Spring 5-5-2018

Role of EPS15 Homology Domain-Containing Protein 4 (EHD4) in the Kidney

Shamma Rahman
University of Nebraska Medical Center

ROLE OF EPS15 HOMOLOGY DOMAIN-CONTAINING PROTEIN 4 (EHD4) IN THE KIDNEY

by

Shamma S. Rahman

A DISSERTATION

Presented to the Faculty of
the University of Nebraska Graduate College
in Partial Fulfillment of the Requirements
for the Degree of Doctor of Philosophy

Cellular & Integrative Physiology
Graduate Program

Under the Supervision of Assistant Professor Erika I. Boesen

University of Nebraska Medical Center
Omaha, Nebraska

January, 2018

Supervisory Committee:

Steven Sansom, Ph.D.

Hamid Band, M.D., Ph.D.

Kaushik P. Patel, Ph.D.

ACKNOWLEDGEMENTS

When I started my journey in the “awe-inspiring” world of graduate studies, I never imagined that I would end up in a kidney lab. I had almost no previous knowledge about the complexity of renal physiology, let alone working with animal models. I am extremely fortunate that I found Dr. Erika Boesen as my mentor during my PhD training. I am truly indebted to her for allowing me to learn and grow as a scientist at my own pace during my time in her lab. I have benefited from the various resources she provided me to expand my scientific knowledge, and I want to thank her for providing me with constructive comments and solutions to my problems during the last 4 years.

My training and transition into becoming a scientist during the last 4 years would not have been possible without the astute guidance of my supervisory committee members: Dr. Steven Sansom, Dr. Kaushik Patel, and Dr. Hamid Band. I am deeply grateful to my supervisory committee for encouraging, supporting, and also challenging me in ways that helped me move forward with my dissertation in a constructive manner.

I would like to thank each and every past and present students, staff, and faculties of the department of Cellular and Integrative Physiology at UNMC. I am very thankful to Dr. Pamela Carmines for not only letting me have an unrestricted access to her laboratory, but also for providing me with helpful information and reminders on graduate school deadlines. I would also like to thank Dr. Lie Gao for letting me use the confocal microscope, even at the oddest hours, that helped tremendously with the progression of my project. The CIP department is blessed to have amazing office staffs, and I would like to thank Cindy, Kim, Pearl, Deb, and Tammy for providing help with external grant submissions and meeting registrations.

I have been extremely lucky that I found Eileen and Mathilde as my labmates. No words can describe the amount of love and gratitude I have for these two amazingly “crazy” persons. In the last 4 years, Eileen and Mathilde have filled my boring and frustrating times in the lab with humor and fun. Not only have they helped me with technical issues in the lab, they have also supported me and lifted my spirit up during difficult times. I cannot thank them enough for the wonderful memories that I made with them in the last 4 years.

I would like to thank my amazing friends here in Omaha: Rahat, Farhana, Nejmun, Duy, Dr. Ali Nawshad, Tinku, and Sara. Living away from home became easier over time because of these wonderful people. They provided me with constant support and love, and have successfully made Omaha a second home for me. A special shout-out to Zeus for meowing outside my door every morning so that I could wake up to come to work. I would like to thank my friends from Bangladesh: Nafis, Esha, and Barna, who have given me constant encouragement and love from afar.

Last, but never the least, I would like to thank my family: Ammu, Abbu, my dearest sister Antara, my cousins Nadia, Samia and Bithi, my nieces Rubab, Tathoi, and Ariya, my nephews Areez, Tajrian, and Ehan, and my mama and mami. I owe my deepest gratitude to all these people for showering me with love and giving me unprecedented support to achieve my dreams. I love you all!

ROLE OF EPS15 HOMOLOGY DOMAIN-CONTAINING PROTEIN 4 (EHD4) IN THE KIDNEY

Shamma S. Rahman, Ph.D.

University of Nebraska Medical Center, 2018

Supervisor: Erika I. Boesen, Ph.D.

In the kidney, endocytic recycling regulates the abundance of channels and transporters in the membrane of the tubular epithelium, and thereby controls the kidney's ability to regulate water homeostasis. In recent years, a family of proteins called Eps15 homology domain-containing (EHD) proteins has emerged as important regulators of the endocytic recycling pathway. Mammals express four paralogs of EHD proteins, EHD1-4, that are expressed in different tissues. Although EHD4 is expressed in the kidney, the specific physiological role of EHD4 in the kidney remains unknown. Therefore, this dissertation was focused to elucidate the physiological role of EHD4 in the kidney. In the mouse kidney, EHD4 was found to be expressed most abundantly in the inner medullary collecting duct (IMCD), a site for fine-tuning final urine concentration. Studying the renal parameters of *Ehd4*$^{-/-}$ (EHD4-KO) mice showed that EHD4-KO mice had a higher urine flow and lower urine osmolality than wild-type (WT) mice. EHD4 was found to be expressed in the hypothalamus, but its deletion did not affect the plasma osmolality or arginine vasopressin (AVP) excretion. EHD4-KO mice were able to exhibit anti-diuretic responses to 24-h water restriction similar to the WT mice, suggesting that the diuretic phenotype of EHD4-KO mice is due to defective renal water and solute handling. Formation of a concentrated urine requires the presence of the renal medullary osmotic gradient, partially contributed by renal urea handling, and fine-tuning of water reabsorption via aquaporin (AQP) 2 in the

IMCD. Given the abundant expression of EHD4 in the IMCD, it was hypothesized that EHD4 regulates AQP2 trafficking in the principal cells and renal urea handling. Both in vivo and in vitro analysis showed that in the absence of EHD4, the apical membrane abundance of AQP2 was significantly attenuated. EHD4 was also found to regulate basolateral membrane abundance of AQP4 in principal cells. Although EHD4 was found to co-localize with AQP2, immuno-complex containing AQP2 did not show the presence of EHD4, suggesting a lack of direct physical interaction between the two proteins. Additionally, EHD4-KO mice had higher urea excretion than WT mice, suggesting a dysfunctional urea handling in these mice. To delineate the exact role of EHD4 in renal urea handling, mice were subjected to a series of experiments involving intake of modified protein diets, which confirmed a role of EHD4 in the regulation of renal urea handling. Overall, this dissertation describes a novel role for EHD4 in the regulation of AQP2, AQP4, and renal urea handling in the kidney.

TABLE OF CONTENTS

LIST OF FIGURES

LIST OF ABBREVIATIONS

AC	adenylyl cyclase
ACBP	acyl-CoA binding protein
AMP	adenosine monophosphate
AQP1	aquaporin 1
AQP2	aquaporin 2
AQP3	aquaporin 3
AQP4	aquaporin 4
Arf	adenosine diphosphate ribosylation factor
AVP	arginine vasopressin
BF	biotinylated fraction
cAMP	cyclic adenosine monophosphate
CD	collecting duct
cPLA2	cytoplasmic phospholipase A 2
CREB	cAMP response element-binding protein
DAPI	4’,6-diamidino-2-phenylindole
dDAVP	d-deamino arginine vasopressin
EDTA	ethylenediaminetetraacetic acid

EH	Eps15 homology domain
EHD1	Eps15 homology domain-containing protein 1
EHD2	Eps15 homology domain-containing protein 2
EHD3	Eps15 homology domain-containing protein 3
EHD4	Eps15 homology domain-containing protein 4
EHD4-HOM	*Ehd4*$^{+/+}$
EHD4-KO	*Ehd4*$^{-/-}$
ELISA	enzyme-linked immunosorbent assay
ENaC	epithelial sodium channel
EP1	prostaglandin E2 receptor 1
EP2	prostaglandin E2 receptor 2
EP3	prostaglandin E2 receptor 3
EP4	prostaglandin E2 receptor 4
EU	euhydrated
FBS	fetal bovine serum
GATA	GATA binding protein
GFP	green fluorescent protein
GTPase	guanosine triphosphatase

IM	inner medulla
IMCD	inner medullary collecting duct
I.P.	intra peritoneal
kD	kilo Dalton
KEB	kidney extraction buffer
LLC-PK1	porcine proximal tubule cell line
MDCK	Madin-Darby canine kidney cell line
$mpkCCD_{c14}$	mouse cortical collecting duct principal cell line clone 14
mRNA	messenger ribonucleic acid
MTAL	medullary thick ascending limb
MVB	multi vesicular body
NCC	sodium chloride cotransporter
NFAT5	nuclear factor of activated T cell 5
NHE	sodium hydrogen exchanger
NIH	National Institute of Health
NKCC2	sodium potassium chloride cotransporter 2
NPF	asparagine-proline-phenylalanine
NT	non-targeting

OM	outer medulla
OVLT	organum vasculosum laminae terminalis
pAQP2	phospho-serine-256-aquaporin 2
PBS	phosphate-buffered saline
pCDNA3	mammalian expression vector
PGE2	prostaglandin E2
PKA	protein kinase A
PKC	protein kinase C
PKG	protein kinase G
PVD	polyvinylidine difluoride
Rab	Ras superfamily of monomeric G protein
Rab11-Fip2	Rab11 family-interacting protein 2
SDS	sodium dodecyl sulfate
SDS-PAGE	sodium dodecyl sulfate polyacrylamide gel electrophoresis
shRNA	short hairpin ribonucleic acid
siRNA	small interfering ribonucleic acid
TAZ	transcriptional coactivator with PDZ-binding motif
TBST	Tris-buffered saline Tween-20

UT-A1	urea transporter A1
UT-A2	urea transporter A2
UT-A3	urea transporter A3
UT-A4	urea transporter A4
UT-B	urea transporter B
V2R	arginine vasopressin V2 receptor
VEGFR2	vascular endothelial growth factor receptor 2
WCL	whole cell lysate
WR	water-restricted
WT	wild type

INTRODUCTION [1] [2]

[1] Parts of the material presented in this section was previously published in:
[1]**Rahman, S. S.,** and Boesen, E. I. Outside the mainstream: novel collecting duct proteins regulating water balance. Am. J. Physiol. Renal Physiol. 311: F1341-F1345 (2016)

[2]**Rahman, S.S**., Moffitt, A. E. J., Trease, A., Foster, F. W., Storck, M., Band, H., Boesen, E. I. EHD4 is a novel regulator of urinary water homeostasis. FASEB J. (2017)

Physiological functions of the kidney

The kidney has three broad physiological functions: secretion of hormones, gluconeogenesis, and maintenance of extracellular homeostasis of pH and blood electrolytes. The functional unit of the kidney, called the nephron, consists of two parts: the glomerulus, which is involved in the ultrafiltration of the blood, and the tubule, which consists of specialized epithelial cells involved in the reabsorption and secretion process (65).

The renal corpuscle consist of glomerular capillaries and the glomerular capsule known as Bowman's capsule. Blood undergoes filtration as it passes through the renal corpuscles, wherein large cells and proteins are retained in the blood in the glomerular capillaries, and water and solutes freely pass into the Bowman's space. The kidneys filter 180 liters of blood each day in an average 70 kg human and the rate at which the kidney filters blood is called glomerular filtration rate (156).

The filtrate entering the Bowman's space then passes into the nephron tubules. The ultrafiltrate undergoes regulated stages of reabsorption, which involves removal of water and solute from the tubular fluid and transporting it back to the blood, and secretion, which involves releasing molecules into the tubular fluid from the epithelium as it passes down the nephron tubules. The first part of the nephron tubule is the proximal convoluted tubule. The apical (luminal) surface of the epithelial cells of the proximal tubules contains dense microvilli and the cytoplasm of these cells contains numerous mitochondria, allowing these cells to participate in the bulk reabsorption of water and solute. Next, the filtrate enters the loop of Henle, which consists of thin descending limb, thin ascending limb, and thick ascending limb. Next, the filtrate passes to the distal convoluted tubule, which is lined by small cuboidal epithelial cells. Finally the filtrate reaches the collecting duct, which consist of two major types of cells: intercalated cells, involved in acid-base

regulation, and the principal cells, involved in the fine-tuning of urine volume and composition. An adult human produces 1 to 2 liters of urine in average, which is regulated by factors like the hydration state, physical activity, environmental conditions, weight, and the health of the person (65, 156).

Urine formation and composition

Urine formation begins as soon as the ultrafiltrate enters the proximal tubules, where complete reabsorption of the essential molecules, such as glucose and amino acids, takes place. About 65-70% of filtered sodium is reabsorbed in the proximal tubule via the sodium-hydrogen exchanger (NHE) (115) and sodium-glucose cotransporter, lining the apical membrane of the proximal tubules. Sodium reabsorption in the proximal tubule is coupled to water reabsorption, wherein water enters and exits the epithelial cells via aquaporin (AQP) 1(140).

The descending thin limb of the loop of Henle is highly permeable to water due to the presence of AQP1 (23, 153), but impermeable to sodium due to a lack of sodium channels and transporters in the membrane (95). On the other hand, the ascending limb of the loop of Henle is permeable to sodium due to the presence of sodium-potassium-chloride cotransporter 2 (NKCC2) (62), as well as NHE, that allows reabsorption of 25% of filtered sodium. However, this section of the nephron is completely impermeable to water due to a lack of any aquaporin water channels (162). Such an arrangement, which is discussed in detail in the following section, allows the formation of concentrated urine. The distal convoluted tubules of the nephron contains the sodium-chloride cotransporter (NCC) (52), which participates in the reabsorption of 5% of filtered sodium. The collecting duct offers the final stages of regulation of the volume and composition of urine, and about 5% of sodium reabsorption occurs via the epithelial sodium channel (ENaC) (54). Water reabsorption in the distal parts of the nephron is variable and this variability allows the

kidney to regulate the water excretion and reabsorption to maintain a constant water balance. A detailed role of the water channels of the collecting duct is discussed in the following section.

Water balance

Maintaining extracellular fluid osmolality is integral for survival. Imbalance in body water can have adverse effect on the cell size and function. The hypothalamus, neurohypophysis, and the kidney are involved in the regulation of water balance in the body (33).

Clinical implications of water imbalance

A failure to maintain water balance can result from different forms of urine-concentrating defects. Diabetes insipidus is such a disorder where the patient produces large volumes of urine. Defects in the synthesis or secretion of arginine vasopressin (AVP) can result in central diabetes insipidus (2), whereas unresponsiveness of the kidney to AVP can cause nephrogenic diabetes insipidus (85, 111). Unmanaged polyuria, such as during diabetes insipidus, can cause the osmolality of the plasma to elevate and result in an often-fatal condition known as hypernatremia. Treatment options for these diseases are limited and a major limiting factor in designing better therapies for such conditions of water imbalance is the lack and gap in the knowledge of the detailed molecular and cellular pathways that regulate the hypothalamic-neurohypophyseal-renal axis. The physiological process of maintaining a net zero water balance is very tightly regulated at the cellular level. It is, therefore, essential to study these pathways to form a comprehensive knowledge of how the body regulates water balance.

Role of the collecting duct in fine-tuning water balance

The ability of the kidney to produce a concentrated urine (i.e. reabsorbing more water) or dilute urine (i.e. excreting more water) depends on the state of water-permeability of the nephron sections. The water-permeability of the nephron structures can be altered by acutely regulating the paracellular and transcellular water flow. The paracellular route is regulated by the tight junction proteins, which act as zippers to seal the intercellular spaces between adjacent epithelial cells (73). The tight junction proteins along the thick ascending limb and collecting duct are highly expressed, making these segments water-impermeable. However, the water-permeability of the collecting duct can be increased by AVP by increasing the transcellular route of water reabsorption via the regulation of the membrane trafficking of aquaporins (AQPs) of the IMCD.

Aquaporins of the kidney

Water homeostasis is a critical process involving the coordinated action of the hypothalamus, including the thirst mechanism and control of AVP release, and the kidneys, where water is either reabsorbed or excreted in the urine. Reabsorption of water from the tubular lumen into the interstitium occurs via specialized water channels called AQPs (96, 198). The kidney expresses different subtypes of AQPs in different segments of the nephron. AQP1 is constitutively expressed in the apical membrane of the epithelium of proximal tubules and thin descending limb of the loop of Henle (96). Although AQP1-mediated water transport in these proximal sections of the kidney contribute to the bulk reabsorption of water, the collecting duct (CD) represents the key site for fine-tuning of water balance by the kidney. AQP2, the apical water channel of the principal cells of the CD, is the only AQP whose presence on the apical membrane of the principal cell is regulated by AVP, and as a result determines the water permeability of the CD (198). Humans harboring mutation in the AQP2 gene develop nephrogenic diabetes insipidus

(34). The principal cells of the CD constitutively expresses AQP3 and AQP4 on the basolateral membrane (140).

General structure and expression profile of AQP2

AQP2 is the water channel found in the apical plasma membrane of principal cells of the collecting ducts of the kidney. Cloning and expression analysis of AQP2 was first performed in 1993 (51) and since then the regulatory mechanisms of AQP2 has been extensively studied. AQP2 is composed of 6 transmembrane α-helices, with both the amino and carboxyl ends facing the inside of the cell (59). The expression and trafficking of AQP2 in the principal cells is regulated by AVP and is required for the water permeability of the collecting duct of the kidney. A large number of different mutations of AQP2 gene have been found and a defect in its trafficking causes nephrogenic diabetes insipidus, where the kidney is unable to reabsorb water and concentrate urine (128). However, most of the time, nephrogenic diabetes insipidus occurs due to a mutation of the vasopressin V2 receptor (129).

AVP-dependent regulation of AQP2

AVP is a major regulator of renal water reabsorption and exerts its effects on the kidney through its G-protein coupled receptor. The collecting duct expresses V2 receptor, a G_s-coupled receptor, on the basolateral membrane of the principal cells. Similar to other G_s-coupled receptors, activation of V2 receptor increases the level of cyclic-AMP (cAMP) and activates protein kinase A (PKA) in the principal cells. Extensive studies on rodents have been performed to understand the effect of AVP on the regulation of AQP2 in principal cells. AVP-mediated regulation of AQP2 can be classified as being short-term, which occurs within minutes, and as long-term, which can take place over several hours to days (75, 140).

The short-term regulation of AQP2 by AVP involves the changes in the cellular localization of AQP2 (139). In the presence of AVP, localization of AQP2 is shifted from the cytoplasm to the apical plasma membrane, and is mediated by a combination of both an increased exocytosis and inhibition of endocytosis of AQP2-containing vesicles (18). AVP mediates the changes in the localization of AQP2 by changing the phosphorylation status of AQP2 that results in an increased forward trafficking of the channel and retention of AQP2 in the apical membrane (126). Exocytosis of AQP2 is dependent on the phosphorylation of the serine-256 residue (50), whereas the phosphorylation of serine-269 strongly favors the retention of AQP2 in the apical plasma membrane and inhibits its endocytosis (124). AVP also reduces the phosphorylation on serine-261 residue (113), although the role of this phosphorylation site in the trafficking of AQP2 remains unknown. In addition to inducing changes in the phosphorylation status of AQP2, AVP also regulates the redistribution of AQP2 by modulating the cytoskeletal proteins such as actin (145).

The long-term effect of AVP on AQP2 involves changes in the total abundance of the channel in principal cells (67), which is regulated in at least two ways. Firstly, AVP increases the half-life of AQP2 protein in principal cells, such as from 9 to 14 hours in cultured principal cells (169). Secondly, AVP increases the transcription of the AQP2 gene, which ultimately increases the translation of AQP2 mRNA (120). The promoter region of AQP2 has binding sites for cAMP responsive element binding (CREB) protein, the binding of which increases the transcription of AQP2 (209).

Much progress has been made into understanding the molecular mechanisms involved, especially as they relate to the classical AVP-AQP2 axis (18, 66, 75, 140). However, recent studies have implicated several novel proteins and local factors in the regulation of water balance, as discussed below, and these may or may not act by influencing the components of the classical linear AVP-AQP2 axis upstream of AQP2.

AVP-independent regulation of AQP2

Several studies have called into question whether cAMP is necessary for apical trafficking of AQP2 downstream of activation of G protein-coupled receptors such as the V2-receptor. A recent study highlighted a disconnect between the time course of cAMP elevation in response to stimulation of these G_s coupled receptors and the apical membrane targeting of AQP2 (150). Treatment of cells with an adenylyl cyclase (AC) inhibitor did not prevent AQP2 membrane targeting (150), and AC6-null mice do not increase cAMP in response to AVP yet still are able to concentrate their urine in response to water restriction or d-deamino-arginine vasopressin (dDAVP), an analog of AVP administration (161). Accordingly, cAMP-independent signaling pathways for AQP2 apical trafficking in response to activation of these receptors await elucidation.

Regulation of AQP2 by prostaglandin E2 (PGE2)

One of the major local factors influencing the trafficking of AQP2 in principal cells is prostaglandin E2 (PGE2). PGE2 is a lipid mediator derived from the metabolism of arachidonic acid, which is converted to PGE2 by the sequential actions of cyclooxygenase-1 and -2 and PGE synthase enzymes. PGE2 exerts its influence via 4 different types of G protein-coupled prostanoid receptors, namely EP1-4 (14). The CD expresses all 4 of these receptors. EP2 is only expressed in the cortical collecting ducts (84), whereas the other EPs are expressed all along the CD (6, 15, 16). EP2 and EP4 are coupled to G_s protein, whereas EP1 and EP3 are coupled mainly to G_i protein (14). This differential coupling pattern of EPs results in evoking opposite effects on AQP2 trafficking, and ultimately on urine-concentrating mechanisms.

In rat IMCD, PGE2 and agonists of EP1 and EP3 have been shown to decrease the AVP-induced water permeability and AQP2 trafficking at a post-cAMP level (78, 132, 191, 211). EP1 retards AQP2 trafficking by activating protein kinase C (PKC) that results

in an increase in the endocytosis of AQP2. In the CD, EP3 couples to G_i and inhibits the synthesis of cAMP, thereby inhibiting the exocytosis of AQP2. Another interesting way by which PGE2 could increase diuresis is by acting on the EP2 located in the papillary interstitial cells. EP2 is the only prostanoid receptor expressed in the papillary interstitial cells and binding of PGE2 to EP2 increases hyaluronan synthesis in these cells (165, 213). Hyaluronan has a high capacity to bind water, and thereby alter the papillary matrix and inhibit water flow (166). Hence, PGE2 can reduce water permeability and increase diuresis within the IMCD through acting on EP1, EP2, and EP3.

Transcriptional regulation of AQP2 gene transcription

Transcriptional regulation represents an important means of long-term regulation of CD function. Unsurprisingly, deletion of a number of transcription factors results in renal developmental abnormalities, phenotypes of nephrogenic diabetes insipidus or urinary concentrating defects (109, 210, 214). However, several such transcription factors have additionally been shown to play a role in water handling independently of developmental effects. Using an inducible system, post-developmental deletion of GATA2 from the nephron induced polyuria and revealed an important role of GATA2 as a direct transactivator of AQP2, as well as regulating V2R and AQP3 mRNA levels, suggesting GATA2 promotes water conservation via multiple mechanisms (210). AVP-independent increases of AQP2 by the ligand-activated transcription factor Farnesoid X receptor was also recently shown to contribute to regulation of urine volume (214). Hyperosmotic stress increases the phosphorylation of TAZ (transcriptional coactivator with PDZ-binding motif, also known as Wwtr1), which is followed by increased physical interaction between TAZ and nuclear factor of activated T cells 5 (NFAT5), reducing NFAT5 activity (80). NFAT5 is an osmoregulatory transcription factor that upregulates the expression of AQP2 in response to calcium and osmotic stress (109), suggesting that TAZ may help to fine-tune

both NFAT5 and AQP2 expression under conditions of osmotic stress. Together, these recent developments show that there is far more to the transcriptional regulation of CD water handling proteins than the classical transcription factor CREB.

Post-translational modifications of AQP2 in principal cells

The role of phosphorylation of AQP2 has been extensively studied by several groups, and it can be readily appreciated from these numerous studies that phosphorylation of AQP2 is one of the most highly regulated post-translational modifications of the channel (125). As described above, AVP increases the forward trafficking of AQP2 to the apical plasma membrane by changing the phosphorylation status of the channel. Phosphorylation of serine-256 residue of AQP2 was the first to be identified (50), and studies over the last decade have identified other phospho-residues, namely serine-261, serine-264, and serine-269 (125). Although PKA is the most well-defined kinase involved in the phosphorylation of AQP2, the channel has other putative sites for other kinases such as PKG, PKC, and casein kinase II (18). Each of the phosphoforms of AQP2 have an effect on the cellular localization of AQP2. Phosphorylation of serine-256 residue increases the exocytosis of AQP2 and is required for facilitating the phosphorylation of serine-264 and serine-269 (70). Phospho serine-269 AQP2 has only been observed exclusively on the apical membrane, suggesting that the phosphorylation of this residue increases the retention of AQP2 in the apical membrane (124). Phospho serine-264 AQP2 resides in the compartments close to the plasma membrane and in early endocytic pathways (48), whereas phospho serine-261 AQP2 is localized in compartments different from the endoplasmic reticulum, Golgi, and lysosomes (71). Phosphorylation of AQP2, therefore, is a critical process in determining the cellular localization of the channel in the principal cells.

Ubiquitination is another form of post translational modification of AQP2 whereby the lysine-270 residue of AQP2 undergoes short-chain ubiquitination and mediates the endocytosis and degradation of AQP2 (82). In addition to ubiquitination, AQP2 also undergoes complex N-glycosylation (7, 68); however, the role of glycosylation of AQP2 is unclear. In oocytes, mutants of non-glycosylated and glycosylated AQP2 are retained in the endoplasmic reticulum due to failure to properly fold the protein (116). In another study it has been shown that glycosylation of AQP2 is necessary for the exit of the protein from Golgi and important for membrane trafficking (68). Together, these studies on the post-translational modifications of AQP2 have shown that these processes are important for the cellular localization and function of AQP2, although the knowledge of these processes is far from complete.

Membrane localization of AQP2 in principal cells

The presence of aquaporins in the apical and basolateral membranes of select regions of the nephron is critical for water reabsorption from the tubular fluid. The cAMP-dependent PKA-mediated phosphorylation of AQP2 downstream of vasopressin V2 receptor activation by AVP has long been recognized to promote the forward trafficking of AQP2 into the apical membrane. The trafficking of AQP2 to the cell membrane from the intracellular vesicles involves passage of the channel through the Golgi apparatus and endosomal compartments. The insertion of AQP2 channel into the plasma membrane involves numerous fission and fusion steps that are regulated by various proteins such as the SNARE complex (18).

As described above, the trafficking of AQP2 in principal cells is regulated by factors such as AVP and PGE2, but under non-stimulated conditions, AQP2 can undergo constitutive recycling (18). In LLC-PK_1 cells, a porcine kidney cell line, inhibition of clathrin-mediated endocytosis resulted in an increased accumulation of AQP2 in the plasma

membrane, which was independent of serine-256 phosphorylation (112). In another study, inhibition of AQP2 recycling in LLC-PK1 cells resulted in accumulation of the channel in the trans-Golgi (64), showing that recycling of AQP2 is critical for the membrane accumulation of the channel. Additionally, induction of actin depolymerization in cultured IMCD cells in the absence of any hormonal stimulation increased the accumulation of AQP2 in the plasma membrane (189), indicating the importance of the cytoskeleton in the trafficking of AQP2. All these observations show that a disruption of either the endocytosis or exocytosis of AQP2 can change the amount of AQP2 in the plasma membrane, implying that the constitutive recycling of AQP2 is a very dynamic process with endocytosis in equilibrium with exocytosis (167). Currently, there is a major gap in understanding this constitutive recycling of AQP2 because the molecular machinery for these processes is poorly characterized.

Roles of AQP3 and AQP4 in the CD

The principal cells of the CD express AQP3 and AQP4 in the basolateral membrane, providing an exit pathway for the water that enters these cells through the AQP2 in the apical membrane. Mice lacking AQP3 develop severe polyuria (114). Albeit less well-studied than AQP2, differences in AQP3 expression or localization to the basolateral membrane can also affect water reabsorption across the CD. Similar to AQP2, AVP regulates AQP3 transcription (36); however, recent studies are showing AVP-independent pathways can also regulate AQP3. Mice lacking acyl-CoA binding protein (ACBP), a protein involved in transporting acyl-CoA esters between different enzymes, were found to have slightly higher urine flow under basal conditions and a reduced ability to conserve water during water restriction, but no apparent difference in sodium or potassium handling (101). Expression and basolateral localization of AQP3 was reduced in the ACBP knockout mice, with no apparent changes in the expression and localization

of AQP1, 2 or 4 (101). Fatty acyl-CoAs can serve as allosteric regulators of cellular proteins such as ryanodine-sensitive Ca^{2+} release channels (40), which are in turn important regulators of AQP2 distribution in principal cells (24), however the mechanism(s) by which ACBP regulates AQP3 expression and localization is unknown.

AQP4, along with AQP3, is expressed in the basolateral side of principal cells; however, unlike AQP2 or AQP3, its abundance is not regulated by AVP (140). Deletion of AQP4 in mice results in polyuria that is milder than that seen in AQP3-null mice (25). Unlike AQP2 and AQP3, the expression of AQP4 is unaffected by water restriction (192). Moreover, sorting of AQP3 and AQP4 to the basolateral membrane occurs separately in the Golgi (3), indicating that there are several non-overlapping cellular pathways regulating these aquaporins in the CD.

Over the decades, studies on the AQPs of the CD have elegantly shown that the cellular apparatus involved in the regulation of these water channels is very complex, and far from being completely characterized. The presence of these water channels in their appropriate membrane is crucial in determining the water permeability of the CD, which in turn regulates the ability of the kidney to maintain water balance. While the AVP-mediated cellular trafficking of AQP2 has been somewhat well-characterized, the constitutive recycling of AQP2 and the other AQPs remain largely unexplored. It is, therefore, imperative to accurately identify and characterize proteins and molecular mechanisms that regulate the cellular localization of these water channels of the CD. Moreover, as the discussion on the role of the kidney and hypothalamus in the maintenance of water balance progresses in the upcoming sections, the importance of the cellular trafficking of other channels and transporters in the regulation of water balance can be appreciated.

Role of the renal medullary interstitium in fine-tuning water balance

The final steps in the maintenance of osmotic homeostasis occur in the kidney, and involves the production of a hypoosmotic or hyperosmotic urine depending on the hydration state of the individual. The osmolality of the renal medullary interstitium provides an osmotic driving force to allow water to exit the tubules, thereby allowing urine to be concentrated. The osmolality of the renal medulla can be increased significantly during states of dehydration to increase the amount of water that is reabsorbed, and thereby, allowing the formation of a hyperosmotic urine, whose osmolality is higher than that of the plasma (172, 174).

The structural arrangement of the nephron is crucial in the generation of the osmotic gradient of the renal medullary interstitium. Three features of the nephron structure come into play to establish this gradient. First, the nephron forms a hairpin loop to allow water and solute exchange between the descending thin limb and the ascending thin limb (174). Second, the ascending thin limb is impermeable to water, but permeable to sodium due to the presence of NKCC2 that actively transports sodium from the tubular fluid into the interstitium, allowing the concentration of the interstitium to build up. Third, the concentration gradient of the interstitium allows reabsorption of water from the water-permeable, but solute-impermeable, descending thin limb. This process, termed countercurrent multiplication, establishes the gradient and contributes to one half of the maximal medullary concentration, with the other half contributed by urea recycling (87). Urea is passively reabsorbed from IMCD via urea transporters of collecting duct and enters the interstitium. The reabsorbed urea then re-enters the thin loop of Henle back into the filtrate, passes the distal tubules and reaches the IMCD, from where it again undergoes passive reabsorption. This re-circulation of urea within renal medulla helps in building up the osmotic gradient (74, 206).

The preservation of the osmotic gradient of the renal medullary interstitium is achieved by a process called countercurrent exchange that involves the vasa recta. The special arrangement of the vasa recta prevents the escape of the solutes from the renal medulla and thereby stops the dissipation of the gradient (130). Two features of the vasa recta allows the preservation of the gradient. First, the blood flow to the renal medulla is very low. Although the kidney receives about 25% of the cardiac output, most of the renal blood flow is directed to the outer cortex and the renal medulla receives only less than 2 to 5% (127) of this blood. Second, the arrangement of the two limbs of the vasa recta allows countercurrent exchange. In the descending limb of the vasa recta water diffuses out of the plasma and solutes from the renal interstitium enters the plasma, thereby making the plasma in this side hyperosmotic. In the ascending limb of the vasa recta, the water diffuses back into the blood and solutes diffuse back to the interstitium. In this way the washing out of the gradient is prevented and the gradient remains preserved.

As described above, urea plays an important role in both the generation and preservation of the renal medullary gradient, the integrity of which is crucial in the maintenance of water balance. The following section discusses the various urea transporters of the kidney that are involved in the renal urea handling.

General structure and expression profile of urea transporters

Urea was first isolated from the urine by Hillaire-Marin Ronelle in 1773 and has been long recognized as an important biological molecule in the urine-concentrating mechanism (206). Being a water-soluble molecule, urea has low permeability through lipid bilayers, and mammalian cells have several types urea transporter (UT) that facilitate the transport of urea down a concentration gradient through the plasma membrane (108). Each UT has 10 predicted transmembrane helices, except for UT-A1, which has 20 transmembrane domains arising from two tandem UT domains (164). The region in the

first and the last five transmembrane helices are highly homologous, and each 5 transmembrane repeat contain a conserved motif with the following sequence: LPXXTXPF. This motif is thought to be critical for urea permeation (164).

Two gene families encode for the urea transporters in mammals: *Slc14a1* and *Slc14a2* (171). The *Slc14a2* gene encodes the UT-A family, whereas the *Slc14a1* gene encodes the UT-B family. There are 6 major isoforms of the UT-A family, each with a distinct expression profile, which are derived by alternative splicing of the same mRNA and alternative promoter of the same gene (47). AVP regulates UT-A1 (179), which is expressed in the apical plasma membrane of principal cells of the IMCD and is involved in the reabsorption of urea in the IMCD. Two distinct forms of UT-A1, 97 kD and 117 kD, have been characterized that arise due to different state of glycosylation of the protein (12). UT-A2 (55 kD) is expressed in the liver and the kidney (143), where UT-A2 is involved in the transport of urea across the apical membrane into the luminal space of the thin descending limb of the nephron (158). UT-A3 is expressed in the IMCD (194), and similar to UT-A1 it has two forms, a 44 kD form and a 67 kD form. In rat IMCD, UT-A3 localizes to the apical membrane and intracellular vesicles (194), whereas in mouse IMCD UT-A3 is localized in the basolateral membrane (184). UT-A4 has only been found in rat kidney medulla (83), and its function currently remains unknown. Both UT-A5 and UT-A6 are expressed in non-renal tissues: UT-A5 in the testis (42) and UT-A6 in the colon (182). UT-B is expressed in several tissues, including in the basolateral and apical membranes of the descending vasa recta (195).

Cellular mechanisms in the regulation of urea transporters

UTs play an important role in the urine-concentrating mechanism in the kidney, and a loss of UT in mammals result in some form of urine-concentrating defect (45, 173).

Urea transportation, therefore, is highly regulated and a major mode of this regulation occurs via the cellular regulation of the UTs.

Regulation of UT-A1

UT-A1 is critical for basal urine-concentrating ability, as shown in mice where transgenic expression of UT-A1 in UT-A1/A3 double knock out mice corrects the urine-concentrating defect in these animals (92). Perfusion of rat IMCD with AVP rapidly increases the facilitated urea permeability (141, 170); the way AVP induces this change is by increasing the trafficking of UT-A1 to the apical membrane (143). AVP has also been shown to increase the apical membrane accumulation of UT-A1 in the IMCD of Sprague-Dawley rats (89). Phosphorylation is a major post translational modification of UT-A1 that influences its membrane trafficking. Phosphorylation of serine-486 and serine-499 by PKA increases the membrane accumulation of UT-A1(11) and both of these phospho forms of UT-A1 primarily localize to the apical membrane. Additionally, UT-A1 is also phosphorylated at serine-494 by PKC, which acts in concert with PKA to increase the insertion of UT-A1 in the apical membrane (9). AMP-activated protein kinase also increases the phosphorylation of UT-A1, but in an AVP-independent manner (91). The accumulation of UT-A1 in the apical membrane is reduced by 14-3-3 proteins, which bind and target UT-A1 for ubiquitination and degradation (41), thereby ultimately reducing urea transport in the IMCD.

The IMCD expresses two isoforms of UT-A1, a more abundant 97 kD form and a less abundant 117 kD form (12, 193). The abundance of the 117 kD isoform is regulated and increases when medullary urea concentration falls, such as during intake of a low protein diet (193), and decreases during high medullary urea concentration, such as during anti-diuresis and high protein diet intake (193). However, the expression of the 117 kD is not regulated by circulating AVP (193).

Regulation of UT-A2

UT-A2, expressed in the thin descending limbs of the kidney nephron, corresponds to the COOH-terminal 397 amino acids of the UT-A1 protein, and is a product of alternative transcription of the parent *Slc14a2* gene, wherein the transcription of UT-A2 begins at exon 13 located 200 kb downstream of exon 1 (133). Both the transcript and protein level of UT-A2 are elevated by chronic treatment with AVP (202). In mice, UT-A2 is required to maintain a high medullary urea concentration when urea supply to the kidney is restricted, such as during low protein diet (196), although UT-A2 is dispensable for inner medullary urea accumulation under basal conditions.

Regulation of UT-A3

UT-A3 is expressed in the IMCD, predominantly in the basolateral membrane of IMCD in mice (184, 194) and is transcribed from exons 1-12 of *Scl14a2* gene (133). UT-A3 undergoes phosphorylation in a cAMP-dependent manner, and phosphorylation of the protein increases its presence in the plasma membrane (10). Additionally, AVP acutely increases the accumulation of UT-A3 in the basolateral membrane of MDCK cells (185), thereby increasing urea flux in these cells. Although UT-A1 is required for the basal urine-concentrating ability in mice, UT-A3 is required for the AVP-mediated increase in urea permeability of the IMCD (92).

Regulation of UT-B

Within the kidney, UT-B is expressed in the descending vasa recta, where it plays an important role in the recycling of urea to maintain the osmotic gradient of the medulla. UT-B is also expressed in the red blood cells and humans lacking this transporter develop a urine-concentrating defect (173). Mice lacking UT-B develop a severe urine-concentrating defect under basal conditions (207) due to impairment of urea recycling in the vasa recta. The concentrating defect in UT-B-null mice is more severe than that in UT-

A2-null mice, suggesting that the countercurrent exchange of urea between ascending and descending vasa recta are more important in the entrapment of medullary urea than the transfer of urea from the vasa recta to the thin limbs (43). Although UT-B deletion in mice does not affect the expression of the IMCD UTs, there is an increase in the expression of UT-A2 in the mice (90). Short-term treatment with AVP in Brattleboro rats reduces UT-B expression, whereas long-term treatment with AVP increases UT-B expression (157).

As apparent from the discussion above, renal urea handling dictates the urine-concentrating ability of the kidney, and a major regulatory arm of the renal urea handling is the cellular regulation of the urea transporters of the kidney. Even after decades of studying these transporters, there are gaps in the understanding of the cellular and molecular machineries involved in the regulation of these urea transporters. In order to better understand these cellular events, it is, therefore, important to properly identify and characterize molecules and proteins involved in the regulation of renal urea handling.

Role of hypothalamus and neurohypophysis in the regulation of water balance

An important aspect of water homeostasis is to be able to sense the changes in plasma osmolality. Neurons in the organum vasculosum laminae terminalis (OVLT) (27, 201), supraoptic and paraventricular nuclei of the hypothalamus (107, 118) have been identified to be involved in osmosensing. It has been proposed that an increase in plasma osmolality, such as during water deprivation, causes membrane depolarization via the activation of calcium channels (17, 110). The nature of the actual stimulus that causes these changes in membrane polarization are unknown, but a role of the mechanical stretch receptors called transient receptor potential vanilloid in osmosensing has been proposed (110). The neurons involved in osmosensing undergo shrinkage in the face of hyperosmolality, and it is proposed that this reduction in cell volume, as well as Angiotensin II (154), allows these cells to stimulate thirst and AVP release.

The brain regions identified to be associated with the perception of thirst are the anterior wall of the third ventricle, the anterior cingulate, parahippocampal gyrus, insula, and the cerebellum (38). These regions of the brain are known to be associated with higher behavioral functions, explaining why thirst is physiologically connected to complex social and emotional behaviors such as motivation. The OVLT senses hyperosmolality and in turn relay the stimuli to the insula and cingula through the thalamic nuclei, initiating the sensation of thirst (72), which is quenched immediately upon drinking. Very recently, other peripheral sodium sensors in the gastrointestinal tract and liver have been identified that are thought to participate in the thirst mechanism (103).

AVP is a major peptide hormone that regulates numerous physiological functions, including the regulation of water balance. AVP is a nonapeptide that is synthesized from a 39-amino acid-long pre-pro hormone (100) in the magnocellular cell bodies of the supraoptic and paraventricular nuclei of the posterior hypothalamus. AVP then binds to

the carrier protein called neurohypophysin and is transported to the axonal terminals of the magnocellular neurons of the posterior pituitary gland (33), where it temporarily stored. It takes almost 2 hours for the complete synthesis and storage of AVP, and the half-life of AVP is around 30 minutes (79). AVP mediates its affect by binding to V1, V2, V3, and oxytocin receptors located in target organs. The V1 receptor is expressed in the vasculature, and binding of AVP to V1 receptor results in vasoconstriction. The V3 receptor is expressed in the pituitary gland. V2 receptors are expressed in the distal tubules and collecting ducts of the kidney, where the binding of AVP stimulates the increase in the water permeability of the CD and allows concentration of urine (33).

Two major stimuli for AVP secretion into the circulation are reduced blood volume and hypertonic plasma, with the latter being the more sensitive stimulus (35). The osmolar threshold of AVP release is almost 5 mOsm/kg lower than the threshold for thirst, allowing AVP to regulate urinary water excretion without the need to drink constantly (33). Apart from osmotic stimulation, the release of AVP is also regulated by several non-osmotic stimuli, such as Angiotensin II, norepinephrine, dopamine, pain, hypoxia, and acidosis (106). Altogether, the stimulation of the osmosensing mechanism of the brain triggers the thirst mechanism and release of AVP to allow conservation of water.

Maintenance of water homeostasis is a complex process that involves the integrative action of the hypothalamus, neurohypophysis, and the kidney. As discussed so far, the regulation of water balance by these organs rely largely on cellular events such as protein trafficking. For example, an important regulatory step that determines the kidney's ability to concentrate urine is the endocytic recycling of AQP2 water channel to the apical membrane of the tubular epithelium. Once in the apical membrane, AQP2 allows entry of water from the tubular fluid into the principal cells, thereby allowing the kidney to reabsorb water. Similar to AQP2, epithelial cells of the kidney's nephrons modify

the composition of urine by selective reabsorption or secretion of solutes and water with the help of various other channels and transporters located on their membranes. A key means of regulating urine composition is via the regulation of the presence and abundance of these channels and transporters on the membrane of the epithelial cells (205). Under steady-state conditions, expression of many of the channels and transporters on the membrane represents the culmination of a very dynamic process, wherein constitutive recycling works in balance with post-synthetic membrane localization, endocytosis and lysosomal degradation (18, 167). Therefore, it is important to understand the intricacies of the endocytic recycling of channels and transporters in the kidney epithelium, and how endocytic recycling plays a role in the adjustment of urine composition and thus water homeostasis.

Endocytic recycling

Endocytic recycling is a cellular process that regulates the composition of the plasma membrane by controlling the uptake and insertion of proteins and other molecules from or into the plasma membrane (61). As discussed in the previous sections, this cellular process is extremely crucial in the regulation of the renal urine-concentrating mechanism. The amount of channels and transporters in the appropriate plasma membrane of the tubular epithelium determines the rate and quantity of water and solute reabsorption, and therefore, endocytic recycling is crucial for normal physiological processes, such as maintenance of water balance.

Cellular events during endocytic recycling

Endocytic recycling regulates the amount of materials extracted from the plasma membrane by endocytosis and the amount that is returned to the plasma membrane. Plasma membrane proteins can be internalized in the cell by either clathrin-dependent or –independent endocytosis (28). Regardless of how proteins are internalized into the cells, the endocytosed proteins arrive into the early endosome first. The fate of the internalized proteins in the cell is, therefore, ultimately determined once it enters the early endosome (81). Inside the early endosome, the internalized proteins undergo sorting, while the endosome starts generating membrane tubules to pass the internalized cargo to the recycling compartments. Depending on the nature of the internalized protein and the state of the cell, the protein may be trafficked to the lysosome for degradation. In most instances, the internalized proteins pass down to the endocytic recycling compartment (ERC) from the early endosome before going back to the plasma membrane (121). It has been proposed that during the early-endosomal maturation the tubules emerging from the early endosome forms the ERC, while the main body of the early endosome becomes what is known as multi-vesicular body (MVB) (155). The ERC has been found to be

localized near the microtubule organizing center and the Golgi apparatus. Trafficking from the ERC to the plasma membrane involves a number of different routes and the nature of the transition primarily depends on the type of internalized protein and the proteins regulating the endocytic recycling (61).

Regulation of endocytic recycling

The sorting and trafficking of cargo during endocytic recycling is regulated by various proteins: Rab- and Arf-GTPases and their effectors; Eps15 homology domain-containing (EHD) proteins 1-4. These regulators of endocytic recycling serve as scaffolding proteins, and regulate the tubulation of the membranes and regulate the activity of motor proteins and membrane fission proteins (61). Several studies have documented the putative roles of the Rab-GTPases and their effector protein in the trafficking of channels and transporters in the collecting duct (29, 176). In particular, large scale proteomic analysis of AQP2-containing vesicles from the principal cells have been shown to contain many of these Rab proteins (5). Very recently, similar analysis of UT-A1-containing vesicles have also revealed the presence of Rab-GTPases (22), suggesting a potential role of these endocytic regulators in the trafficking of AQP2 and UT-A1. Although these studies have only characterized the Rab proteins, limited to no data on the roles of EHD proteins on the trafficking of renal channels and transporters is present. In recent years, the importance of EHD proteins in the regulation of endocytic recycling have emerged and the overall aim of this dissertation is focused to elucidate the novel role of these proteins in the kidney. The following section discusses these EHD proteins and what is currently known about their cellular and physiological roles.

EHD proteins

The C-terminal Eps15 homology domain-containing (EHD) proteins emerged as important regulators of endocytic recycling almost a decade after the discovery of the Rab-GTPases. Mammals express four members of EHD proteins: EHD1-4 (135). Through their interactions with Rab proteins these EHD proteins regulate endocytic recycling (212).

Structural features and cellular functions of EHD proteins

EHD proteins consist of 534-543 amino acid residues. The full-length EHD protein contains two helical regions, a conserved ATP-binding domain, a linker region, and a C-terminal EH domain (181). The function of these EH domains is to mediate highly specific protein-protein interactions between the EH domain of EHD proteins and the tripeptide motif asparagine-proline-phenylalanine of the interacting partner (168). The degree of sequence homology of the EH domains among the EHD proteins range from 53.0% to 81.5% (135). In the cytoplasm, EHD proteins bind to ATP and undergo dimerization, which allows the EHD proteins to bind to and associate with membrane tubular proteins. The hydrolysis of ATP of the EHD proteins destabilizes the vesicle membrane and results in membrane scission.

Expression profile and physiological functions of EHD proteins

Tissue distribution analysis of the EHD proteins has revealed abundant expression across tissues, including the heart (63), brain (26), kidney (58), and in cell types of various origins (180). Although recent studies involving EHD-null mice have started to highlight the importance of these proteins in different physiological processes (4, 31, 56, 160), very little is known regarding the precise functions of EHD proteins in vivo.

Emerging understanding of the physiological roles of EHD proteins

In recent years, EHD proteins have emerged as important regulators of endocytic recycling of membrane proteins. Although reports on the specific functions of EHD proteins in the body is currently limited, studies with global EHD knockout mice have started shedding some light on the understanding of the physiological roles of EHD proteins. Both EHD1 and EHD4-null mice develop small testis (57, 160), indicating a role of these EHD members in the male germ cell development. Additionally, EHD proteins have been shown to be important in regulating cardiac membrane protein trafficking via their interaction with ankyrin-B (63). In particular, EHD3 has been demonstrated to be involved in the anterograde trafficking of Na/Ca exchanger and $Ca_v1.2$ in ventricular mycocytes (31), as well as T-type Ca channels in the atria (32). These studies have shown that EHD3 regulates cardiac membrane excitability in mice.

Both EHD3 and EHD4 regulate the trafficking of internalized proteins in the early endosomes (136, 178). In HeLa cells, deletion of EHD4 results in enlargement of the early endosomal compartments, with proteins destined for degradation being aggregated in the early endosome (178). This study has demonstrated that EHD4 is required for the exit of cargo from the early endosomes to the recycling and late endosomes. Although EHD3-null mice do not develop any pathological phenotype (56), a recent study with mice lacking both EHD3 and EHD4 have shown that the combined deletion of both these members result in a glomerular pathology called renal thrombotic microangiopathy (56). This report also demonstrated that in EHD3-null mice, there is a compensatory functional upregulation of EHD4 within the glomerular endothelial cells, where the expression of EHD4 is usually low, suggesting a potential role of EHD4 in the renal microvasculature. Although this report elegantly highlighted an important role of EHD4 in the renal microvasculature, the specific role of EHD4 in the kidney tubule remains unknown. While the proteomic database of inner

medullary collecting duct cells maintained by the NIH Epithelial Systems Biology Laboratory shows hits for EHD4 (http://helixweb.nih.gov/ESBL/Database/index.html; last accessed on 10/10/2016), no information is available on the exact role of EHD4 in these cells. Accordingly, the main focus of this dissertation is to elucidate the physiological role of EHD4 in the kidney.

Objectives of this dissertation

Endocytic trafficking of membrane proteins is an important cellular event that determines the kidney's ability to concentrate urine and thus regulate water homeostasis (46). As described above, the fate of internalized proteins are determined in the early endosome and one of the important regulators of early endosomal activity is EHD4 (178). The study of George et. al. (56) indicate that EHD4 is able to compensate for the loss of EHD3 in mice, but the exact role of EHD4 in the kidney remains unknown. Based on the expression profile of EHD4 in the collecting duct cells derived from the aforementioned proteomic database, **the aim of this dissertation, therefore, was to determine the roles of EHD4 in the kidney, particularly in the regulation of water homeostasis. This dissertation will test the hypothesis that EHD4 regulates the formation and composition of urine in mice by regulating channel and transporter membrane abundance in the collecting duct.** As such, the study is divided into three broad aims and the objectives of each of these aims are as follows:

Aim 1: To evaluate the physiological role of EHD4 in the regulation of urine formation and composition at the whole body level.

Aim 2: To investigate the role of EHD4 in the regulation of AQP2 trafficking in principal cells of the collecting duct.

Aim 3: To determine the role of EHD4 in the regulation of renal urea handling.

Each aim will be presented in the one of the following chapters, with each chapter containing an introduction explaining the rationale for the Aim, the methods used to study the Aim, the results generated, and a discussion of the findings. At the end of the chapters, a final comprehensive Discussion section is presented to provide a cohesive amalgamation of the findings of all three Aims.

CHAPTER I: ROLE OF EHD4 IN THE REGULATION OF URINE FORMATION AND COMPOSITION [3]

[3] The material presented in this chapter was previously published: **Rahman, S.S**., Moffitt, A. E. J., Trease, A., Foster, F. W., Storck, M., Band, H., Boesen, E. I. EHD4 is a novel regulator of urinary water homeostasis. FASEB J. (2017)

Introduction

Recently, the study of EHD knockout mice has begun to reveal key physiological processes to be regulated by these proteins, such as EHD3-regulated maintenance of cardiac membrane excitability (31) and EHD1- and EHD4-dependent development of testes size and spermatogenesis in male mice (57). Moreover, it has been reported (56) that mice lacking both EHD3 and EHD4 develop renal thrombotic microangiopathy-like glomerular lesions in association with reduced glomerular VEGFR2 expression, signifying the importance of these proteins in glomerular filtration barrier homeostasis. This study (56) also showed that mice lacking only EHD3 do not develop such renal pathology due a compensatory increase in EHD4 within the glomerular endothelium. Interestingly, glomerular EHD4 staining was very low under baseline conditions in wild-type mice, and appeared restricted to endothelial cells (56). Although this previous study indicated an important role for EHD3/4 in the glomerulus, whether EHD4 might play a role in trafficking of proteins in the tubular and collecting duct system has remained unanswered. Additionally, the NIH Epithelial Systems Biology Laboratory's proteomic databases (http://helixweb.nih.gov/ESBL/Database/index.html; last accessed on 10/10/2016) of inner medullary collecting duct cells and mpkCCD$_{c14}$ cells (an immortalized mouse cortical collecting duct cell line), revealed EHD4 expression in the collecting duct, suggesting that EHD4 may play one or more additional roles in the kidney. However, to date, the role of EHD4 *per se* in normal renal physiology has not been directly addressed. **The aim of this chapter, therefore, was to determine the roles of EHD4 in the kidney, particularly in the regulation of water homeostasis given the proteomics-based evidence of collecting duct EHD4 expression.**

Methods

Animals

All animal studies were approved in advance by the Institutional Animal Care and Use Committee at the University of Nebraska Medical Center. Experiments were conducted on 12 to 18-week old male and female *Ehd4*$^{-/-}$ (EHD4-KO) mice (n = 6 for male; n = 5 for female), generated as described previously (56) on the C57Bl/6 background. Age-matched male and female C57Bl/6 (WT) mice (n = 9 for male; n = 4 for female) were used as control mice (Jackson Laboratories, Bar Harbor, ME). The animals were housed in cages maintained at room temperature, 60% humidity with a 12/12 hour light/dark cycle. The mice were given free access to normal rodent chow (7012, Harlan Teklad, Madison, WI) and drinking water except as described below.

Baseline urinary analysis

Animals were placed in individual metabolic cages for 24 hours for comparison of baseline physiological parameters, specifically food intake, water intake and urine output. Animals had free access to food and water during the experiment and were returned to their home cage at the end of the experiment. “Spot” urine samples were also collected following spontaneous voiding. Urine samples were stored at -80 °C until analysis. Urine osmolality was analyzed by freezing point depression using an osmometer (model 3250, Advanced Instruments, Norwood, MA) and plasma osmolality using a vapor pressure osmometer (Model 5520, Wescor, Logan, UT). Electrolyte concentrations of the samples were measured using Ion Selective Electrode technology (MEDICA *Easy*Electrolytes, Medica Corporations, Bedford, MA). AVP and creatinine concentrations were measured according to the manufacturer’s instructions using a Arg8-Vasopressin ELISA kit (Enzo Life Sciences, Farmingdale, NY) and QuantiChrom™ Creatinine assay kit (Bioassay Systems LLC, Hayward, CA) respectively.

Response to acute water loading

Each mouse underwent intra-peritoneal (I.P.) injection of 2 ml sterile water and was placed in a metabolic cage for 6 hours during which food and water were withheld (55). Urine samples were collected hourly for 6 hours and stored at -80 °C until analysis of osmolality, as described above.

Response to 24-h water restriction

Male WT and EHD4-KO mice (n = 6-7 in each group) were placed in individual metabolic cages with access to food and water. The mice were allowed to acclimate to the cage for the first 24 hours, followed by a 24 hour baseline collection period, then a 24 hour water restriction period during which no drinking water was provided. During these periods, urine was collected under paraffin oil (to prevent evaporation), then stored at -80 ^{o}C for later analysis of osmolality, as above. To test for compensatory changes in EHD protein expression in response to water restriction, female EHD4-KO mice underwent a similar protocol except that one group continued to receive access to water throughout the second 24 hour collection period (euhydrated or EU EHD4-KO mice, n = 4) and the other group was water-restricted (WR EHD4-KO mice, n = 6). At the end of the EU or WR period, animals were sacrificed to collect renal tissues for immunoblotting and immunofluorescence analysis.

Response to acute amiloride injection

As a test of epithelial sodium channel (ENaC) activity in vivo, EHD4-KO and WT mice received I.P. injections of amiloride (5 mg/kg) (EMD Chemicals, Inc., San Diego, CA) and an equivalent volume of vehicle (polyethylene glycol) (163). Mice were placed in metabolic cages immediately after the injection. Food and water were withheld, and urine was collected over a 4-h period. The difference in urine volume and sodium excretion

between vehicle and amiloride treatments for each mouse was calculated and compared between groups.

Response to acute furosemide injection

As a test of Na-K-2Cl cotransporter 2 (NKCC2) activity in vivo, EHD4-KO and WT mice received I.P. injections of furosemide (40 mg/kg) (Hospira Inc., Lake Forest, IL) (86) and an equivalent volume of vehicle (polyethylene glycol) on two separate occasions. Immediately after the injections, the mice were placed in metabolic cages, food and water were withheld, and urine was collected for a 4-hour period. The difference in urine volume and sodium excretion between vehicle and furosemide treatments for each mouse was then calculated and compared between groups.

Tissue homogenate preparation

Mice were sacrificed by thoracotomy under isoflurane anesthesia, accompanied by cardiac puncture and exsanguination to allow for blood and tissue collection. Plasma was obtained upon centrifugation of heparinized whole blood, while the other tissues were snap-frozen in liquid nitrogen and stored at -80 °C. One kidney of each mouse was dissected into inner medulla (IM), outer medulla (OM) and cortex, while the other was cut longitudinally for histological analyses and immersion-fixed in 10% neutral buffered formalin then paraffin-embedded. Additional WT mice were used for isolation of nephron segments for EHD4 immunoblotting. The Percoll gradient centrifugation method was used to obtain separate preparations of proximal tubules and distal tubules from a collagenase-digested cortical tubular suspension, following methods described previously with minor modifications (199, 200). Medullary thick ascending limbs (mTALs) were freshly prepared from the inner stripe of the outer medulla by a minor modification of the method described previously (208). Inner medullary collecting ducts (IMCDs) were isolated from the renal inner medulla using a modified version of the protocol described previously (94).

Hypothalamic tissue was collected and processed as described by Nørregaard *et al.* (147) and was analyzed for EHD1 and EHD3 expression levels by Western blotting. Renal tissues were homogenized in kidney extraction buffer (KEB: 50 mM Tris pH 7.4, 0.1 mM EDTA, 0.1 mM EGTA, 10% glycerol, pH 7.4; 200 µl for each IM sample or 10X w/v for OM and cortex) and a cocktail of protease inhibitors (final concentrations: 1 mM phenylmethylsulfonyl fluoride, 2µM Leupeptin [Sigma-Aldrich, St. Louis, MO], 1 µM Pepstatin A [Sigma-Aldrich, St. Louis, MO], a 1:1000 dilution of 0.1% Aprotinin [Sigma-Aldrich, St. Louis, MO], 14.3 mM 2-mercaptoethanol and 10 µl/ml Phosphatase inhibitor cocktail [Sigma-Aldrich, St. Louis, MO]). Supernatant from the homogenates was collected after centrifugation at 10,000 *g* for 5 minutes at 4 °C and protein concentration of each sample was measured using the Bradford method (Bio-Rad protein assay kit, Bio-Rad Laboratories, Hercules, CA). Homogenates were stored at -80 °C until further analyses were carried out.

Quantitative immunoblot analysis

Expression levels of different proteins in the renal tissues were analyzed by resolving extracts on SDS-PAGE, followed by subsequent electric transfer to polyvinylidene difluoride (PVD) membrane (Bio-Rad). The PVD membranes were blocked with Odyssey® Blocking Buffer (LI-COR® Biosciences, Lincoln, NE) for 1 hour and then incubated overnight in an optimized concentration of the respective primary antibody at 4°C. After multiple washes in 10 mM Tris-Buffered Saline and 0.05% Tween-20 (TBST), the membranes were incubated in appropriate fluorophore-conjugated secondary antibodies (1:10000 dilution, Alexa Fluor® conjugates, ThermoFisher Scientific, Rockford, IL) and the membranes were scanned, viewed and analyzed with an Odyssey Infra-red Imaging System. Beta-actin (1:5000 dilution, Sigma-Aldrich, St. Louis, MO) was used as a loading control. The following primary antibodies were used: rabbit anti-EHD1, anti-

EHD2, anti-EHD3 and anti-EHD4 (1:1000 dilution, generated as described previously) (58); rabbit anti-EHD4 (ab-83859, 1:1000 dilution, AbCam, Cambridge, MA); goat anti-AQP2; (sc-9882, 1:2000 dilution, Santa Cruz Biotechnology, Dallas, TX); rabbit anti-NKCC2 (AB-3562P, 1:1000 dilution, EMD Millipore, Cincinnati, OH); rabbit anti-phospho-NKCC1-Thr212/Thr217 (ABS1004, 1:1000 dilution, EMD Millipore Corporation); rabbit anti-αENaC (AB-3530P, 1:500 dilution, EMD Millipore Corporation).

Immunofluorescence staining and histological analyses of kidneys

Paraffin-embedded kidney sections from WT and EHD4-KO mice (n = 3-4 per group; 3-5 images per IM section) were de-paraffinized with xylene and then dehydrated with absolute ethanol. The sections were subjected to rehydration by serial immersion in 90, 80 and 70% ethanol followed by antigen retrieval by heating in citrate buffer for 20 min. After washing in 1X PBS and blocking in 5% FBS in 1X PBS for 1 hour, the sections were incubated with primary antibodies against AQP2 (1:2000 dilution) overnight at 4 °C. Fluorescently-tagged secondary antibodies (1:500 dilution) were added for 1 hour, followed by washing and addition of mounting solution containing 4',6-diamidino-2-phenylindole (DAPI) (VectaShield, Vector Laboratories, Burlingame, CA). The sections were imaged using a confocal microscope (Leica TCS SP8, Leica Microsystems, Buffalo Grove, IL) at 60X magnification. Apical membrane abundance of AQP2 was quantified by measuring the pixel intensities of the channels within a consistent defined region of the apical membrane using the image analysis tool ImageJ (freely downloaded from https://imagej.nih.gov/ij/). The analysis was performed in a blinded manner in 3-5 images of inner medulla in each mouse. In addition, hematoxylin and eosin, Masson's trichrome and Periodic Acid-Schiff-stained kidney sections were viewed by light microscopy and general morphology was evaluated for qualitatively in a blinded manner.

Statistical analyses

Statistical analyses were performed using GraphPad Prism 6 for Windows (GraphPad Software Inc., La Jolla, CA). All data are shown as the mean ± SEM. Results from experiments yielding a single data point per group were analyzed by Student's t-test or one-way ANOVA, or two-factor ANOVA to test for main effects of genotype and sex. Experiments yielding repeated measures were examined by two-way ANOVA for repeated measures. Bonferroni correction was used for post-hoc analysis and a P value < 0.05 was considered statistically significant.

Results

Expression pattern of EHD4 varies across nephron segments

Western blot analysis confirmed expression of EHD4 in freshly isolated mouse glomeruli, proximal and distal tubular cells, IMCDs, mTALs (Fig. 1). The highest expression of EHD4 in nephron segments studied was observed in the IMCD-enriched nephron preparation. Cross-contamination of the other preparations with collecting ducts was checked by blotting for AQP2, with a positive signal present in the distal tubular preparation, IMCD and inner medulla but absent from proximal tubules, mTALs and glomeruli.

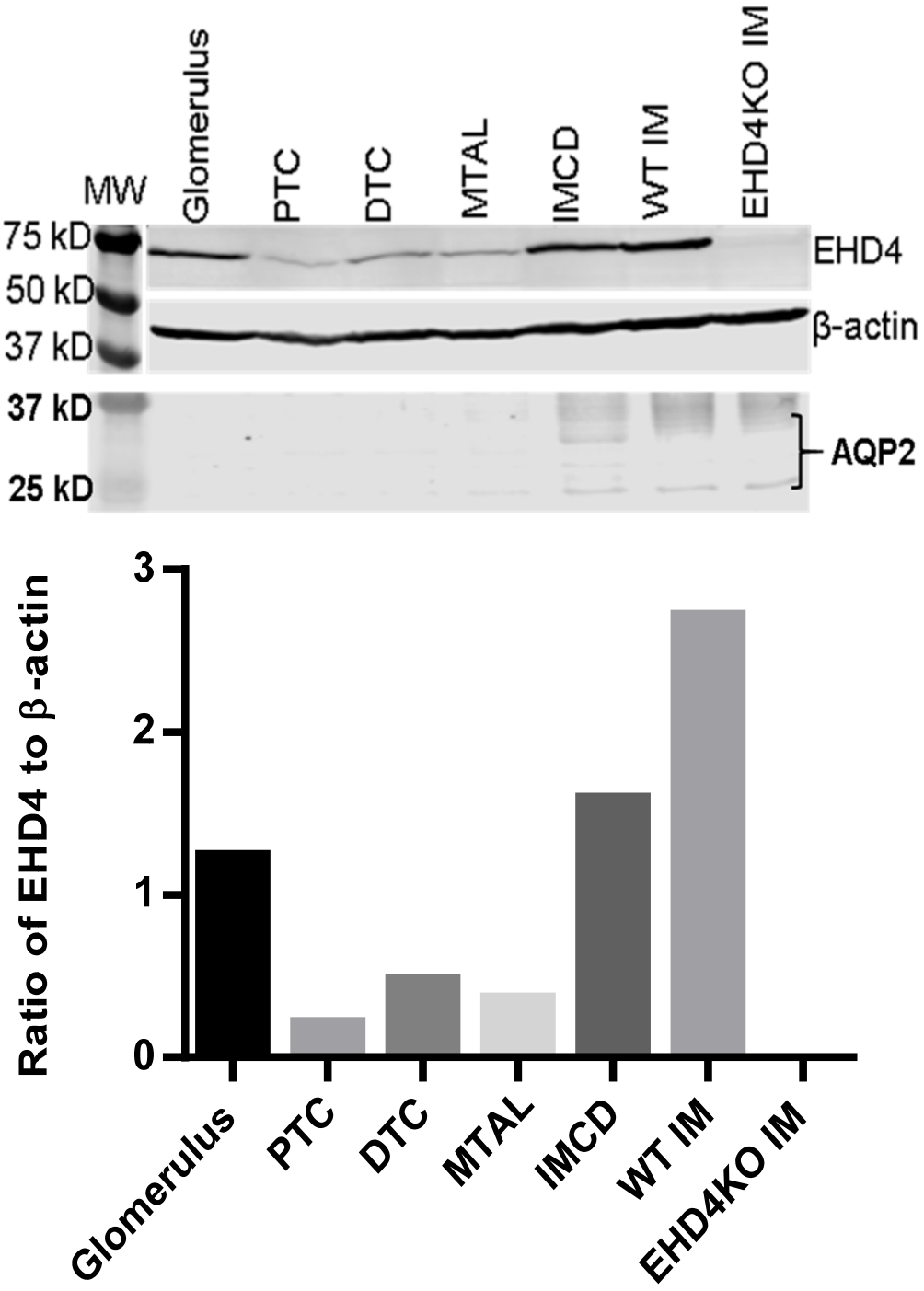

Figure 1: Expression profile of EHD4 across nephron segments. Immunoblot of EHD4 in enriched nephron segments from a C57Bl/6 mice (n = 1). An equal amount of protein was loaded from homogenates of glomeruli, proximal tubular cells (PTC), distal tubular cells (DTCs), mTAL, IMCD, and IM from WT and EHD4-KO mice. Homogenates were tested for cross-contamination by blotting for AQP2.

Deletion of EHD4 had no apparent effect on the kidney morphology in mice

Kidneys of the EHD4-KO mice appeared to develop normally, and although light microscopy showed subtle differences in the amount of cytoplasm between WT and EHD4-KO tubular cells (blinded analyses performed by Dr. Kirk Foster), no significant morphological defect was observed in kidneys of EHD4-KO mice (Fig. 2). Kidney-to-body weight ratio was comparable between WT and EHD4-KO mice (male: 6.1 ± 0.14 for WT vs. 6.2 ± 0.24 mg/g for EHD4-KO mice, $P = 0.77$; female: 5.4 ± 0.17 for WT vs. 5.0 ± 0.25 mg/g for EHD4-KO mice, $P = 0.18$).

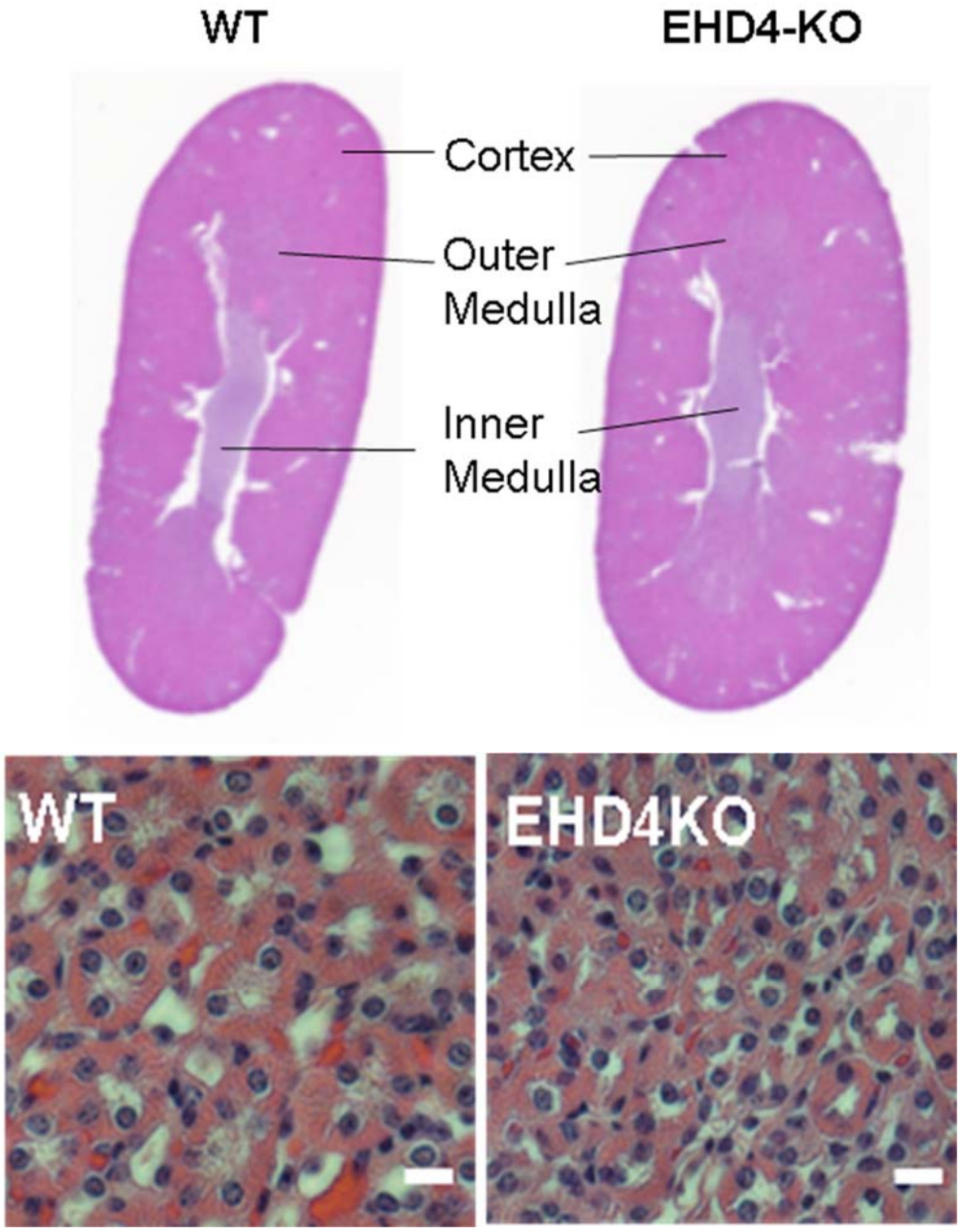

Figure 2: Effect of EHD4 deletion on gross renal morphology. Representative hematoxylin and eosin staining of whole kidney sections and IM of female WT and EHD4-KO mice. Original magnification X40; scale bar = 10 μm.

Absence of compensatory upregulation of other EHD proteins in EHD4-KO mice

EHD proteins have been previously reported to be upregulated during the absence of other EHD proteins (56). Therefore, the expressions of EHD1, EHD2, and EHD3 were next analyzed in the kidney of WT and EHD4-KO mice. There was no significant compensatory increase in the total abundance of EHD1 and EHD3 in kidneys of EHD4-KO mice (Fig. 3A & B). EHD2 expression was too low for accurate quantification.

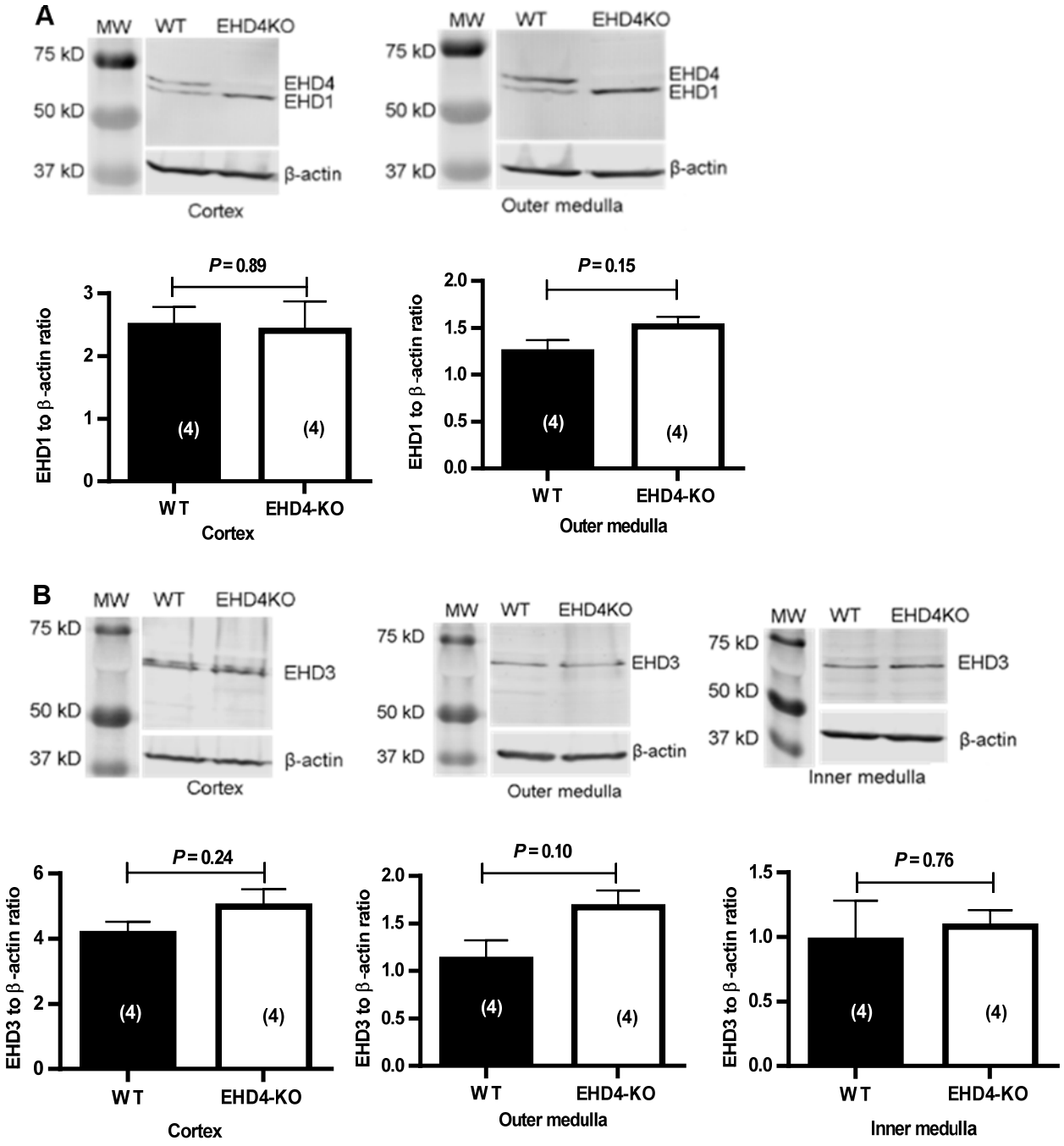

Figure 3: Renal expression of EHD1 and EHD3 in the absence of EHD4. Representative Western blots and densitometric analysis of (A) EHD1 and (B) EHD3 in cortex, outer, and inner medulla of the kidney of WT and EHD4-KO mice. Graphed data are means ± SEM of n (in parentheses). *P* values were determined by unpaired *t* test.

EHD4-KO mice produce higher volumes of dilute urine than WT mice under baseline conditions

The presence of EHD4 in IMCD and mTAL suggested a potential role in both urine formation and concentration. Under 24-hour baseline conditions, water intake was slightly (~20%) but significantly higher in EHD4-KO mice compared to WT mice ($P_{genotype} < 0.05$; Fig. 4A); food intake was not significantly different between WT and EHD4-KO mice (Fig. 4B). Notably, EHD4-KO mice produced significantly higher volumes of urine than WT mice (by ~140-160%; $P_{genotype} < 0.0001$; Fig. 5A). Urine osmolality of EHD4-KO mice was almost 50% lower than that of WT mice ($P_{genotype} < 0.0001$; Fig. 5B). Osmolality of spontaneously voided "spot" urine revealed a similar significant difference ($P_{genotype} < 0.01$; Fig. 5C). Body weights of WT and EHD4-KO mice were comparable (females: 23.0 ± 0.6 g in WT vs 23.4 ± 0.7 g in EHD4-KO, $P = 0.65$; males: 28.5 ± 2.1 g in WT vs 28.3 ± 1.6 g in EHD4-KO, $P = 0.88$). Plasma creatinine levels were not significantly different between WT and EHD4-KO mice (males: 0.21 ± 0.04 for WT vs. 0.20 ± 0.04 mg/dL for EHD4-KO mice, $P = 0.67$; female: 0.26 ± 0.02 for WT vs. 0.25 ± 0.03 mg/dL for EHD4-KO mice, $P = 0.95$). Plasma osmolality was measured in these and in additional mice from which tissues were collected for analyses described below. Plasma osmolality was not significantly different between WT and EHD4-KO mice ($P_{genotype} = 0.6$), or male and female mice ($P_{sex} = 0.2$), nor were there sex differences in the impact of EHD4-KO ($P_{interaction} = 0.7$; males: 326 ± 4 mOsmol/kg H_2O for n = 13 WT vs. 331 ± 8 mOsmol/kg H_2O for n = 10 EHD4-KO mice; female: 321 ± 5 mOsmol/kg H_2O for WT vs. 321 ± 2 mOsmol/kg H_2O for EHD4-KO mice, n = 8 in both groups). There was no sex differences in the effects of EHD4 gene deletion on the above parameters ($P_{interaction} > 0.05$ in all cases). Accordingly, the biochemical and histological analyses described below were performed on either male or female mice to conserve tissue.

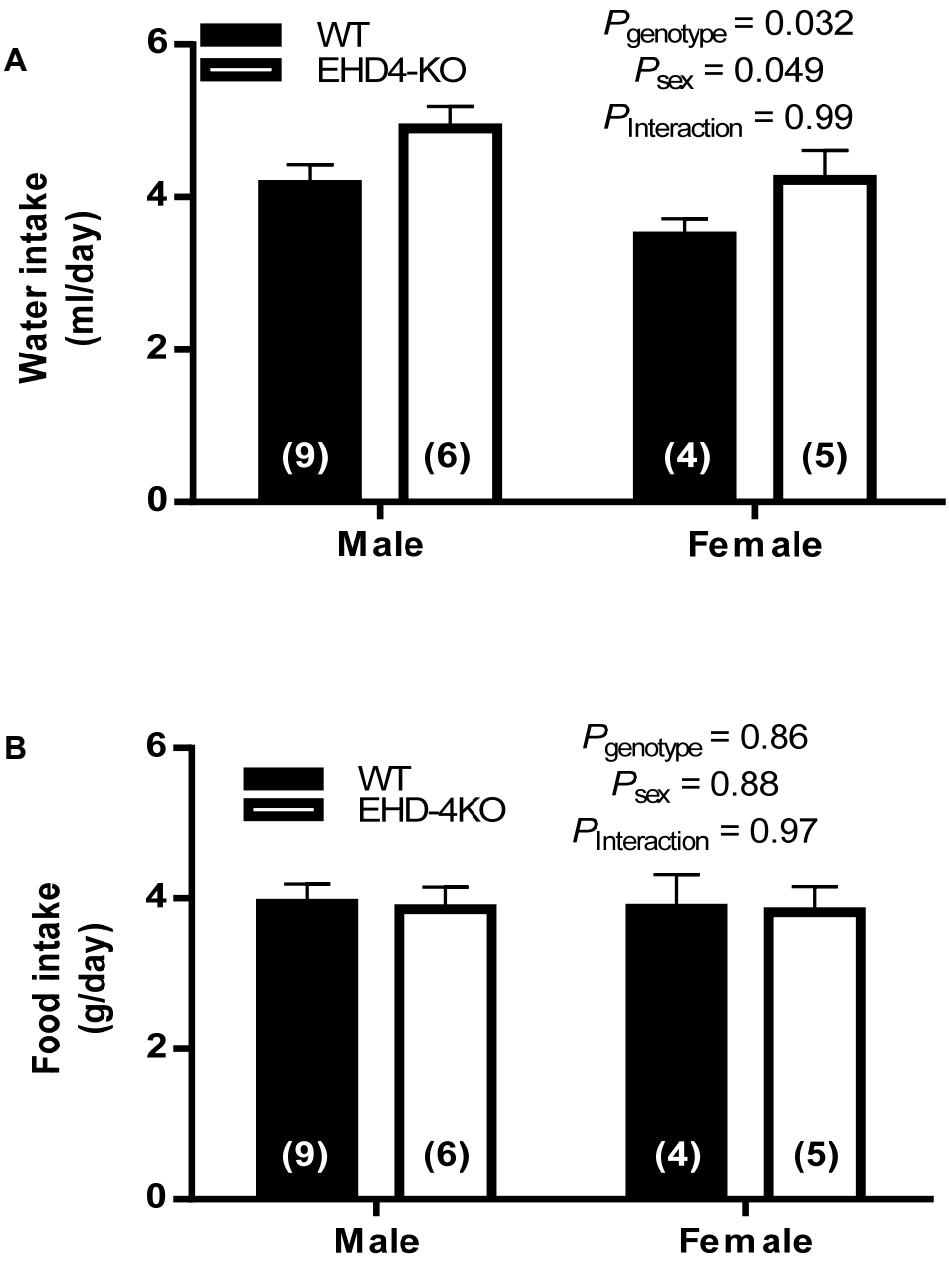

Figure 4: Effect of EHD4 deletion on general metabolic parameters in mice. Data presented are 24 h water intake (A) and food intake (B) of male and female EHD4-KO mice. All values are means ± SEM of n mice (in parentheses). Data were analyzed by 2-factor ANOVA, testing for main effects of genotypes ($P_{genotype}$), sex (P_{sex}), and the interaction between sex and genotype ($P_{interaction}$). * $P < 0.05$ for EHD4-KO vs. WT mice of each sex, by post hoc test.

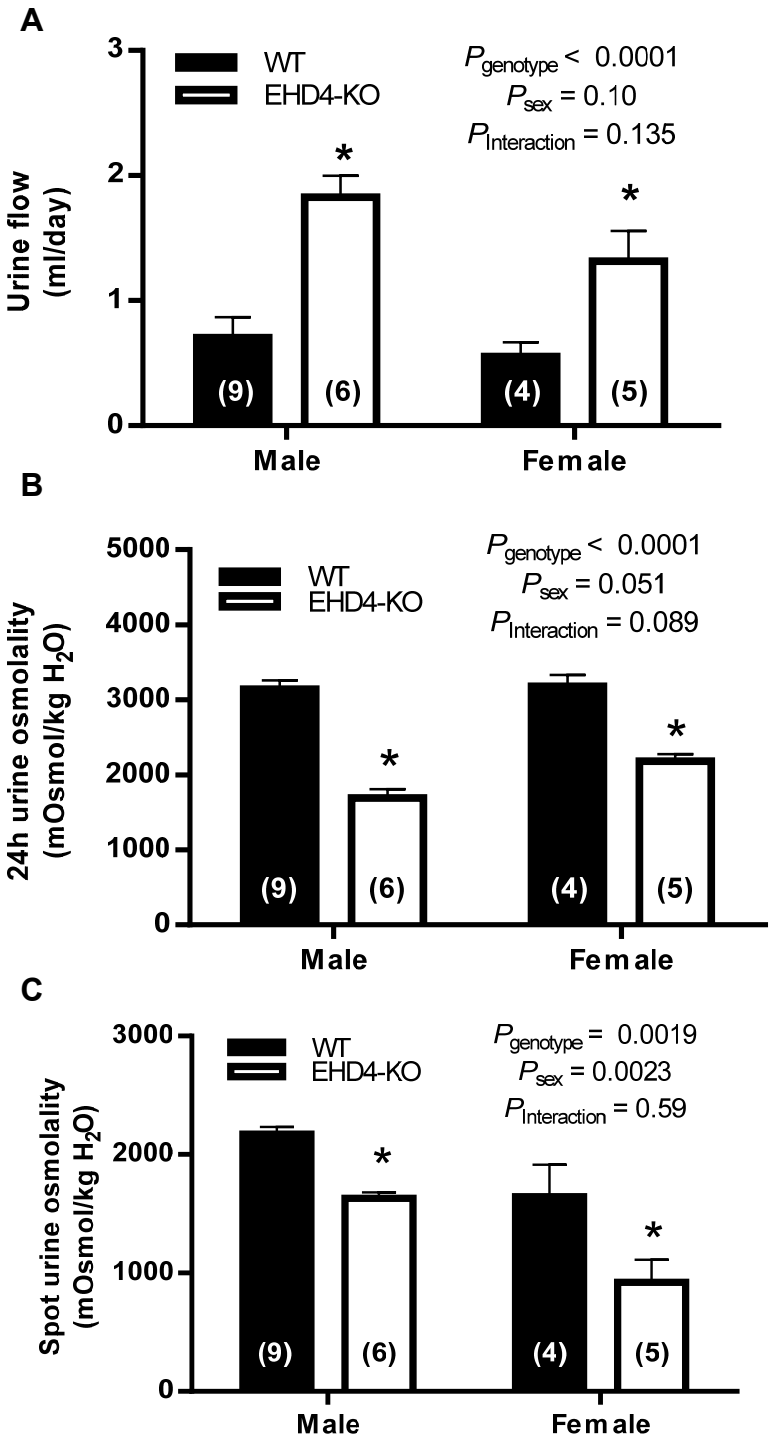

Figure 5: Effect of EHD4 deletion on urine formation and composition in mice. Data presented are 24 h urine flow (A) and urine osmolality (B) of male and female EHD4-KO mice. Spot urine osmolality is shown in (C). All values are means ± SEM of n mice (in parentheses). Data were analyzed by 2-factor ANOVA, testing for main effects of genotypes ($P_{genotype}$), sex (P_{sex}), and the interaction between sex and genotype ($P_{interaction}$). * $P < 0.05$ for EHD4-KO vs. WT mice of each sex, by post hoc test.

EHD4-KO mice show an exaggerated diuretic response to an acute water load

To further test the role of EHD4 in renal water handling independent of voluntary water intake, the mice were subjected to an acute water load by I.P. injection. Cumulative urine excretion showed that the EHD4-KO mice displayed an exaggerated response to water loading compared to WT mice ($P_{interaction} < 0.05$ for both sexes; Fig. 6), and both male and female EHD4-KO mice had excreted almost 75% of the water load by the end of 6 hours whereas WT mice excreted less than 50% (Fig. 6A and B).

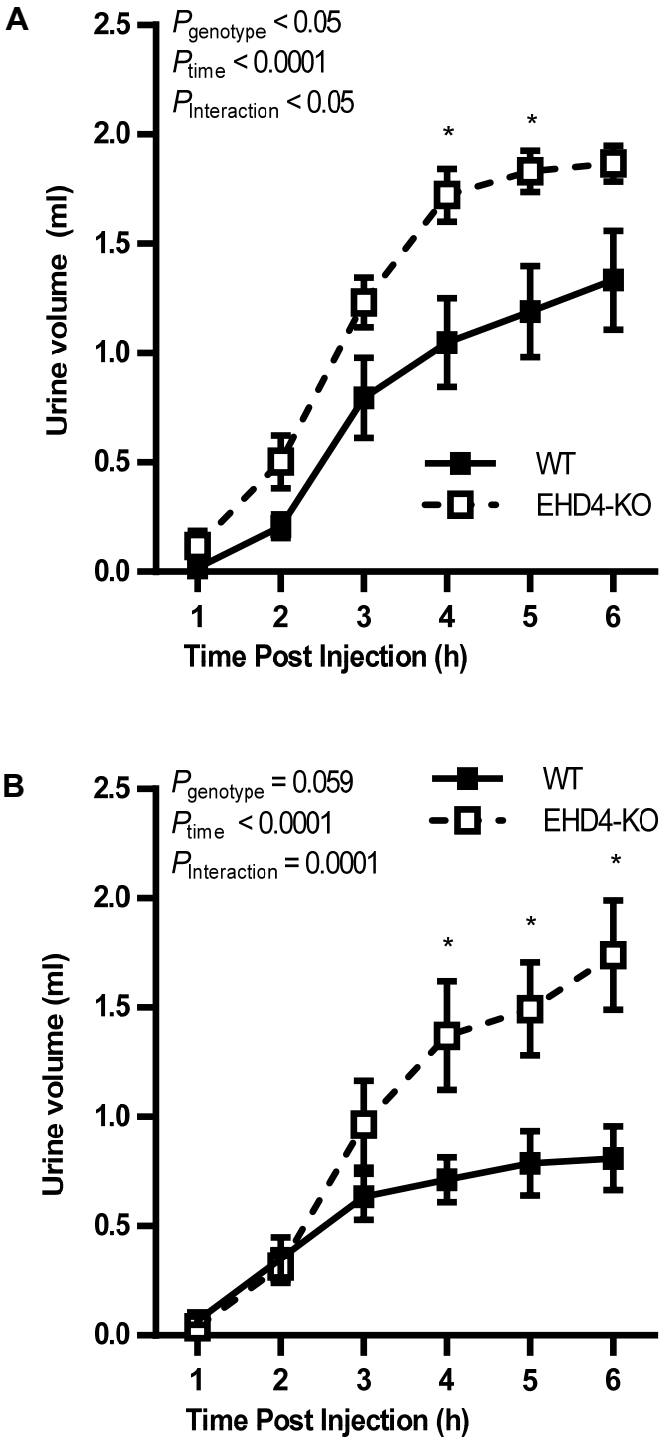

Figure 6: Response of EHD4-KO mice to an acute water load as compared to WT mice. Cumulative urine volume of male (A) and female (B) WT and EHD4-KO mice over 6 h after injection of 2 mL sterile water i.p. Data were compared by 2-factor repeated-measures ANOVA, testing for main effects of genotype ($P_{genotype}$), time (P_{time}), and the interaction between time and genotype ($P_{interaction}$). * $P < 0.05$ for EHD4-KO vs. WT mice at the corresponding time-points.

Responses to 24-h water restriction are similar between WT and EHD4-KO mice

To assess the contribution of EHD4 to the urine-concentrating mechanism, WT and EHD4-KO mice were subjected to 24-h water restriction. After 24-h water restriction, male WT and EHD4-KO mice showed a similar decline in urine flow and increases in urine osmolality ($P_{interaction} > 0.05$ in both cases; Fig. 7A and 7B). However, EHD4-KO mice maintained significantly higher urine flow and lower urine osmolality compared to WT mice even after water restriction ($P_{genotype} < 0.05$ in each case; Fig. 7).

Although the total abundance of AQP2 did not increase in WT or EHD4-KO after 24-h water restriction (Western blot; data not shown), the apical intensity of AQP2 increased significantly in both the groups (Fig. 8). However, the apical intensity of AQP2 in EHD4-KO mice was significantly lower than that in WT mice under baseline conditions (Fig. 8).

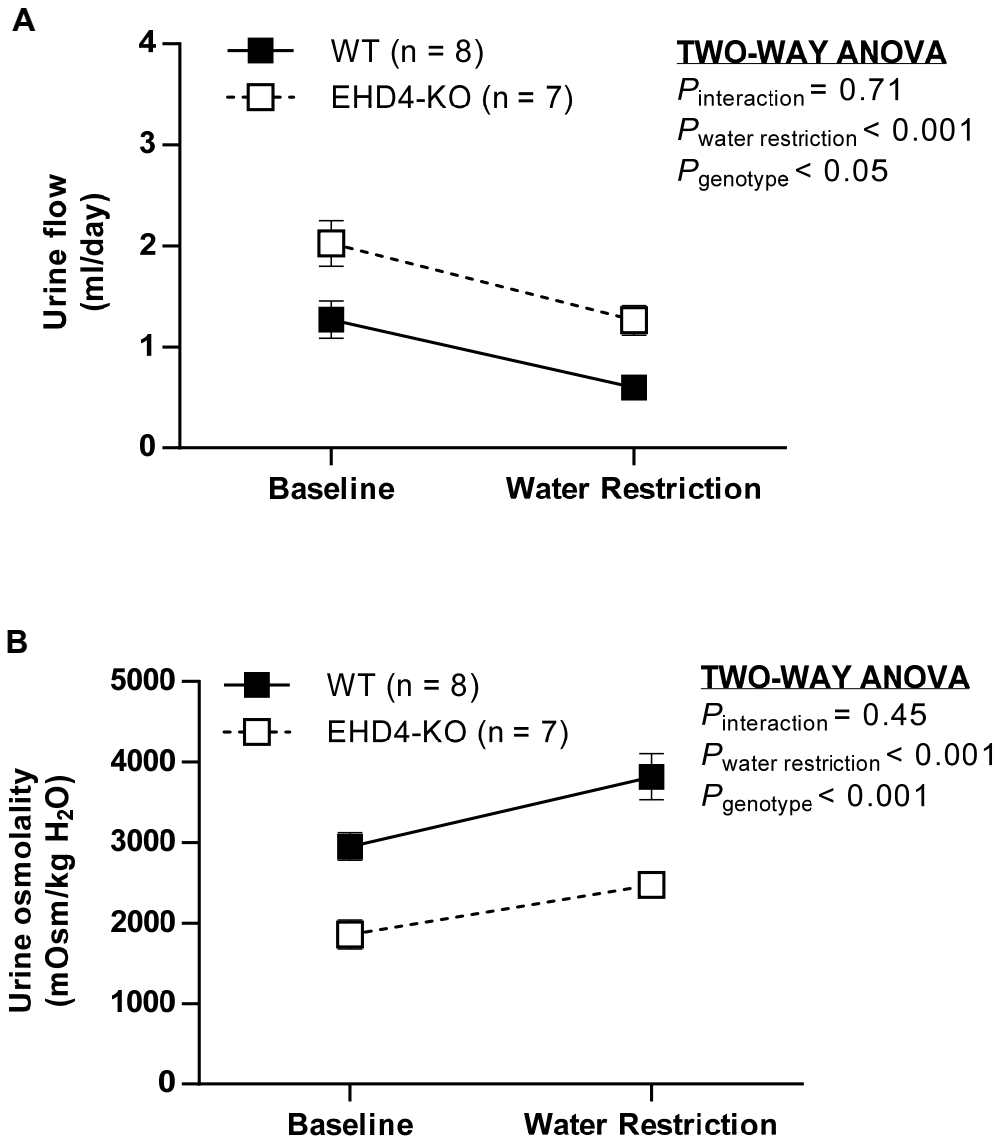

Figure 7: Response of EHD4-KO mice to 24 h water restriction as compared to WT mice. Urine flow (A) and osmolality (B) of male WT and EHD4-KO mice before and after 24 h water restriction. Data were compared by 2-factor repeated-measures ANOVA, testing for main effects of genotype ($P_{genotype}$), water restriction ($P_{water\ restriction}$), and the interaction between water restriction and genotype ($P_{interaction}$). Graphed data are means ± SEM of n mice (in parentheses). *P < 0.05 for EHD4-KO vs. WT mice at the corresponding time points.

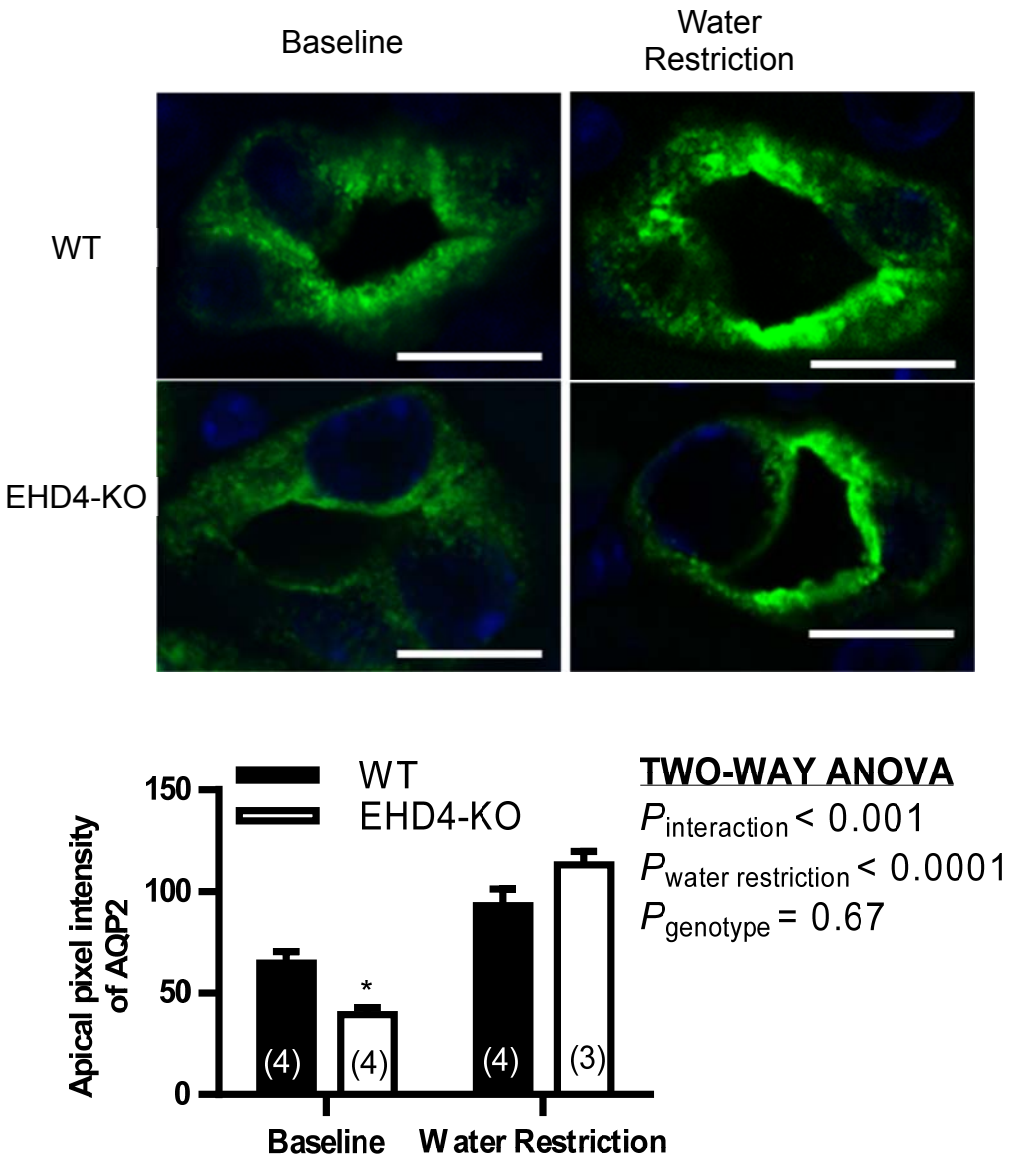

Figure 8: Changes in cellular localization of AQP2 in EHD4-KO mice before and after 24 h water restriction as compared to WT mice. Representative immunofluorescent images and blinded quantification of the pixel intensity of AQP2 in the apical membrane of principal cells in the IM of male WT and EHD4-KO mice before and after 24 h water restriction. Scale bars, 10 μm. Data were compared by 2-factor repeated-measures ANOVA, testing for main effects of genotype ($P_{genotype}$), water restriction ($P_{water\ restriction}$), and the interaction between water restriction and genotype ($P_{interaction}$). Graphed data are means ± SEM of n mice (in parentheses). *P < 0.05 for EHD4-KO vs. WT mice at the corresponding time points.

Anti-diuretic responses during 24-h water restriction are independent of EHD proteins

To determine whether there was a compensatory increase in other EHDs during water restriction in EHD4-KO mice, female EHD4-KO mice were subjected to either EU conditions or water-restricted conditions for 24 hours (Fig. 9). Immunoblots of EHD1, EHD2 and EHD3 in renal cortex, OM and IM showed similar expression of these proteins in both EU and WR EHD4-KO mice (Fig. 10 A-C).

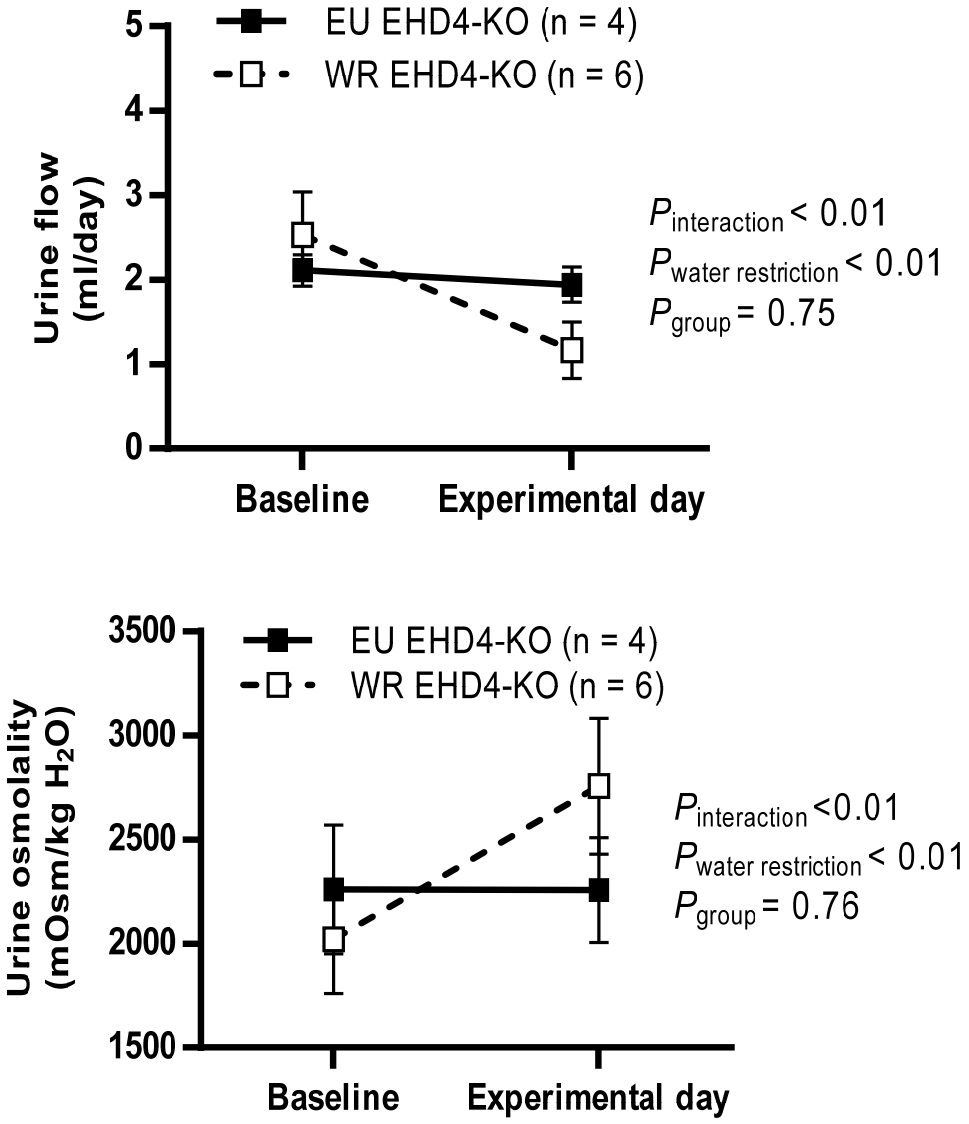

Figure 9: Comparison of antidiuretic responses of EU and WR female EHD4-KO mice. Antidiuretic responses to 24 h water restriction were evaluated in terms of changes in urine flow and osmolality. All mice received access to water on the baseline day, whereas only EU (n = 4), not WR (n = 6), EHD4-KO mice received water on experimental day. Data were compared by 2-factor repeated-measures ANOVA, testing for main effects of experimental group (P_{group}), water restriction ($P_{water\ restriction}$), and the interaction between water restriction and group ($P_{interaction}$). Graphed data are means ± SEM of n mice (in parentheses).

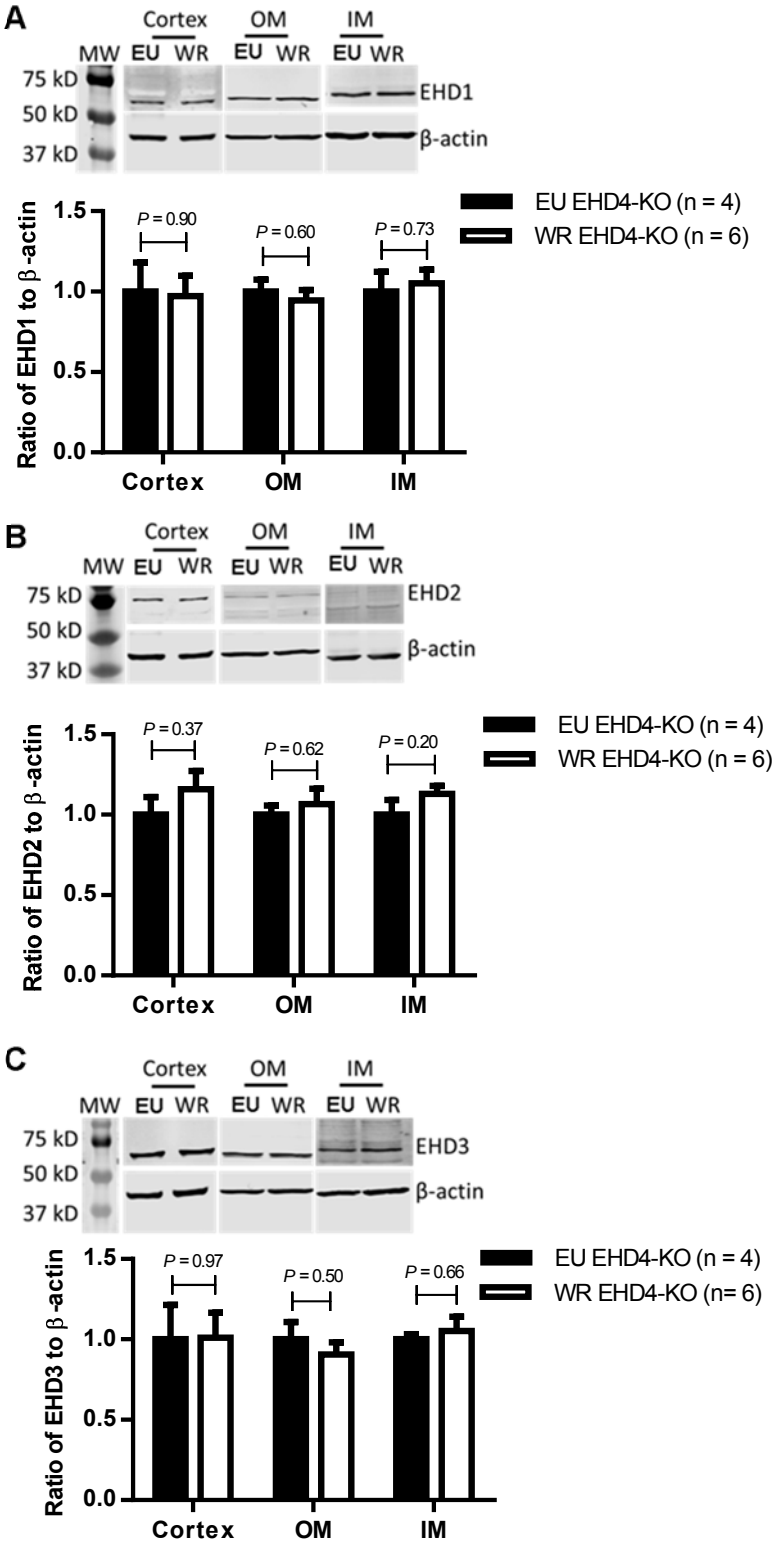

Figure 10: Comparison of expressions of EHD1, 2, and 3 in EU and WR female EHD4-KO mice. Representative Western blots and densitometric analysis of (A) EHD1, (B) EHD2, and (C) EHD3 in the renal cortex, OM, and IM tissues of EU and WR EHD4-KO mice collected at the end of the experimental day. All mice received access to water on the baseline day, whereas only EU (n = 4), not WR (n = 6), EHD4-KO mice received water on experimental day. Please note that renal cortex, OM, and IM tissues were blotted separately, and data for each region were normalized to the mean for EHD group. The mean densitometric data for each region is shown on a single graph for ease of presentative but comparisons of relative expression between different regions of the kidney cannot be made from these data. All data are means ± SEM of n mice (in parentheses). *P* values were determined by unpaired *t* test.

Hypothalamic expression of EHDs

To begin to address whether the polyuric phenotype observed in the EHD4-KO mice could also involve a central component, since the EHD4-KO mouse used is a global knockout, hypothalamic tissue were blotted for EHDs. EHD4 was found to be expressed in the hypothalamus (Fig. 11A), as was EHD1, whose expression was significantly upregulated in EHD4-KO mice (Fig. 11B). EHD3 was also expressed in the hypothalamus but no difference in expression was observed between WT and EHD4-KO mice (Fig. 11C). Baseline plasma osmolality of EHD4-KO and WT mice was found to be comparable (Fig. 12A). Despite EHD4-KO mice having increased urine volumes, their 24 hour urinary AVP excretion, an indirect index of circulating AVP, was comparable to that of WT mice (Fig. 12B).

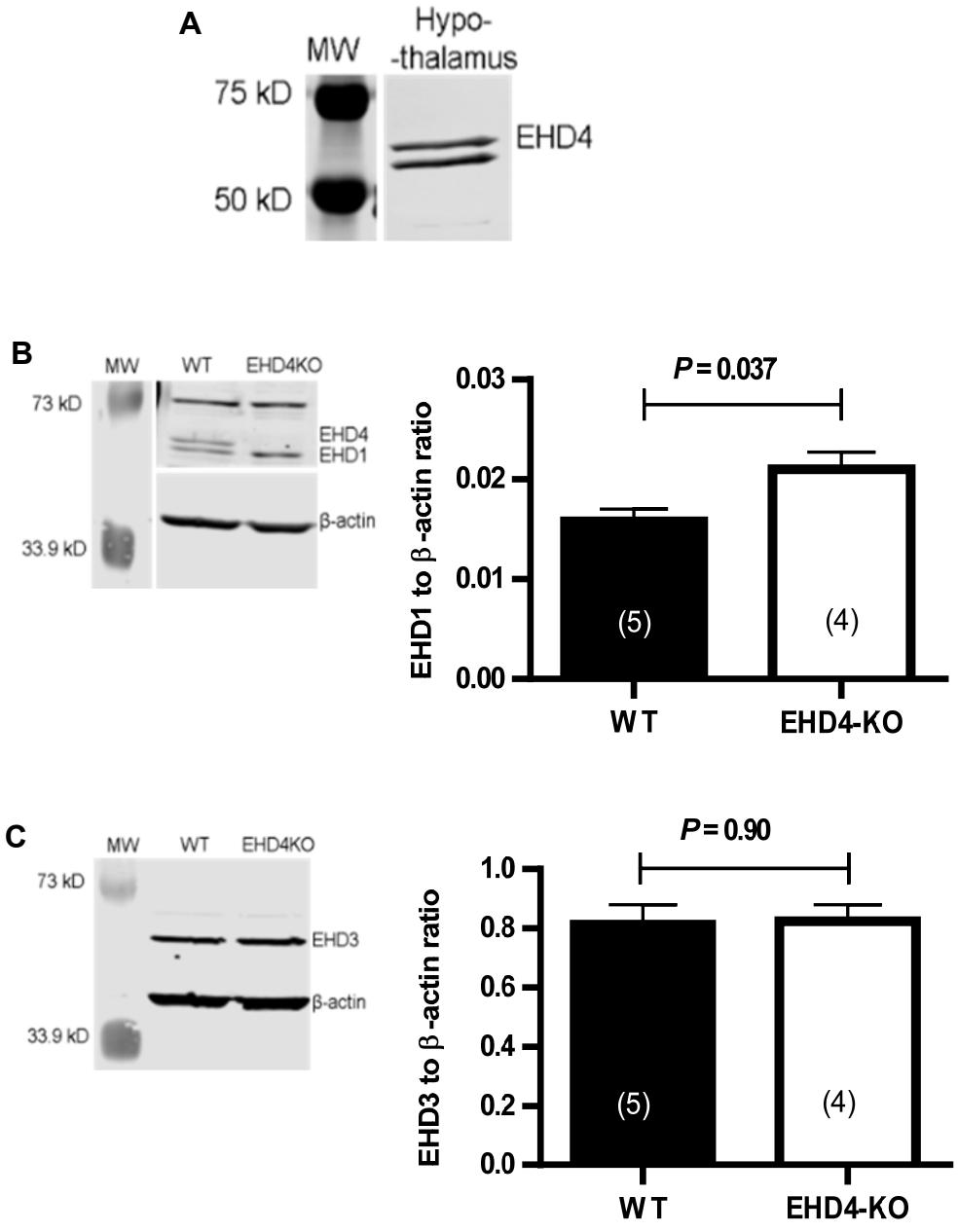

Figure 11: EHDs are expressed in the hypothalamus. Western blot analysis of hypothalamic expression of EHD4 (A) in a WT mouse and EHD1 (B) and EHD3 (C) in WT and EHD4-KO mice. Data were compared by unpaired *t* test and are means ± SEM of n mice (in parentheses).

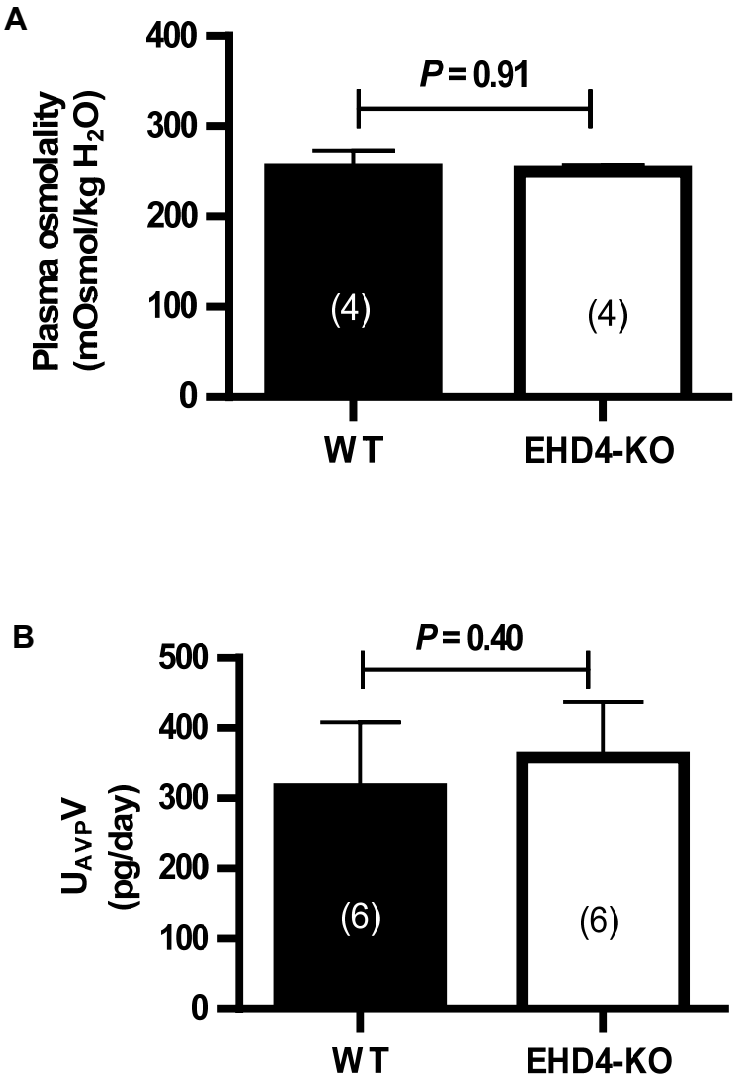

Figure 12: EHD4 deletion does not affect plasma osmolality or urinary AVP. (A) Plasma osmolality of female WT and EHD4-KO mice. (B) Urinary AVP excretion rate in male WT and EHD4-KO mice. Data were compared by unpaired *t* test and are means ± SEM of n mice (in parentheses).

EHD4-KO and WT mice have similar urinary sodium excretion and exhibit comparable responses to furosemide

Renal sodium handling plays an important role in the urine-concentrating mechanism. Therefore, the effect of EHD4 deletion on the urinary sodium excretion was tested. There was no significant difference in urinary sodium excretion between the two genotypes under basal conditions (Fig. 13).

Sodium ion concentration is an important determinant of extracellular fluid osmolarity. Epithelial sodium channel (ENaC), which is abundantly expressed in the collecting duct, finely regulates sodium reabsorption. To test if the activity of this channel is regulated by EHD4, amiloride was administered (a blocker of ENaC) in WT and EHD4-KO mice. Amiloride failed to generate any natriuretic response in both WT and EHD4-KO mice (Fig. 14A). No significant difference in expression of the alpha subunit of the ENaC (αENaC) was seen between groups (Fig. 14B).

The Na-K-2Cl cotransporter 2 (NKCC2), which is expressed by the mTAL plays a key role in establishing and maintaining the urinary concentrating mechanism. To test if the activity of this cotransporter is regulated by EHD4, WT and EHD4 KO mice were challenged with furosemide to block NKCC2. Responses are expressed as the differences in sodium excretion and urine production between acute vehicle and furosemide treatments. The natriuretic and diuretic responses after furosemide injection were comparable between the genotypes (Fig. 15A and 15B). Consistent with this finding, total and phosphorylated NKCC2 protein expression levels in renal outer medulla were similar between the two genotypes (Fig. 15C).

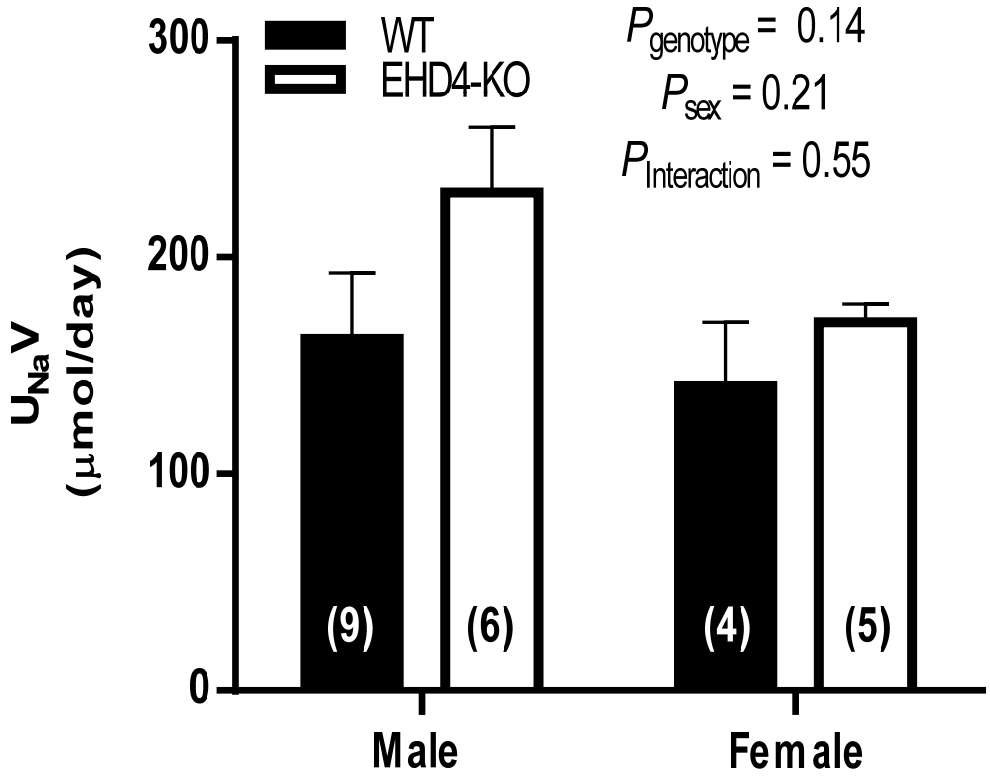

Figure 13: Effect of EHD4 deletion on sodium excretion. Data presented for 24 h urinary sodium excretion ($U_{Na}V$) of WT and EHD4-KO mice. All values are means ± SEM of n mice (in parentheses). Data were analyzed by 2-factor ANOVA, testing for main effects of genotypes ($P_{genotype}$), sex (P_{sex}), and the interaction between sex and genotype ($P_{interaction}$).

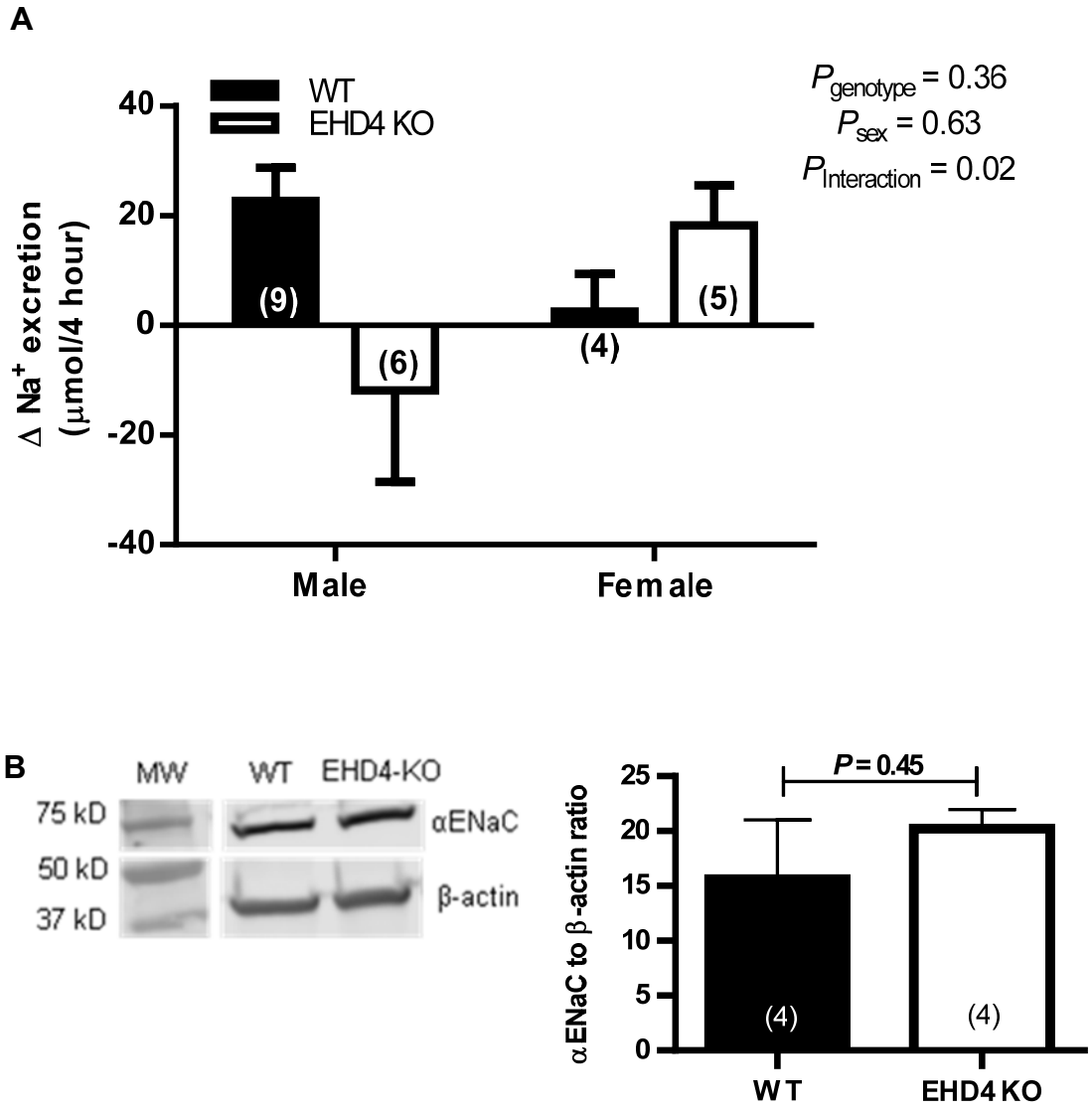

Figure 14: Effect of EHD4 deletion on ENaC activity in vivo. Changes in (Δ) urinary sodium excretion (A), calculated as the difference between values recorded in response to amiloride and vehicle. Data were analyzed by 2-factor ANOVA, testing for main effects of genotypes ($P_{genotype}$), sex (P_{sex}), and the interaction between sex and genotype ($P_{interaction}$). (B) Representative immunoblot and quantification of αENaC in cortex of female WT and EHD4-KO mice. Data are presented as means ± SEM of n mice (in parentheses) and were analyzed by unpaired *t* test.

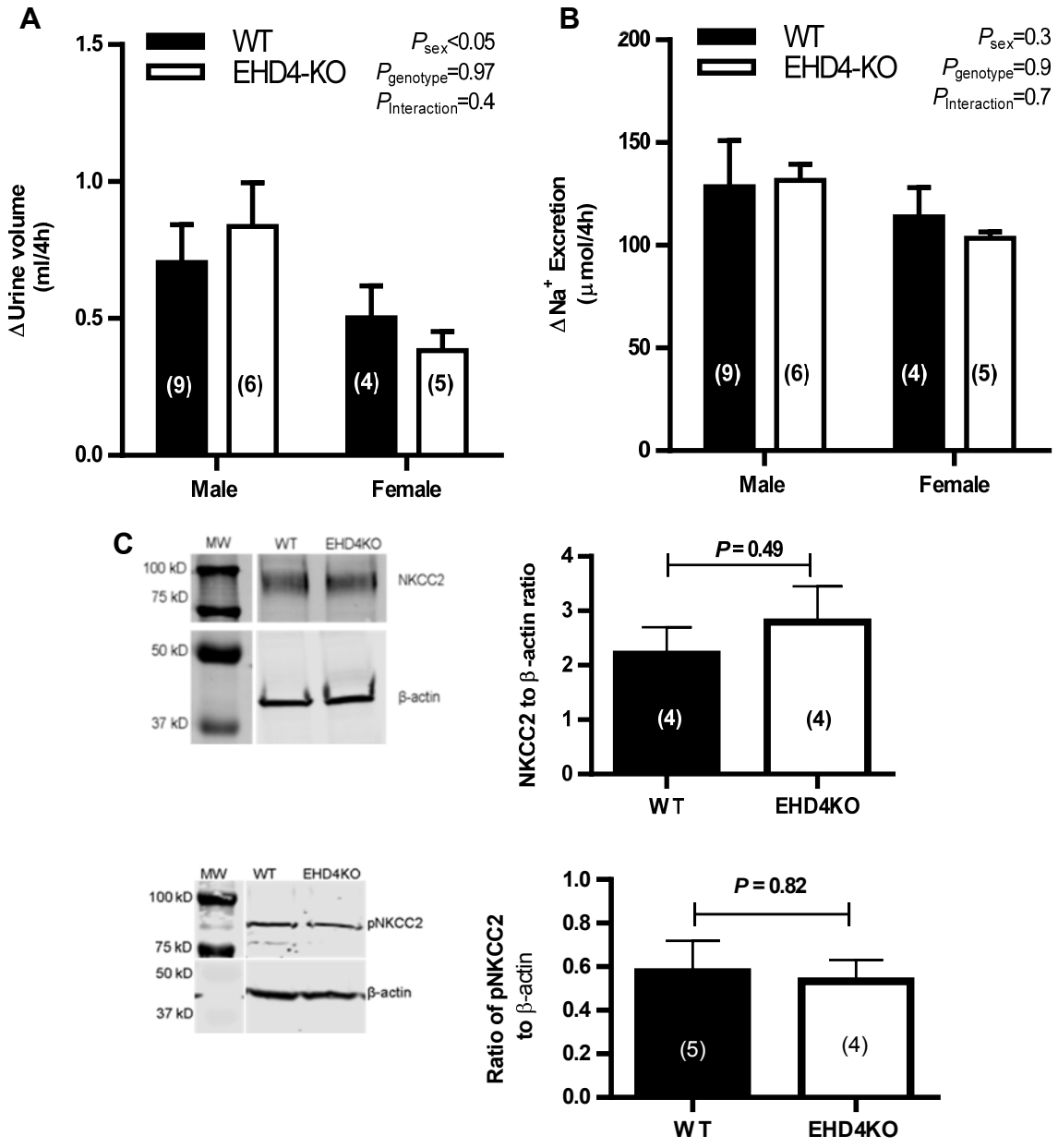

Figure 15: Effect of EHD4 deletion on NKCC2 activity in vivo. Changes in (Δ) urine volume (A) and urinary sodium excretion (B), calculated as the difference between values recorded in response to furosemide and vehicle. Data were analyzed by 2-factor ANOVA, testing for main effects of genotypes ($P_{genotype}$), sex (P_{sex}), and the interaction between sex and genotype ($P_{interaction}$). (C) Representative immunoblot and quantification of NKCC2 and pNKCC2 in OM of female WT and EHD4-KO mice. Data are presented as means ± SEM of n mice (in parentheses) and were analyzed by unpaired *t* test.

Discussion

This chapter focused on elucidating the physiological roles of EHD4 in the kidney, particularly in the regulation of urine formation and composition. These findings show that in the kidney, EHD4 is expressed differentially across the nephron, and that global deletion of EHD4 in mice results in a phenotype of mild, apparently nephrogenic, diabetes insipidus, with EHD4-KO mice showing increased excretion of osmotically dilute urine.

To better understand the functional roles of EHD4 in the kidney it was determined whether EHD4 protein was expressed in segments of the nephron important in urinary concentration and salt and water homeostasis. George *et al.* (58) had shown previously that EHD4 is expressed in the kidney, based on the analysis of whole kidney lysates, with immunofluorescence staining indicating expression by glomerular endothelial cells and peritubular capillaries (56). Moreover, the proteome databases constructed by the NIH ESBL reported EHD1-4 expression in the IMCD and EHD1 in the proximal convoluted tubule at the protein level as determined by mass spectrometry (104). Unfortunately, I have been unable to successfully immunostain the kidney sections using the currently available batches of rabbit polyclonal EHD4 antibodies, whether obtained from Abcam or custom-generated by a vendor as described previously (58). I observed via Western blot that EHD4 was expressed highly in the glomerulus and IMCD, with some expression in the distal tubular cells, mTAL and proximal tubular cells. Additionally, single tubule RNA sequencing data generated by Lee *et. al.* showed that EHD4 mRNA was highest in thin ascending limb (104); however, it was beyond our technical capabilities to isolate the thin ascending limbs to confirm protein expression by Western blot. The presence of EHD4 in IMCD and mTAL raised the question of whether this protein might play a role in the urinary concentrating mechanism. Consistent with this hypothesis, EHD4-KO mice were found to produce an increased volume of osmotically dilute urine compared to WT mice under

baseline conditions. This phenotype is suggestive of a defect in water reabsorption and potentially a defect in urine concentrating ability in the absence of EHD4. Although EHD4 is abundantly expressed in the glomerulus, there was no significant difference in plasma creatinine level between WT and EHD4-KO mice, suggesting that EHD4 probably does not regulate urine formation and composition by modulating GFR. However, plasma creatinine is not a very precise indicator of GFR, and therefore, the role of EHD4 in modulating the GFR would require further analyses.

Further supporting our hypothesis that EHD4-KO mice display altered renal water handling, EHD4-KO mice excreted higher volumes of urine than WT mice when administered with an acute intraperitoneal water load. That the response was larger in EHD4-KO mice compared to WT mice confirms that water handling by the kidney is regulated in part by EHD4. Plasma osmolality of EHD4-KO mice was similar to that of WT mice, suggesting that even though they have increased excretion of dilute urine, EHD4-KO mice are able to maintain osmotic homeostasis under normal conditions. EHD4-KO mice consumed slightly but significantly elevated amounts of water compared to the WT mice. While comparison of raw volumes of water intake and urine output collected using metabolic cages is complicated by an unavoidable degree of urine evaporation during the funneling and collection process, the percentage increase in water intake (~20%) was much smaller than the increase in urine flow measured by metabolic cage collections (~140-160%). This finding can be interpreted to argue against primary polydipsia being a likely cause of the phenotype observed in EHD4-KO mice, although extensive additional experiments would be needed to rule this out definitively. This disparity in the apparent increase in water intake compared to urine output also suggests that mechanisms in addition to thirst may help to offset excess renal loss of water, possibly including enhanced gastrointestinal water absorption or reduced insensible water loss.

Excretion of small volumes of concentrated urine is a classic anti-diuretic response to water restriction, and EHD4-KO mice show a similar anti-diuretic response in terms of urine volume and urine osmolality as the WT mice. Moreover, expression of no other EHD protein was increased when EHD4-KO were water-restricted. Together, these data suggest that the renal response to water restriction occurs independently of EHD4. However, even after water restriction, EHD4-KO mice still displayed lower urinary osmolality and higher urine flow compared with WT mice, indicating that EHD4 is required to achieve maximal urine concentrating ability. Retention of the anti-diuretic response to water restriction suggests that other regulators of AVP-dependent water transport are still operational in EHD4-KO mice; whether this might be in part due to a functional role of the remaining EHD proteins (EHD1 and EHD3) expressed by the collecting duct is an intriguing prospect that could be addressed in future studies by collecting duct specific knockout of combinations of EHD proteins.

As EHD4 was found to be expressed in the mTAL, its role in the regulation of the activity of NKCC2, an important cotransporter involved in setting up the osmotic gradient for urine concentration, was tested. The data, however, shows that EHD4 deletion does not affect the activity of NKCC2, as suggested by the comparable diuretic and natriuretic responses to furosemide in EHD4-KO and WT mice. Further, if EHD4 had a major role in NKCC2-trafficking, evidence of salt-wasting in EHD4-KO mice is to be expected. Although the metabolic cage data gives the appearance of a slight trend towards increased urinary sodium excretion in male EHD4-KO mice, 2 of the 9 WT mice had relatively lower sodium excretion than the rest of the group, which had similar levels of sodium excretion to the EHD4-KO mice. I did not observe any compensatory upregulation of ENaC alpha subunit expression in EHD4-KO mice, although changes in activity of ENaC or other distal sodium transporters masking the effects of the loss of EHD4 on NKCC2 cannot be ruled out.

Unfortunately, the approach to understand the role of EHD4 in regulating ENaC using amiloride was unsuccessful, possibly due to insufficient dosage and the results from this study remains inconclusive. Which and how many proteins in the kidney interact directly or indirectly with EHD4 is currently unknown.

While these results clearly support a nephrogenic origin of diabetes insipidus seen in EHD4-KO mice, other possible explanations for their diuretic phenotype could include primary polydipsia (as discussed above), or defective AVP secretion from the hypothalamus, along with a faulty AVP-induced signaling cascade in the principal cells of the collecting duct. However, 24-hour urinary AVP excretion, which allowed me to indirectly assess circulating AVP (69), was comparable between WT and EHD4-KO mice, thereby suggesting that the defect in water reabsorption is not due to low circulating AVP. Direct measurement of circulating AVP would be ideal, however this is challenging to do in mice due to the potential confounding influences of stress, anesthesia and hypovolemia-induced AVP secretion. Although urinary excretion of AVP represents an indirect index of circulating AVP, it has been shown by others that water-loading reduces urinary AVP excretion (53), supporting that this represents an indirect but physiologically-viable measurement. Both EHD4 and EHD1 are expressed in the hypothalamus, with an increase in EHD1 expression in the hypothalamus of EHD4-KO mice, suggesting that upregulation of EHD1 might compensate for the absence of EHD4. This suggests that in EHD4-KO animals, AVP synthesis or secretion may not be defective but that EHD4-KO mice develop a polyuric phenotype despite similar circulating AVP. This in turn could suggest a faulty renal response to AVP in EHD4-KO mice. I tried unsuccessfully to immunostain kidney sections for the V2 receptor due to technical difficulties with the commercial antibody, and so an effect on V2 receptor localization cannot be ruled out. EHD4-KO mice were also able to concentrate their urine in response to water restriction,

suggesting that the AVP-V2R-AQP2 axis possibly remains intact in EHD4-KO mice. Additionally, the apical membrane accumulation of AQP2 increased to a similar level in WT and EHD4-KO post-24-h water restriction. This indicates that the forward trafficking of AQP2 to the apical membrane during water restriction is functional in EHD4-KO mice, and further suggests that a major defect at the level V2 receptor is unlikely to underlie the phenotype observed in the EHD4-KO mice.

The sum total of the data so far suggest that the apical accumulation of AQP2 in the EHD4-KO mice were significantly lower than in WT mice under baseline conditions. This indicates a possible role of EHD4 in the trafficking of AQP2 under baseline conditions. **The current working hypothesis is, therefore, that EHD4 plays a role in regulating apical trafficking of AQP2 in the collecting duct under baseline conditions.**

CHAPTER II: ROLE OF EHD4 IN THE REGULATION OF AQP2 TRAFFICKING IN PRINCIPAL CELLS OF THE COLLECTING DUCT [4]

[4] Parts of the material presented in this chapter was previously published: **Rahman, S.S**., Moffitt, A. E. J., Trease, A., Foster, F. W., Storck, M., Band, H., Boesen, E. I. EHD4 is a novel regulator of urinary water homeostasis. FASEB J. (2017)

Introduction

The water permeability of the collecting duct is finely regulated by the presence or absence of AQP2 in the principal cells. Endocytic recycling plays an important role in the regulation of the presence of AQP2 in the apical membrane (18). Endocytic recycling of AQP2, as like other membrane proteins, starts with the entry of AQP2 into the early endosome (188). The transition of AQP2 from the early endosome to the other endosomal compartments depends on the state of the cell. In unstimulated cells, mere inhibition of endocytosis has been shown to result in an accumulation of AQP2 in the plasma membrane (112), indicating that the recycling process of AQP2 is very dynamic and can occur constitutively. In the presence of factors such as AVP and PGE2, the rate of insertion of AQP2-containing vesicles can be significantly regulated. AVP increases the phosphorylation of residues of AQP2 that favors its exocytosis (113, 123, 138, 144), whereas PGE2 may retard the exocytosis of AQP2 (148). In addition to these exogenous factors, the recycling of AQP2 depends on the presence of several different types of cellular proteins (18). AQP2-containing vesicles have been found to contain proteins that regulate endocytic recycling (5). One such protein, called Rab11-Fip2, has been shown to be important in the forward trafficking of AQP2 (137). Rab11-Fip2 is known to interact with EHD proteins (136) and is important in the trafficking proteins from the recycling endosome to the plasma membrane (30). Although separate previous studies have established common interacting partners between AQP2 and EHD proteins, to our knowledge no studies have been performed to delineate the direct role of EHD proteins in the regulation of AQP2 trafficking.

Experiments in the previous chapter demonstrated a reduced accumulation of AQP2 in the apical membrane of principal cells of EHD4-KO mice under baseline conditions, suggesting a role of EHD4 in the regulation of AQP2 trafficking. The membrane

abundance of AQP2 in EHD4-KO mice was increased during the water-restricted period, which indicates that EHD4 may only be required for the constitutive recycling of AQP2 in principal cells. **Therefore, it is hypothesized that EHD4 regulates the trafficking of AQP2 in principal cells, and in the absence of EHD4, membrane accumulation of AQP2 in the principal cells will be reduced.** A major aim of this chapter is, therefore, to study the effect of EHD4 deletion and depletion on AQP2 trafficking in in vivo and in vitro models of principal cells, and to understand the cellular and molecular mechanisms of how EHD4 may regulate AQP2. In the first series of experiments, the total cellular and membrane abundance of AQP2 is assessed in the presence and absence of EHD4. In order to identify the cellular mechanisms that might be involved in the regulation of AQP2 by EHD4, a protein-protein interaction profile will be generated and the interaction between EHD4 and AQP2 will be tested by immunoprecipitation. Depletion of EHD4 has been previously shown to increase the activity of Rab5 proteins and enlarge the early endosome of HeLa cells (178). In a separate study, a similar increase in the activity of Rab5 proteins and early endosomal length were observed in murine macrophages when PGE2 was administered to the cells (203). PGE2 is a well-known negative regulator of AQP2 and reduces the accumulation of AQP2 in the apical membrane of principal cells. Because the cellular and physiological effects of EHD4 deletion is similar to that of increased PGE2 synthesis, an additional line of investigation will be performed to test to see if EHD4 regulates the synthesis of PGE2.

Collecting ducts constitutively express AQP3 and AQP4 in the basolateral membrane of principal cells to provide an exit route for water, and previous studies have reported that mice lacking AQP3 or AQP4 can develop urine-concentrating defects (25, 114). Therefore, this chapter will also assess the role of EHD4 in the regulation of AQP3 and AQP4 in the principal cells of the collecting duct.

Methods

Animals

All animal studies were approved in advance by the Institutional Animal Care and Use Committee at the University of Nebraska Medical Center. Baseline metabolic cage experiments were conducted on 12 to 18-week old male and female EHD4-KO mice (n = 6 for male; n = 5 for female) and age-matched male and female C57Bl/6 mice (WT) (n = 9 for male; n = 4 for female (Jackson Laboratories, Bar Harbor, ME) as described in CHAPTER I (page no.31) to collect baseline urine.

Cell culture

The mouse cortical collecting duct principal cell line (mpkCCD$_{c14}$ cells) was generously shared by Dr. Mark Knepper (NIH). These cells are known to express AQP2 endogenously, and are widely accepted as a good in vitro model principal cell line to study AQP2 trafficking (67). The cells were grown in modified DMEM/F-12 medium with composition as described in (67) and were seeded on permeable filters (Transwell®, 0.4-μm pore size, 1-cm^2 growth area, Corning Costar, Cambridge, MA) at a density of 50,000 cells/well for Western blotting and immunofluorescent analysis, and 100,000 cells/well for surface biotinylation unless otherwise stated.

Cell transfection

EHD4-siRNA transfection: Cells were grown to 70-80% confluency in a 6-well dish and subjected to Lipofectamine-2000-mediated transient transfection with 20 pmol/well solution of either a non-targeting (NT) siRNA (Catalogue# D-001210-01-05, Dharmacon™, Lafayette, CO) or an EHD4-specific siRNA (sequence: 3' UGGAGGACGCCGACUUCG-AUU 5') (Dharmacon™). Expression of EHD4 was measured in the transfected cells (by Western blot) after 48 hours to ensure knock down of EHD4.

EHD4-shRNA transfection: Cells were subjected to Lipofectamine 2000-mediated transfection followed by retroviral transduction with either a NT or an EHD4-specific shRNA (sequence: 3' GAAGGCTCGAGAAGGTATATTGCTGTTGACAGTGAGCGATC-GCCCATCAATGGCAAGATATAGTGAAGCCACAGATGTATATCTTGCCATTGATGGG CGACTGCCTACTGCCTCGGACTTCAAGGGGCTAGAATTCGAGCA 5') and positively selected for with 2 μg/mL puromycin (Sigma-Aldrich, St. Louis, MO). Transfected cells were grown on the filter for 3 days in complete media before switching to serum/hormone-free media. To simulate baseline conditions, 0.1 nM d-deamino-arginine vasopressin (dDAVP) (Sigma-Aldrich, St. Louis, MO) was applied on the basolateral side for 24 h, while 10 nM dDAVP was used as a stimulatory dose of dDAVP (67). At the end of the 24-h period, cells were extracted and lysed as described below.

GFP-EHD4 plasmid transfection: Cells were grown on cover slips at a density of 50,000 cells/well in a 24-well dish and allowed to grow to a 80-90% confluency. Next, the cells were subjected to Lipofectamine-2000-mediated transfection with GFP-tagged EHD4 pCDNA3 plasmid, previously generated as described in (58). For transient transfection in each well, 7.5 μL Lipofectamine-2000 (Catalogue# 11668-027, ThermoFisher Scientific, Rockford, IL) and 3 μg plasmid DNA were separately diluted in 100 μL Opti-MEM™ (Catalogue# 31985070, ThermoFisher Scientific) and allowed to incubate at room temperature for 20 minutes. During this incubation period, growth medium from each well was removed and 1 mL Opti-MEM™ was added to each well. After the incubation, diluted Lipofectamine-2000 was added to the diluted plasmid DNA and the mixture was incubated for another 20 minutes to allow complex formation. Finally, 250 μL of the final DNA-Lipofectamine complex was slowly added to each well containing Opti-MEM™ and cells were incubated for 6 hours in the transfection media. After the final incubation, the transfection medium was removed and complete growth media was added to the cells.

Cells were allowed to grow for 48 hours post-transfection in the complete media before performing immunofluorescent staining. Cells treated with Lipofectamine-2000 but no GFP4-EHD4 plasmid were used as negative controls.

Cell lysate preparation

Confluent mpkCCD$_{c14}$ cells were subjected to lysis by M-PER™ mammalian protein extraction reagent (78501, ThermoFisher Scientific, Rockford, IL) containing 1 mM phenylmethylsulfonyl fluoride, 2 µM Leupeptin, 1 µM Pepstatin A, 0.1% Aprotinin, and 10 µL/mL Phosphatase inhibitor cocktail (Sigma-Aldrich, St. Louis, MO). Cells were incubated in the lysis buffer for 1 hour at 4 °C, followed by centrifugation of the lysates at 13,000 *g* for 10 minutes. Supernatant was collected and protein concentration of the lysate was measured as described in CHAPTER I (page no. 33). Lysates were stored at -80 °C until further analyses were performed.

Surface biotinylation

Control and EHD4 shRNA-transfected mpkCCD$_{c14}$ cells were seeded at a density of 100,000 cells/well on semipermeable filters of Transwell systems and cultured for 3 days prior to performing surface biotinylation as described in (152). Briefly, cells were treated with dDAVP (0.1 nM for baseline stimulation) for 24 h at 37°C at the basolateral sides. At the end of the 24-h period, cells were washed three times with ice-cold PBS-CM (10 mM PBS containing 1 mM $CaCl_2$ and 0.1 mM $MgCl_2$, pH 7.5), followed by incubating the cells for 45 min at 4°C in ice-cold biotinylation buffer (10 mM triethanolamine, 2 mM $CaCl_2$, 125 mM NaCl, pH 8.9) containing 1 mg/ml sulfosuccinimidyl 2-(biotinamido)-ethyl-1,3-dithiopropionate (Sulfo-NHS-SS-biotin, ThermoFisher Scientific, Rockford, IL) on the apical side. Cells were then washed once with quenching buffer (50 mM Tris-HCl in PBS-CM, pH 8.0) and twice with PBS-CM, followed by lysing the cells as described above. The lysates were sonicated at 2 × 6 pulses at 20% of amplitude and centrifuged at 10,000 g

for 5 min at 4°C. Next, the supernatant was transferred to columns (Pierce Spin Column Snap Cap, Catalogue# 69725) (ThermoFisher Scientific, Rockford, IL), which were previously loaded with 200 µl Neutravidin agarose resin (ThermoFisher Scientific, Rockford, IL) and incubated for 60 min at room temperature with end-over-end mixing. At the end of the 60-minute incubation, the columns were centrifuged at 8000 rpm for 1 minute and the flow through was discarded. After washing with degassed PBS containing protease inhibitors for 6-8 times, 50 µL of 1X sample buffer containing 50 mM DTT was added to the column and incubated for 60 min at room temperature. The final flow-through was collected in a 1.5 mL tube and heated at 65 °C for 10 minutes before proceeding to Western blotting. Lysates of cells that did not undergo biotinylation, but were otherwise prepared identically to biotinylated cells, including purification via Neutravidin agarose column, were used as a negative control. Total loaded protein was analyzed by Revert™ Total Protein Stain (LI-COR® Biosciences, Lincoln, NE).

Co-immunoprecipitation of AQP2 and EHD4

Confluent monolayer of mpkCCD$_{c14}$ cells were grown on permeable filters at a density of 150,000 cells/well in a 6-well dish for 3 days. For the final 24 hours, either no or 1 nM dDAVP (to stimulate AQP2 expression) was added to the basolateral side of the cells. Next, the cells were subjected to lysis as described above, followed by centrifugation at 13,000 *g* at 4 °C to collect the supernatant. AQP2 antibody was added to the supernatant at a 1:250 w/w ratio and incubated for 1 hour at 4 °C. Then, 20 µL of resuspended Protein A/G Plus-Agarose (sc-2003, Santa Cruz Biotechnology, Dallas, TX) kept at room temperature were added to the samples, and samples were incubated overnight at 4 °C on a rocker platform to ensure uniform mixing. Immunoprecipates were collected the following day by centrifugation of the samples at 1,000 *g* for 5 minutes and the supernatant was discarded. The pellets were washed with 1 mL 1X PBS for 5 times,

each time repeating the centrifugation step above. After the final wash, the supernatant was discarded and 40 µL of 1X electrophoresis sample buffer containing 10% glycerol, 50 mM Tris-HCl (pH 6.8), 2% SDS, 0.005% bromophenol blue, and 2% 2-mercaptoethanol was added. Samples were heated for 15 minutes at 60 °C and subjected to SDS-PAGE to blot for EHD4. Cell lysates that were not incubated in AQP2 antibody but otherwise prepared identically to lysates with AQP2 antibody, including incubation with Protein A/G Plus-Agarose, were used as negative controls.

Quantitative immunoblotting of aquaporins

Expression levels of AQP2, AQP3, AQP4, phospho-serine256-AQP2 (pAQP2), and EHD4 in the renal tissues and cell lysates were analyzed by immunoblotting as described in CHAPTER I (page no. 34). The following primary antibodies were used: goat anti-AQP2 (sc-9882, 1:2000 dilution); goat anti-AQP3 (sc-9885, 1:1000 dilution), and goat anti-AQP4 (sc-9888, 1:1000 dilution) (Santa Cruz Biotechnology, Dallas, TX); rabbit anti-pAQP2 (ab-109926, 1:1000 dilution, AbCam, Cambridge, MA); rabbit anti-EHD4 (ab-83859, 1:1000 dilution, AbCam, Cambridge, MA).

Immunofluorescence staining of aquaporins

Paraffin-embedded kidney sections from WT and EHD4-KO mice (n = 3-4 per group; 3-5 images per IM section) were subjected to immunofluorescent staining as described in CHAPTER I (page no. 35). Membrane abundance of AQP2, AQP3, AQP4 and pAQP2 was quantified by measuring the pixel intensities of the channels within a consistent defined region of the apical (for AQP2 and pAQP2) or basolateral (for AQP3 and AQP4) membrane using the image analysis tool ImageJ (freely downloaded from https://imagej.nih.gov/ij/). The analysis was performed in a blinded manner in 3-5 images of inner medulla in each mouse.

To analyze localization of AQP2 and GFP-tagged EHD4 in cultured principal cells, mpkCCD$_{c14}$ cells were plated on cover slips as described above. Cells were fixed in 4% formaldehyde in 1X PBS for 20 minutes. Next, cells were washed in 1X PBS for 5 minutes and subjected to permeabilization by 0.075% Triton X-100 for 20 minutes. Cells were then blocked in 2 mg/ml BSA in 1X PBS for 30 minutes, followed by incubation in primary antibodies for 1 hour at 37°C. Fluorescently-tagged secondary antibodies (1:500 dilution) (Alexa Fluor® conjugates, ThermoFisher Scientific, Rockford, IL) were added next and cells were incubated for 1 hour at room temperature. Finally, cells were washed 3 times in 1X PBS, and mounting solution containing DAPI was added. The analysis was performed in 3-4 images for each treatment group (n = 3 per treatment group, with n being the number of separate experiments).

The following primary antibodies were used: goat anti-AQP2 (1:2000 dilution), goat anti-AQP3 (1:100 dilution), goat anti-AQP4 (1:100 dilution), rabbit anti-pAQP2 (1:1000 dilution), rabbit anti-GFP (ab-6556, 1:200 dilution, AbCam, Cambridge, MA).

Measurement of PGE2

Cells were plated in a 6-well dish at a density of 100,000 cells/well. After 24 hours, the complete growth media were removed and a serum/hormone-free media was added to the cells. Next, the cells were subjected to siRNA transfection as described above and were allowed to grow for 48 hours. At the end of the 48-h period, 1 mL media surrounding the cells was collected and the amount of PGE2 released was measured. PGE2 level in urine and cell culture media was measured according to the manufacturer's instructions with a PGE2 ELISA kit (Catalogue# 514010, Cayman Chemicals, Ann Arbor, MI).

Protein-protein interaction map

The protein-protein interaction map for EHD4 was generated using the bioinformatics tool STRING ver. 10.5 (available at www.string-db.org). STRING 10.5 is a database of known and predicted protein interactions. The interactions were derived from four sources: genomic context, high-throughput experiments, coexpression, and existing knowledge from literature database. The minimum required interactions score was set at medium confidence of 0.400, with the highest score being 0.900.

Statistical analyses

Statistical analyses were performed using GraphPad Prism 6 for Windows (GraphPad Software Inc., La Jolla, CA) as described in CHAPTER I.

Results

EHD4 deletion reduces accumulation of AQP2 in the apical membrane and AQP4 in the basolateral membrane of principal cells

As urine osmolality of euhydrated mice was reduced and urine flow increased in EHD4-KO mice compared to WT mice, total cellular abundance of AQP2, AQP3, and AQP4, as well as pAQP2 in the renal inner medulla of these two genotypes were compared. As shown in Figures 16A and 17A, there was no difference in the total AQP2 and pAQP2 protein level in the inner medullas of the two groups. However, immunofluorescence staining of AQP2 as well as pAQP2 was more dispersed within principal cells of EHD4-KO mice compared to WT mice, which showed a clear apical localization of AQP2 in principal cells of the collecting duct (Fig. 16B and 17B). Moreover, apical pixel intensity of both AQP2 and pAQP2 was significantly reduced (~20% for AQP2 and ~40% for pAQP2) in EHD4-KO mice compared with WT, indicating reduced membrane accumulation of AQP2 and pAQP2 in EHD4-KO mice. Additionally, a robust decline in the basolateral membrane intensity of AQP4 staining in EHD4-KO mice (~70% reduction) was found when compared to the WT mice, although total staining of AQP4 also appeared to be significantly reduced in EHD4-KO mice (Fig. 18A). Using the same AQP4 antibody, Western blot analysis showed a slight reduction in glycosylated-AQP4 and a significant increase in non-glycosylated-AQP4 (Fig. 18B). Basolateral abundance of AQP3 (Fig. 19) was comparable in both the genotypes.

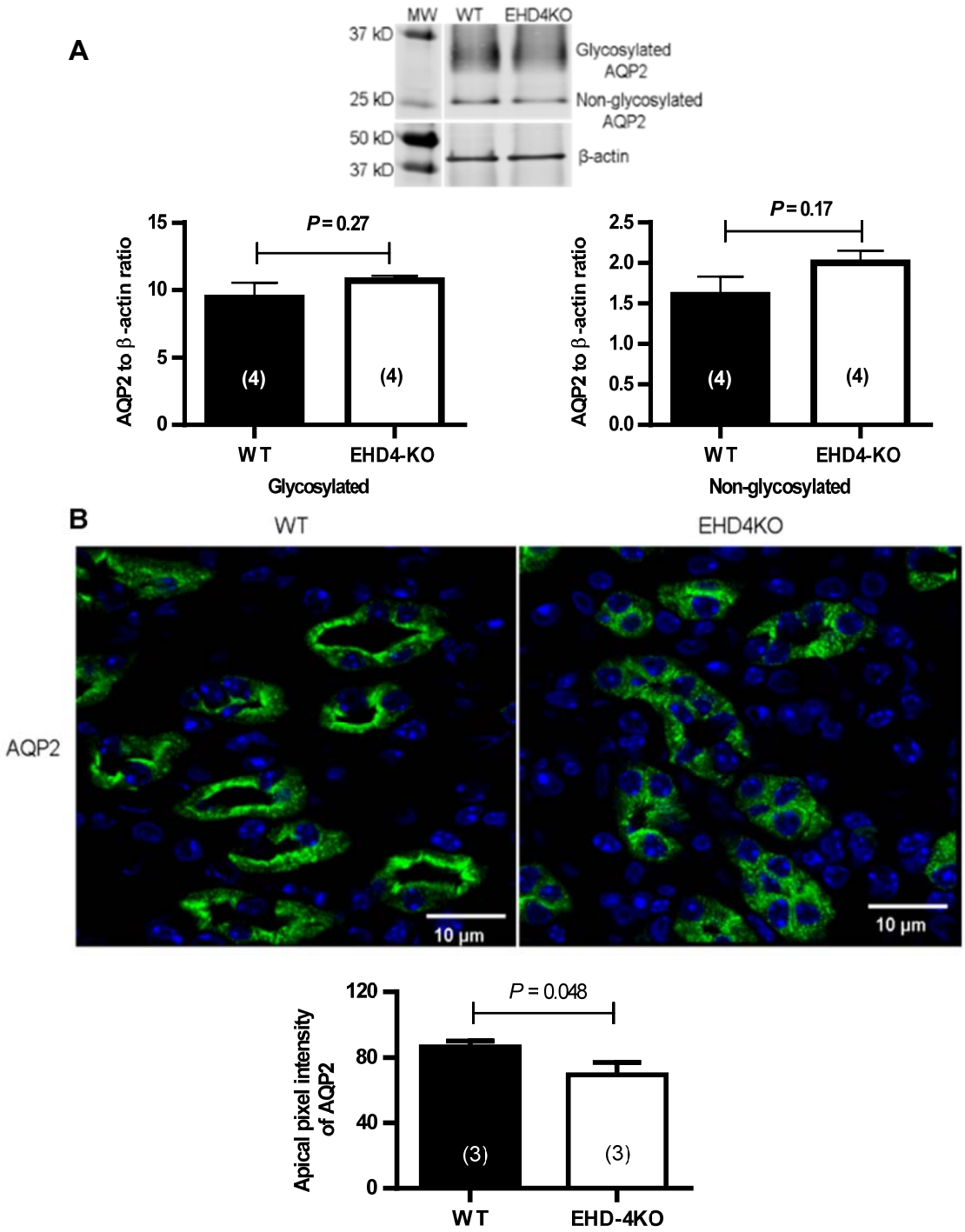

Figure 16: EHD4 regulates localization of AQP2 in the IM of mice kidney. (A) Representative immunoblot and densitometric quantification of AQP2 in the IM of female WT and EHD4-KO mice. (B) Representative immunofluorescent image and blinded quantification of apical intensity of renal IM of male WT and EHD4-KO mice with AQP2 antibody. Original magnification, X60. Graphed data are means ± SEM of n mice (in parentheses). *P* values were determined by unpaired *t* test.

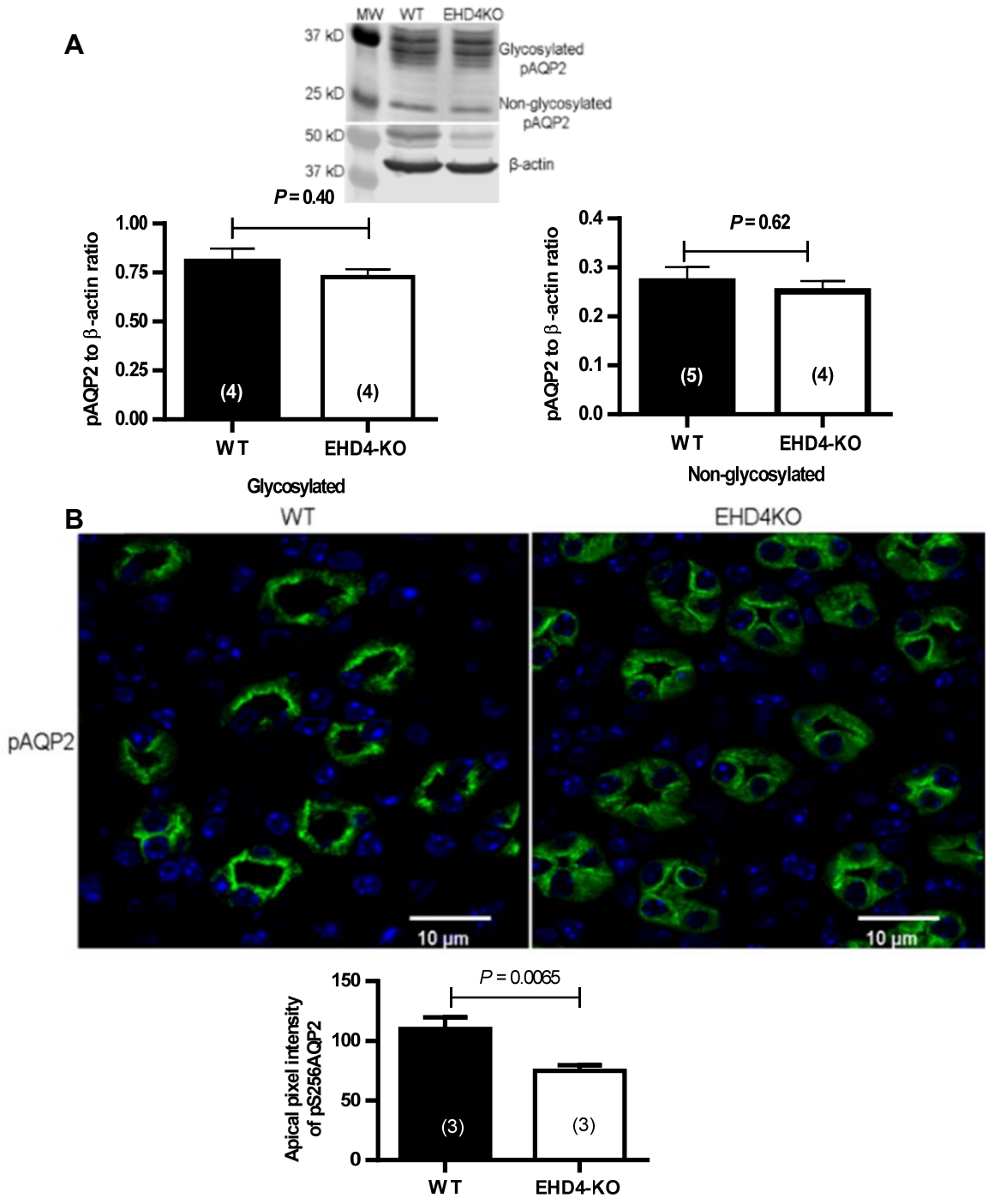

Figure 17: EHD4 regulates localization of pAQP2 in the IM of mice kidney. (A) Representative immunoblot and densitometric quantification of pAQP2 in the IM of female WT and EHD4-KO mice. (B) Representative immunofluorescent image and blinded quantification of apical intensity of renal IM of male WT and EHD4-KO mice with pAQP2 antibody. Original magnification, X60. Graphed data are means ± SEM of n mice (in parentheses). *P* values were determined by unpaired *t* test.

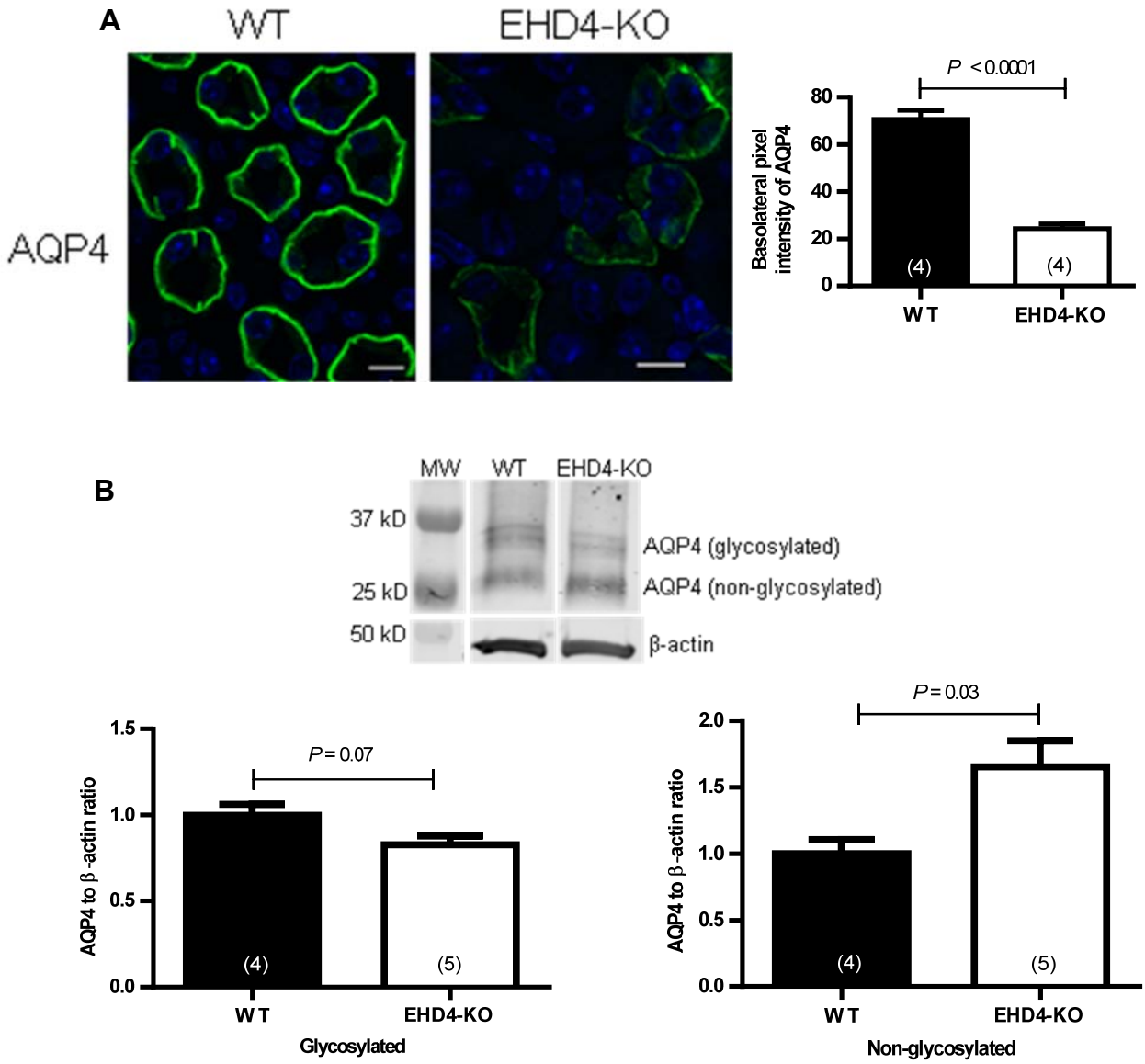

Figure 18: EHD4 regulates expression of AQP4 in the basolateral membrane of the collecting duct. (A) Representative immunofluorescent images and blinded quantification of AQP4 in the IM of male WT and EHD4-KO mice. Scale bars, 10 μm. (B) Representative immunoblot and densitometric quantification of glycosylated and non-glycosylated AQP4 in the IM of male WT and EHD4-KO mice. Graphed data are means ± SEM of n mice (in parentheses). *P* values were determined by unpaired *t* test.

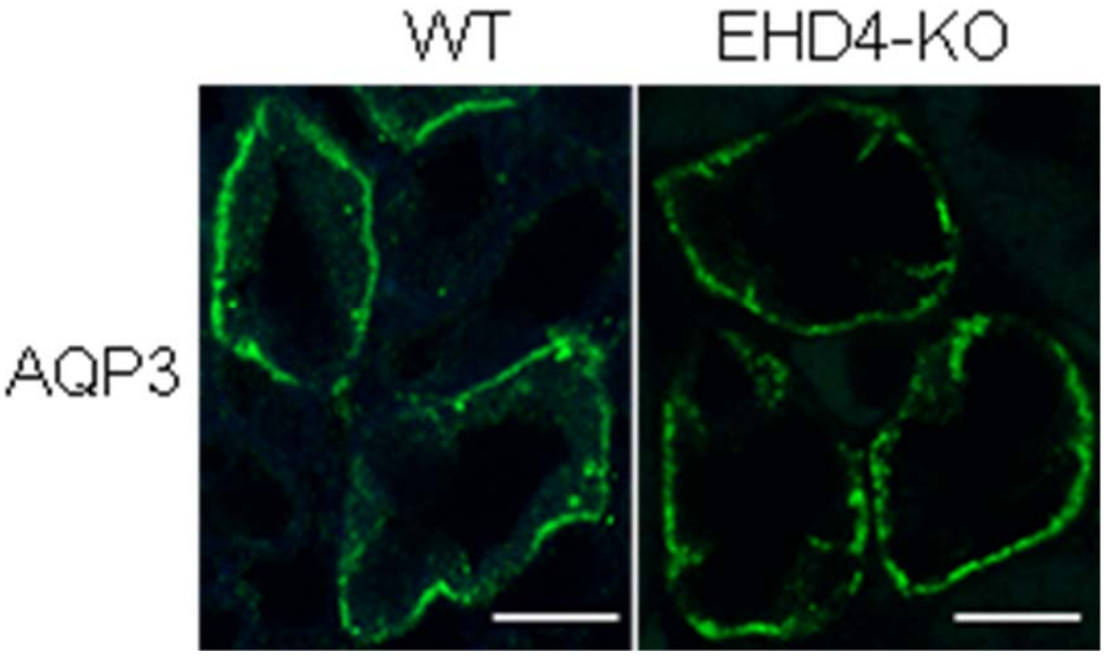

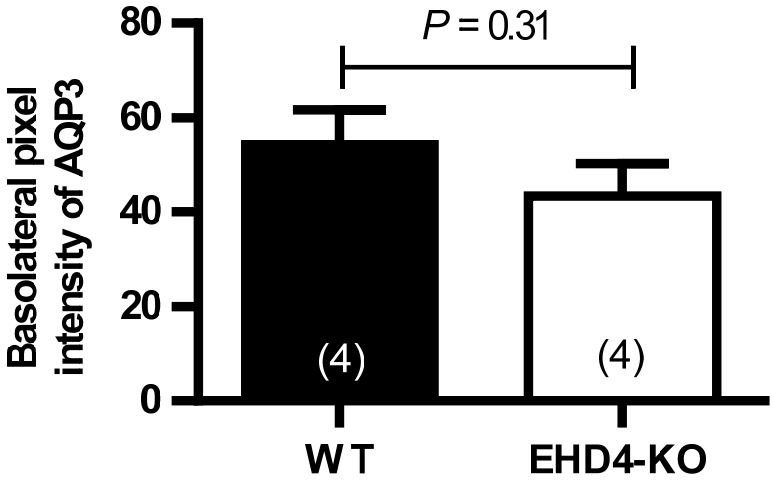

Figure 19: Effect of EHD4 deletion on the basolateral expression of AQP3. Representative immunofluorescent images and blinded quantification of AQP3 in the IM of male WT and EHD4-KO mice. Scale bars, 10 μm. Graphed data are means ± SEM of n mice (in parentheses). *P* values were determined by unpaired *t* test.

EHD4 deletion decreases the accumulation of glycosylated AQP2 in the apical membrane of cultured principal cells

Although the blinded quantification of the apical membrane pixel intensity of AQP2 immunofluorescence staining presented in Figure 16 suggests that EHD4-KO mice have reduced apical membrane AQP2 abundance, it remains possible that some of the difference in intensity detected may reflect a difference in the sub-apical space as well as or rather than the apical membrane itself. To further confirm the role of EHD4 in the regulation of apical membrane AQP2 localization in principal cells under baseline conditions, mpkCCD$_{c14}$ cell line was stably transfected with either NT or EHD4-specific shRNA. Transfection with EHD4-shRNA resulted in an almost 65% reduction in the expression of EHD4 protein as compared to that in control cells (Fig. 20). These mpkCCD$_{c14}$ cells are known to express AQP2 endogenously and the expression of AQP2 is upregulated in a dose-dependent manner in the presence of dDAVP (67), which was also demonstrated in cultured cells used in this study (Fig. 21). As shown in Figure 18, knock down of EHD4 in mpkCCD$_{c14}$ cells did not significantly affect the total abundance of AQP2 at baseline (0.1 nM dDAVP) or after a 10 nM stimulatory dose of dDAVP ($P_{genotype} > 0.05$), and dDAVP increased the expression of glycosylated and non-glycosylated AQP2 in both control and EHD4-shRNA cells in a similar manner ($P_{dDAVP} = 0.013$, $P_{interaction} > 0.05$), indicating an EHD4-independent effect of dDAVP on the total expression of AQP2. Surface biotinylation of apical AQP2 revealed that knock down of EHD4 in mpkCCD$_{c14}$ cells significantly reduced the apical level of glycosylated but not non-glycosylated AQP2 compared to that observed in NT-shRNA (control) cells (Fig. 22), corroborating the reduction in apical immunofluorescence staining observed in EHD4-KO mouse kidney sections in Figure 16.

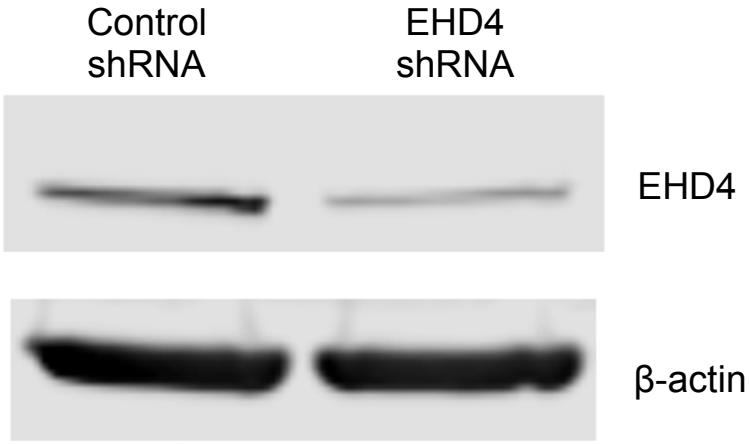

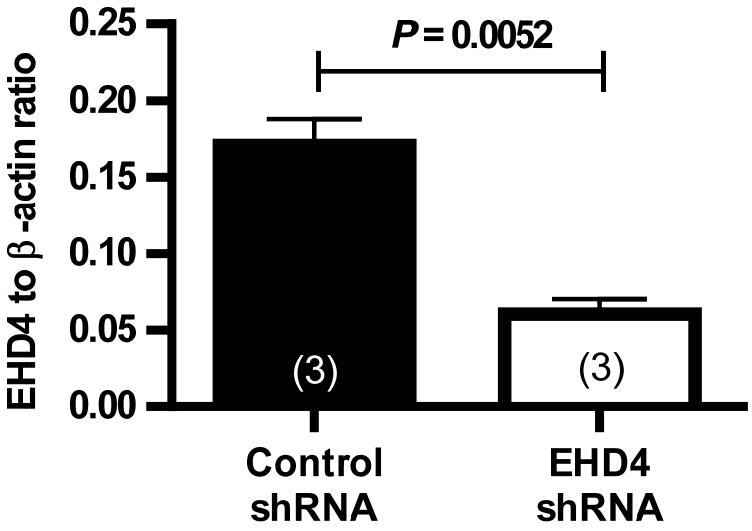

Figure 20: EHD4 expression in shRNA-transfected mpkCCD$_{c14}$ cells. Representative immunoblot and densitometric quantification of EHD4 in mpkCCD$_{c14}$ cells transfected with either non-targeting (control) or EHD4-specific shRNA. Graphed data are means ± SEM of n separate experiments (in parentheses). *P* values were determined by unpaired *t* test.

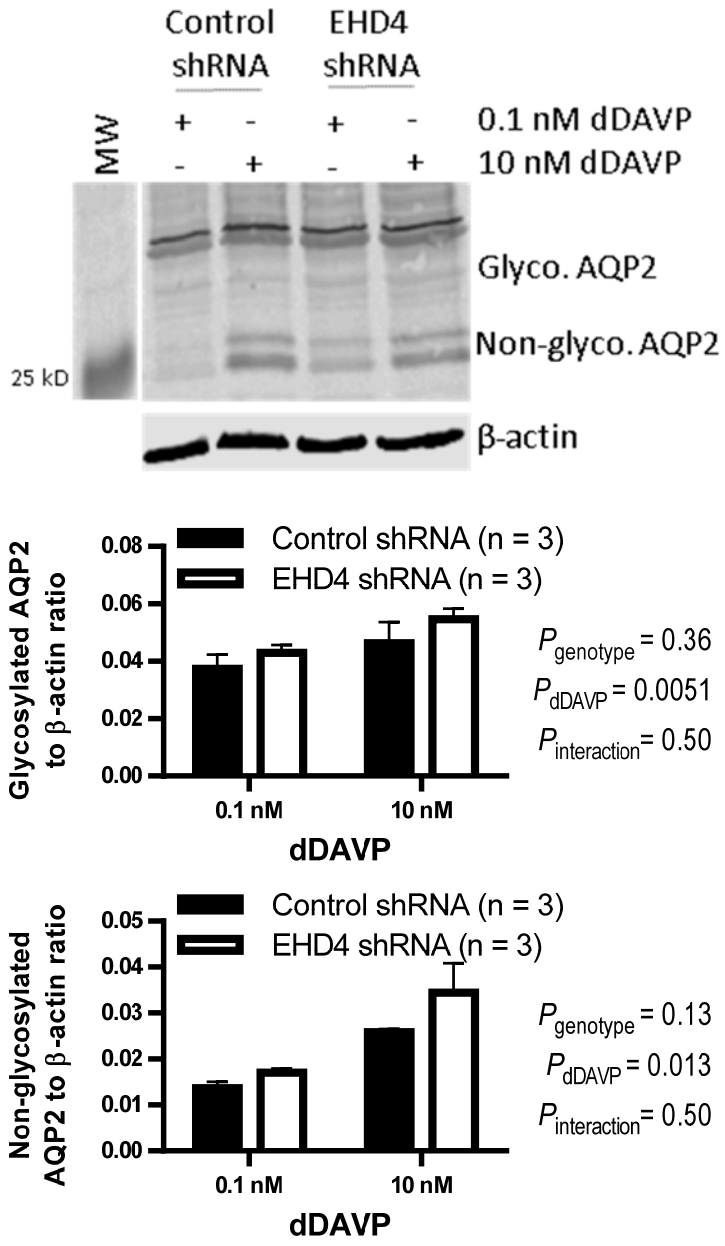

Figure 21: Effect of EHD4 knockdown on the expression of total AQP2 in mpkCCD$_{c14}$ cells. Representative immunoblot and densitometric quantification of glycosylated and non-glycosylated AQP2 in control and EHD4-shRNA cells treated with 0.1 nM dDAVP (baseline stimulation) for 24 h, followed by a stimulatory dose of 10 nM dDAVP. Graphed data are means ± SEM of n separate experiments (in parentheses). *P* values were determined by 2-factor ANOVA to test for the effects of genotypes ($P_{genotype}$), dDAVP (P_{dDAVP}), and the interaction between dDAVP and genotype ($P_{interaction}$).

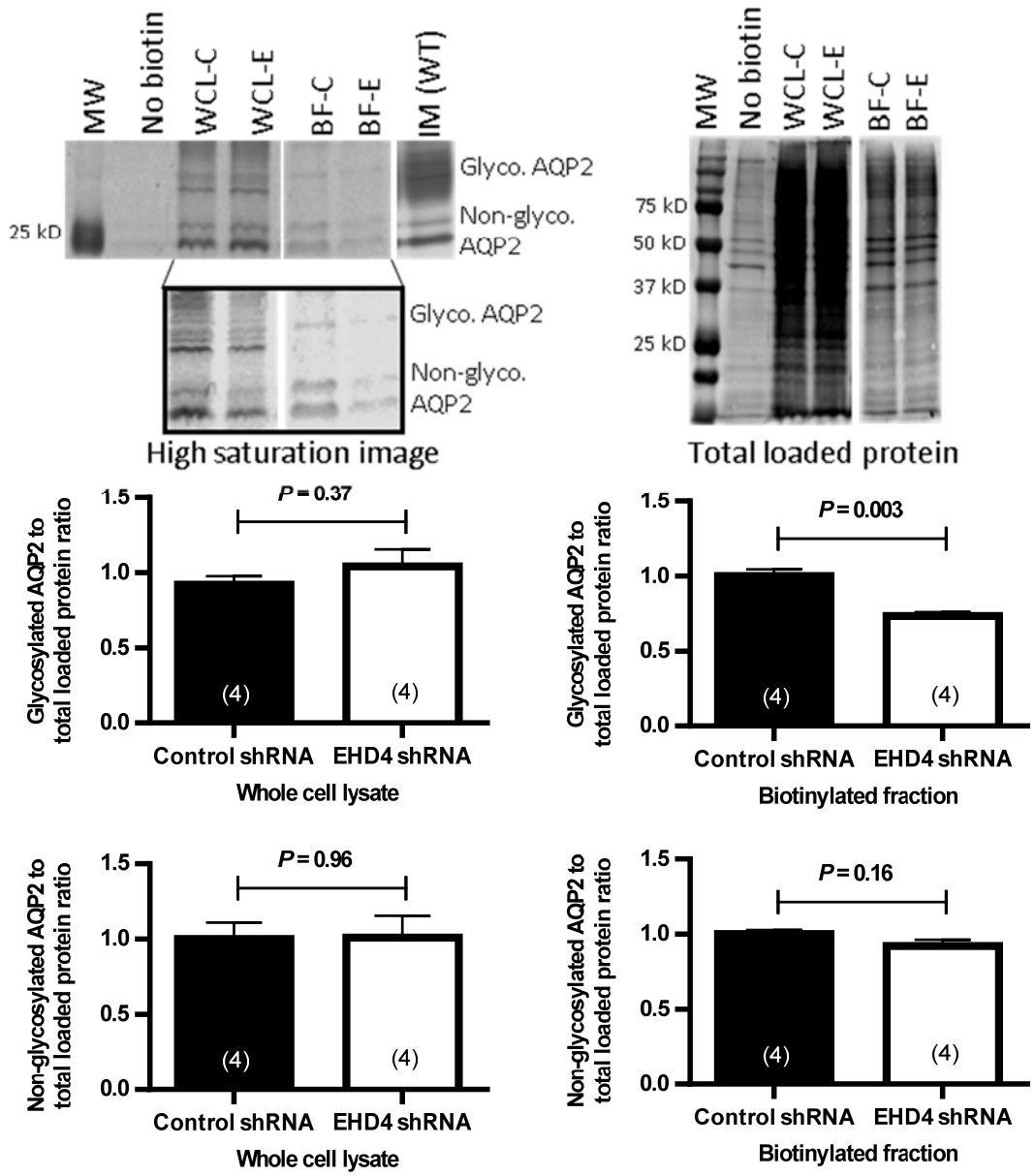

Figure 22: Effect of EHD4 knockdown on the cell surface expression of AQP2 in mpkCCD$_{c14}$ cells. Representative immunoblot and densitometric quantification of AQP2 after surface biotinylation of mpkCCD$_{c14}$ cells. Lysates of cells that did not undergo biotinylation, but were otherwise prepared identically to biotinylated cells, including purification via the Neutravidin agarose column, were used as a negative control. Total AQP2 surface and cytosolic fractions that were not passed through column) in whole-cell lysate (WCL; C = control, E = EHD4-shRNA) and biotinylated-AQP2 fractions (BF; C = control, E = EHD4-shRNA) were loaded and the appropriate bands for glycosylated and non-glycosylated AQP2 were confirmed by running a WT IM homogenate. A high saturation image of the same blot is shown below to show the bands in the BF samples more clearly. Total loaded protein was used for normalizing the quantification of AQP2 intensity. For representative images of Western blots, white gaps indicate where intervening lanes were spliced out, with vertical alignment maintained as per the original blot. Graphed data are means ± SEM of n separate experiments (in parentheses). *P* values were determined by unpaired *t* test.

Protein-protein interaction profile of EHD4 shows possible interaction of EHD4 with regulators of water reabsorption and AQP2 trafficking

To understand the role of EHD4 in the regulation AQP2 trafficking in principal cells, an interaction profile of EHD4 using STRING ver. 10.5 (Fig. 23) was generated. Three of the EHD4-interacting proteins, namely Rab5a, Rab5b, and Rab5c, were discovered as proteins involved in the regulation of water reabsorption (KEGG pathway ID: 04962, false discovery rate = 0.000347). Interactions between EHD4 and Rab5 proteins were all derived from text-mining. Additionally, EHD4 was also shown to interact with Rab11-Fip2 (interaction score = 0.892), an important regulator of AQP2 shuttling (137).

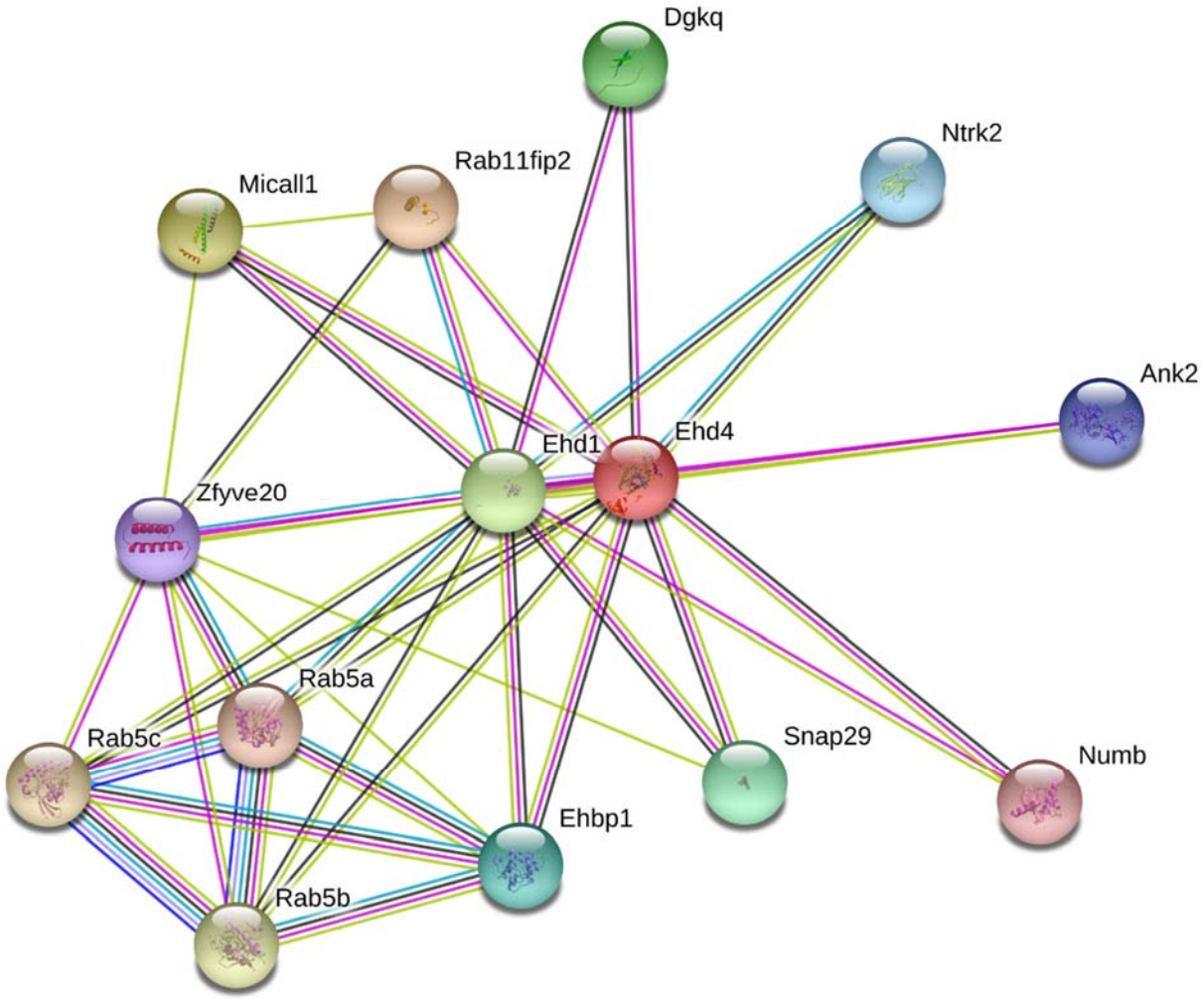

Figure 23: Protein-protein interaction profile of EHD4. STRING ver. 10.5 was used to generate the predicted interaction profile of EHD4 in mouse. The minimum confidence score was set at 0.400, with the highest score being 0.900.

EHD4 co-localizes, but may not physically interact, with AQP2 in cultured principal cells

To better understand the interaction between EHD4 and AQP2, the cellular localization of EHD4 and AQP2 was examined in mpkCCD$_{c14}$ cells transfected with GFP-tagged EHD4 pCDNA3. Transfected cells containing GFP-EHD4 show the characteristic localization of EHD4 in pleomorphic tubulovesicular structures in the perinuclear region and around the cell periphery (58) (Fig. 24). When co-stained with AQP2 antibody, GFP-EHD4 was found to localize with AQP2 in the transfected mpkCCD$_{c14}$ cells (Fig. 25), indicating that EHD4 exists in close proximity to AQP2. To test if EHD4 physically interacts with AQP2, immunoprecipitation of AQP2 from mpkCCD$_{c14}$ cells (Fig. 26) was performed. As shown in Figure 26, EHD4 was not found in the immunoprecipitates containing AQP2, suggesting a lack of direct physical contact between AQP2 and EHD4.

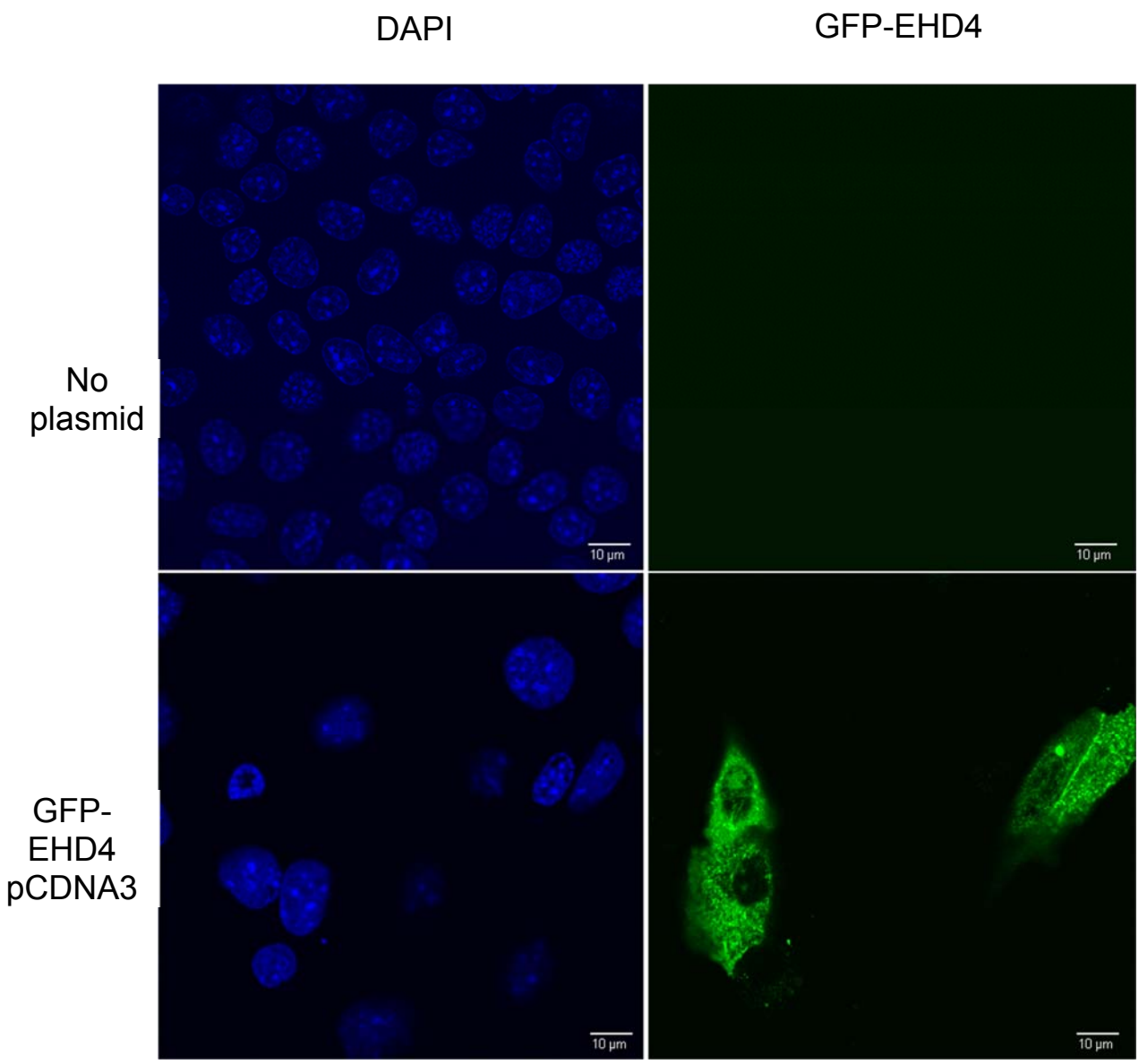

Figure 24: Transfection of mpkCCD$_{c14}$ cells with GFP-tagged EHD4 pCDNA3. Representative immunofluorescent image of cultured mpkCCD$_{c14}$ cells transfected with or without GFP-tagged EHD4 pCDNA3. Original magnification, X60.

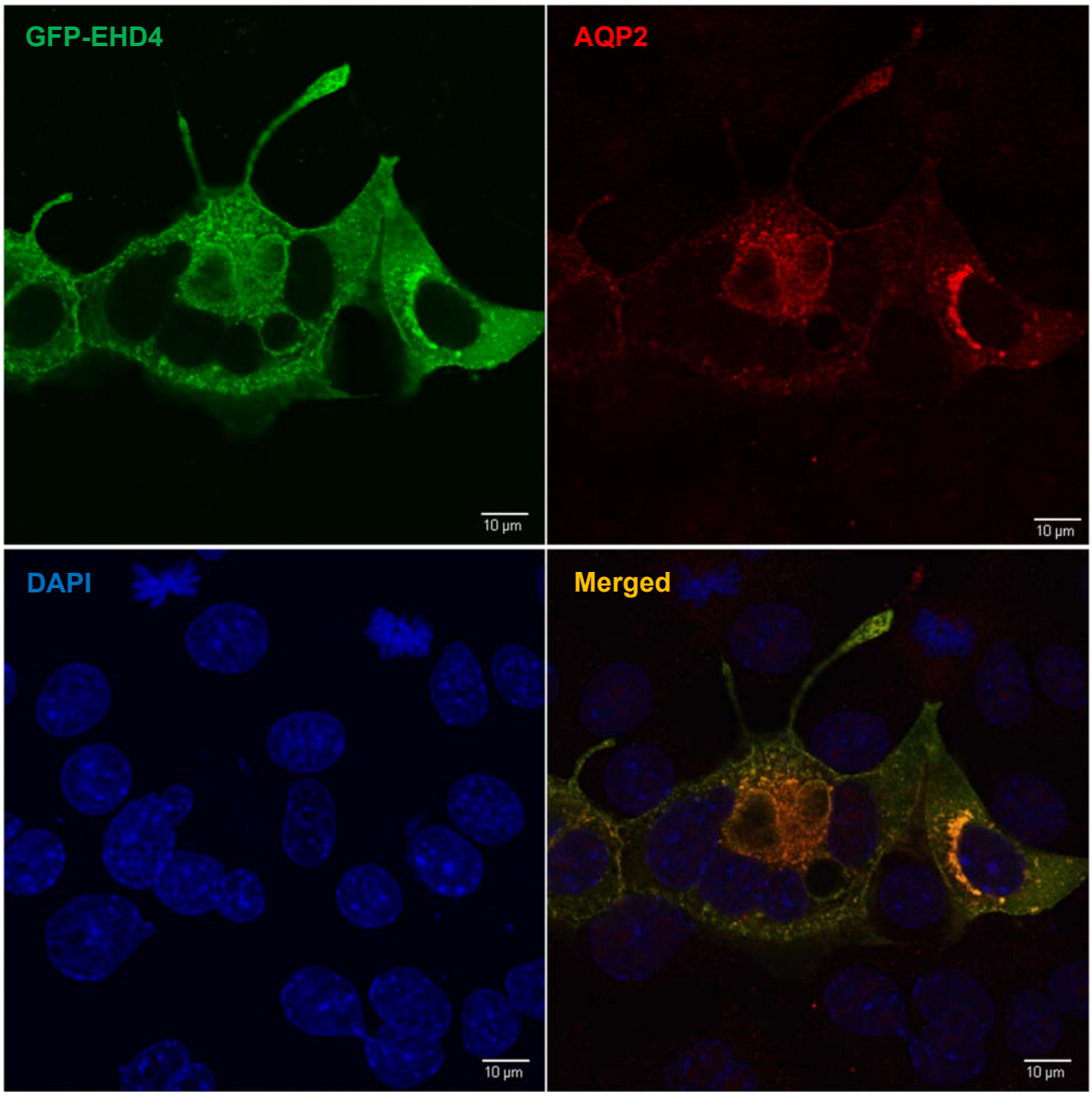

Figure 25: EHD4 co-localizes with AQP2 in mpkCCD$_{c14}$ cells. Representative immunofluorescent image of cultured mpkCCD$_{c14}$ cells transfected with or without GFP-tagged EHD4 pCDNA3 and co-stained with AQP2. Original magnification, X60.

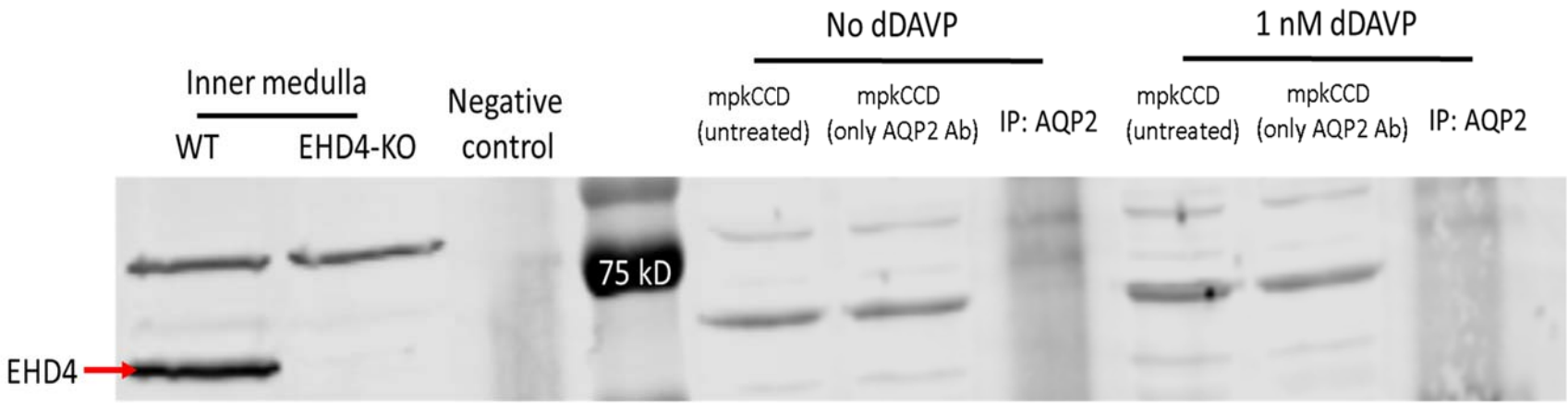

Figure 26: EHD4 is absent in the immunoprecipitate containing AQP2. Representative immunoblot of EHD4 after immunoprecipitation of AQP2 from $mpkCCD_{c14}$ cells. Cell lysates that were not incubated in AQP2 antibody but otherwise prepared identically to lysates with AQP2 antibody, including incubation with Protein A/G Plus-Agarose, were used as negative controls. Additional cells were treated with 1 nM dDAVP for 24 h to amplify the total expression of AQP2 in order to collect more immunoprecipitate. IM homogenates from WT and EHD4-KO mice were loaded to correctly identify the EHD4 band.

EHD4 deletion increases the urinary PGE2 excretion in mice

To test the hypothesis that EHD4 regulates PGE2 synthesis, the urinary PGE2 excretion in WT and EHD4-KO mice was measured. Urinary PGE2 excretion of EHD4-KO mice was significantly higher than that in WT mice (Fig. 27), indicating a potential role of EHD4 in the regulation of PGE2 synthesis.

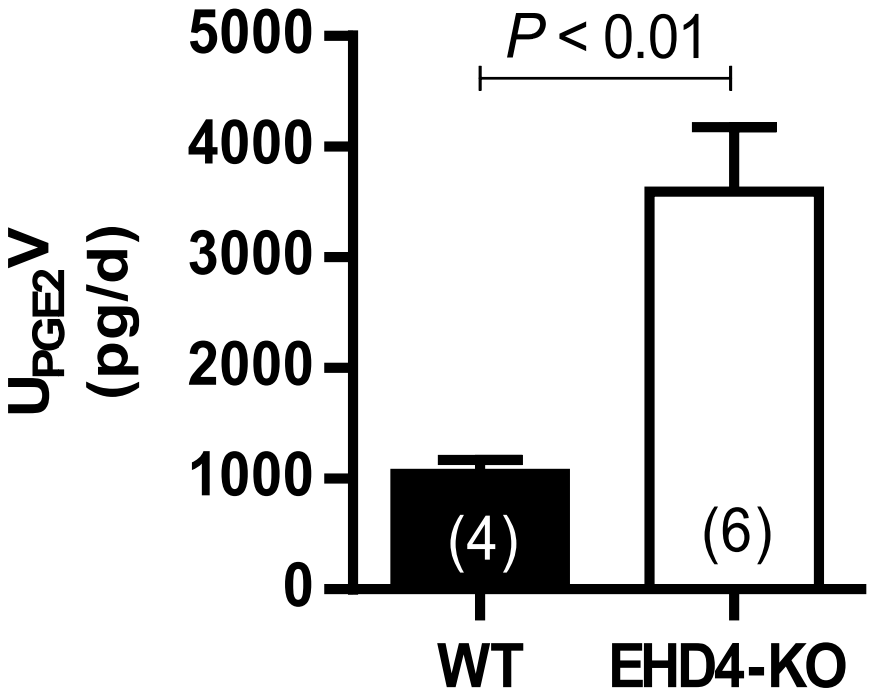

Fig 27: Effect of EHD4 deletion on the urinary PGE2 excretion in female mice. WT and EHD4-KO female mice were placed in metabolic cages for 24 hours and urine was collected to measure urinary PGE2 excretion. Data shown are mean ± SEM for n mice (in parentheses). Data were compared using unpaired *t-test*.

EHD4 regulates the synthesis of PGE2 in cultured principal cells

To test the role of EHD4 in the regulation of PGE2 synthesis in principal cells, EHD4 expression was transiently knocked down in mpkCCD$_{c14}$ cells with EHD4-siRNA and measured the amount of PGE2 released into the media as an indicator of PGE2 synthesis. EHD4-siRNA transfection caused a robust (~92%) reduction in the expression of EHD4 expression in mpkCCD$_{c14}$ cells within 48 hours (Fig. 28). Moreover, EHD4-siRNA treated cells released significantly more PGE2 into the surrounding media than control NT-siRNA cells (Fig. 29), indicating an increased synthesis of PGE2 in EHD4-depleted cells.

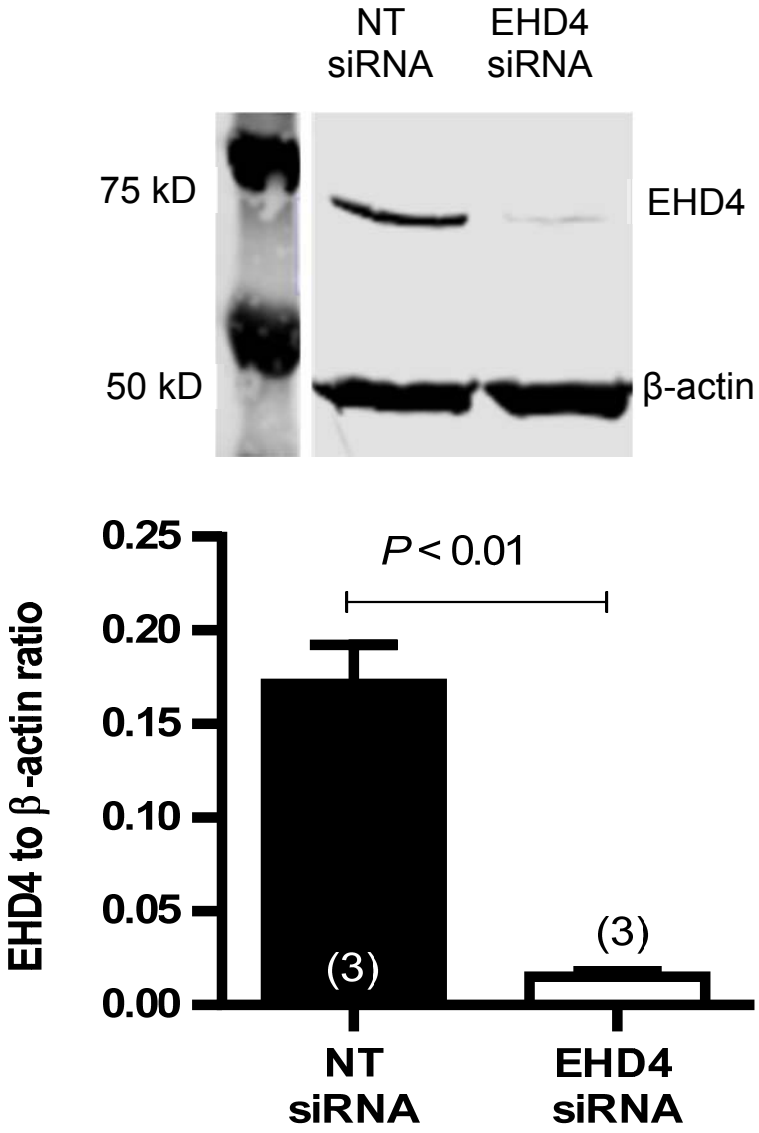

Figure 28: EHD4 expression in siRNA-transfected mpkCCD$_{c14}$ cells. Representative immunoblot and densitometric quantification of EHD4 in mpkCCD$_{c14}$ cells transfected with either non-targeting (NT) or EHD4-specific siRNA for 48 h. Graphed data are means ± SEM of n separate experiments (in parentheses). *P* values were determined by unpaired *t* test.

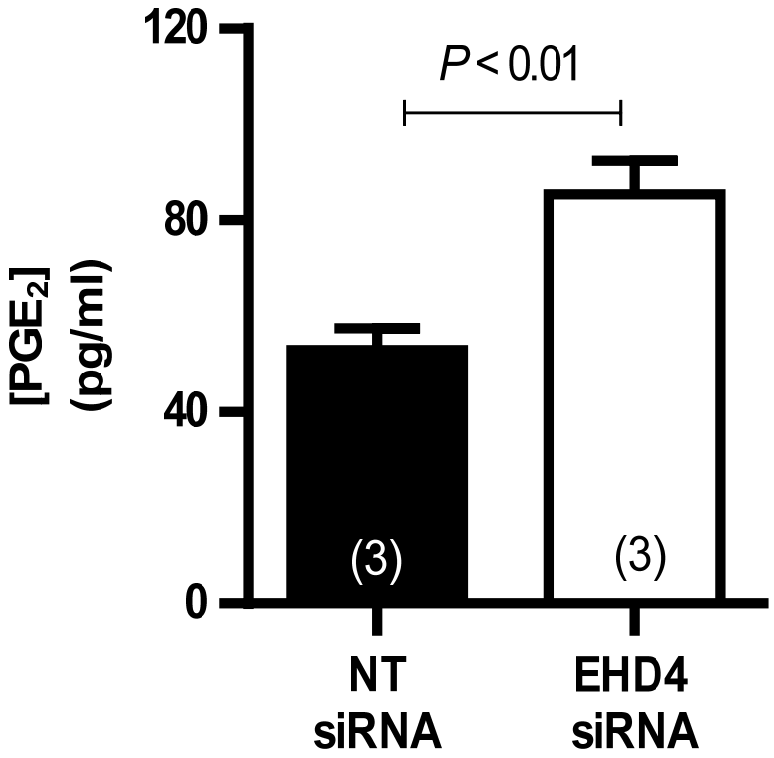

Figure 29: EHD4 regulates the synthesis of PGE2 in mpkCCD$_{c14}$ cells. Data are presented for the concentration of PGE2 level in the media surrounding siRNA transfected mpkCCD$_{c14}$ cells collected after 48 h of transfection. Graphed data are means ± SEM of n separate experiments (in parentheses). *P* values were determined by unpaired *t* test.

Discussion

This section focused on the role of EHD4 in the regulation of AQP2 trafficking in principal cells of the collecting duct. These data show that when EHD4 is deleted the membrane abundances of AQP2 and AQP4 is significantly reduced. It was also found that EHD4 co-localizes with AQP2 in principal cells, but may not physically interact with AQP2. Moreover, EHD4 has been found to regulate the synthesis of PGE2 both in vivo and in vitro, providing an additional mode of regulation of the trafficking of AQP2 in principal cells.

In the absence of EHD4, the subcellular distribution of both AQP2 and pAQP2 was found to be altered in the principal cells of the kidney. In collecting duct principal cells of WT mice, AQP2 and pAQP2 were more apically localized, whereas in EHD4-KO mice, these proteins were dispersed throughout the principal cells. Moreover, the apical accumulation of both AQP2 and pAQP2 was significantly reduced in the absence of EHD4, as evident from the reduced immunofluorescence staining intensity quantified at the apical membrane of EHD4-KO mice. The regions of interest for this blinded analysis of the confocal immunofluorescence images were drawn close to and including the apical membrane. It therefore remains possible that some of the AQP2 staining intensity included in the analyzed regions was attributable to a difference in sub-apical as well as apical AQP2. However, surface biotinylation of mpkCCD$_{c14}$ cells following silencing of EHD4 also demonstrated a significant reduction of glycosylated AQP2, suggesting that the reduced immunofluorescence intensity detected reflected a reduced apical localization of AQP2. Together, these findings indicate that less AQP2 is available in the apical membrane to facilitate water reabsorption in EHD4-KO mice, which may contribute to the polyuria in these mice.

Under baseline conditions, AQP2 is constitutively trafficked between the apical membrane, subapical vesicles and basolateral membranes (75), and when AVP levels are

low, AQP2 is mainly localized to the sub-apical endocytic vesicles (138). Binding of AVP to its V2 receptor in the principal cells induces the phosphorylation of AQP2 at ser-256 residue (138) and allows its translocation to the apical membrane (139). At the level of molecular interactions, this seemingly simple trafficking process requires the coordinated activities of multiple molecules. AVP binding to its receptor triggers several downstream signaling pathways: cAMP-mediated PKA activation, elevated intracellular Ca^{2+} level, and activation of other protein kinases (146). Phosphorylation of AQP2 is followed by reorganization of the actin cytoskeleton (187, 190) and allows traffic of AQP2 to the apical membrane. Accordingly, AQP2 trafficking within the cell involves the intricate interactions of many proteins (18). To our knowledge, no studies to date have determined whether AQP2 might directly bind with EHD4, therefore, it was examined if EHD4 physically interacts with AQP2 in principal cells. The immunoprecipitation data do not support direct physical interaction between AQP2 and EHD4; however the complex nature of AQP2 trafficking allows the possibility of EHD4 being a part of AQP2 traffic regulation through an indirect interaction with components of the endocytic traffic machinery. For example, actin cytoskeleton dynamics has been suggested to be regulated by EHD proteins via their interaction with Syndapin (PACSIN) I and II (13, 60) and therefore provides potential for the involvement of EHD proteins in AQP2 trafficking. Moreover, absence of Rab11-Fip2, one of the interacting partners of EHD proteins (136), disrupts the recycling of AQP2 (137), providing another possible link to the involvement of EHD proteins in AQP2 trafficking. Additionally, EHD4 was found to co-localize with AQP2 in principal cells, strongly indicating a close proximity of the two proteins and a possible indirect interaction between the two proteins. The lack of EHD4 may eventually reduce the association of AQP2 with important trafficking proteins, and thereby stall the constitutive recycling of AQP2. Further biochemical analyses to define the mechanism and molecular interactions by which EHD4 regulates AQP2 represent an exciting future direction.

AVP is a potent stimulator of the forward trafficking of AQP2. In the presence of AVP, AQP2-containing vesicles shift from the sub-apical region and fuse with the apical membrane, thereby increasing the amount of AQP2 in the apical membrane of principal cells (18). It could be possible that EHD4 deletion stalls the forward trafficking of AQP2 in the principal cells that ultimately reduces the membrane availability of AQP2. However, the data showed a similar increment in the amount of AQP2 in the apical membrane of both WT and EHD4-KO mice after water restriction. This data suggest that the forward trafficking of AQP2 may occur independently of EHD4. It is currently not known which part of the AQP2 recycling process is regulated by EHD4. Trafficking of membrane proteins like AQP2 through the endosomal system is a very dynamic process and in order to study the transition of AQP2 through each of the endosomal compartment in the absence of EHD4 would require a more sophisticated tool such as live-cell imaging technique coupled to pulse-chase experiments rather than a routine immunofluorescence analysis. Co-staining AQP2 with specific endosomal compartment marker would only provide a snap shot of the total process, and therefore, would not be an ideal technique for assessing the role of EHD4 in the constitutive recycling of AQP2. Because there is an overall reduction, and not absolute absence, of AQP2 in the apical membrane in the absence of EHD4, it is very likely that the speed of AQP2 recycling becomes very slow EHD4-depleted principal cells, and such a hypothesis can only be tested using live-cell imaging, which was beyond the feasible and technical scope of this study.

PGE2 is the primary product of arachidonic acid metabolism pathway and is a known negative regulator of AQP2 trafficking (148). Several studies has defined the role of PGE2-mediated AQP2 regulation as an additional mode of increasing water permeability of the collecting duct (149, 183). The data has so far suggested that the role of EHD4 in the regulation of AQP2 trafficking is AVP-independent. Moreover, EHD4 was

observed to co-localize with AQP2 in principal cells, but EHD4 and AQP2 could not be precipitated together. Although it is possible that EHD4 may interact with AQP2 indirectly, an alternative mechanism of regulation of AQP2 by EHD4 cannot be ruled out. Therefore, additional pathways that may be involved in the regulation of AQP2 in the absence of EHD4 were examined. PGE2 regulates AQP2 as well as other proteins that are also regulated by EHD4 (203). These observations provided us with grounds for analyzing the effect of EHD4 on the production of PGE2. Both the in vivo and in vitro data have shown that EHD4 regulates the synthesis of PGE2. In mice, the deletion of EHD4 resulted in an increase in the urinary PGE2 excretion, which was further confirmed in our cultured principal cells where knock down of EHD4 resulted in increased synthesis of PGE2. These data suggest that in the absence of EHD4 there is an increased production of PGE2, which may then inhibit the recycling of AQP2 in principal cells. Production of PGE2 in a cell depends on the translocation of cytosolic phospholipase A2 (cPLA2) enzyme to the membrane in order to initiate the metabolism of arachidonic acid (39). It could be possible that EHD4 regulates the translocation of cPLA2 and thereby regulates the synthesis of PGE2. The exact mechanism of how EHD4 regulates PGE2 synthesis awaits further investigation.

AQP4 makes an important contribution to the water permeability of the inner medullary collecting duct (25). As visualized by confocal immunofluorescence staining, there was a robust attenuation of the basolateral accumulation of AQP4, but not AQP3, in EHD4-KO mice, indicating that exit of water from the principal cells may also be impaired in these mice. However, a divergent expression profile of AQP4 was observed in EHD4-KO mice via immunoblotting. Although the total abundance of inner medullary AQP4 was similar between WT and EHD4-KO mice (bands quantified together), there was a significant increase in the non-glycosylated AQP4 (lower band) and a slight decrease in

glycosylated AQP4 (upper band) in EHD4-KO mice. One possible technical explanation for the discordant Western blot and immunofluorescent staining data could be that the antibody used for AQP4 has a preferential selectivity for glycosylated-AQP4 epitope in immuno-stained kidney sections, reducing the apparent overall abundance. Current understanding of AQP4 trafficking to the basolateral membrane is limited, in part due to technical challenges associated with studying the basolateral membrane of the collecting duct, and the exact role of EHD4 in this mechanism awaits further investigation. Previous studies have shown that sorting of AQP3 and AQP4 in trans-Golgi network for the basolateral membrane occurs separately (3), which could explain why only AQP4 membrane accumulation, and not AQP3, was reduced in EHD4-KO mice. In addition, the lack of a change in localization of AQP3 in EHD4-KO mice demonstrates that there is specificity in terms of which proteins EHD4 regulates. Current understanding of AQP4 trafficking to the basolateral membrane is limited and the exact role of EHD4 in this mechanism needs further investigation.

Similar to the data on AQP4, I also observed a significant reduction in the membrane abundance of glycosylated APQ2 only. Glycosylation is an important post-translational process for proper targeting of membrane proteins (197), including AQP2 (68). Around 25% of the newly-synthesized AQP2 undergoes glycosylation and this post-translational process is required for the exit of AQP2 from the Golgi and eventual sorting at the plasma membrane (68). My data on the reduced level of only the glycosylated AQP2 and AQP4 suggest a possible role of EHD4 in the regulation of exit of newly-synthesized AQPs from the Golgi in the principal cells. However, very little is known about the exact role of glycosylation on AQP trafficking, which makes interpreting these data difficult. Data so far suggest that the AVP-stimulated forward trafficking of the AQP2 does not require EHD4. It is possible that trafficking of subapical AQP2-containing vesicles that have

already exited Golgi do not require EHD4 to be inserted into the plasma membrane. Although there no increase in the total amount of other EHD paralogs in the EHD4-KO mice, it is possible that there is functional compensation by another EHD paralog allows the exit of some of the AQP2-containing vesicles from the Golgi in the absence of EHD4.

Altogether, data from this chapter show that EHD4 regulates the cellular distribution of AQP2 and AQP4 in the principal cells. The reduced accumulation of AQP2 and AQP4 in their respective membrane in EHD4-KO mice may be responsible for the diuretic phenotype in these animals. Additionally, deletion of EHD4 increases the synthesis of PGE2 in the principal cells, which might be responsible for the reduced membrane accumulation of AQP2 in principal cells. Although the aquaporins were mainly investigated in this chapter to understand the role of EHD4 in renal water handling, several other renal processes may be affected by the deletion of EHD4 and contribute to the observed phenotype. Urea uptake and recycling within the inner medulla, and the renal medullary osmotic gradient are additional important factors in underlying renal water reabsorption and urinary concentrating ability. Analysis of the role of EHD4 in renal urea handling and whether EHD4 might regulate urea transporters is, therefore, the focus of the next section.

CHAPTER III: ROLE OF EHD4 IN THE REGULATION OF RENAL UREA HANDLING

Introduction

Maintenance of constant plasma osmolality is vital to sustaining normal physiological functions and is tightly regulated by the kidney. Kidneys have the ability to regulate water excretion independently of sodium excretion, thereby allowing conservation of this major cationic osmotic constituent of the plasma. When required, kidneys are able to concentrate the urine from an osmolality of ~290 to ~1200 mOsm/kg H_2O simply by increasing the amount of water reabsorbed in the collecting ducts (174). In this way, kidneys are able to produce a "hyperosmotic" urine — urine with an osmolality greater than that of the plasma. The architecture of the nephron segments within the kidney (151, 174) allows establishment of a progressively increasing osmotic gradient starting from the cortico-medullary boundary to the tip of the papillary inner medulla. This osmotic gradient of the renal interstitium drives the sodium-independent water reabsorption in the kidney. Establishment and maintenance of this osmotic gradient also depends on the tight cellular regulation of the abundance of water and solute transporters as well as other proteins in the tubular epithelium and renal vasculature. These regulatory steps, in addition to other factors such as central osmoreceptors and voluntary water intake, act in concert to keep the plasma osmolality constant.

Urea, generated in the liver by the breakdown of protein, is one of the two major osmotic constituents of the inner medullary osmotic gradient, and is the predominant solute in the urine during strong anti-diuresis (174). High interstitial urea concentration within the inner medulla is established by renal urea recycling that occurs via the various renal urea transporters. Urea reabsorption in the kidney is passive, and the permeability of the tubule to urea varies across the nephron section (117). As the filtrate moves along the nephron, urea concentration in the tubular lumen keeps increasing due to disproportional reabsorption of water, and the urea concentration reaches the highest in

the medullary collecting duct, where this high concentration of tubular urea drives the passive reabsorption of urea via the urea transporters, thereby setting the steep interstitial osmotic gradient (117).

Urea transporters comprise 2 large subfamilies, UT-A and UT-B (88), and each member of these subfamilies are differentially expressed in mammalian tissues. Of the UT-A subfamily, UT-A1, A2, A3, and A4 are all expressed in the kidney tubular epithelium, whereas UT-B is expressed in the renal vasculature, specifically the descending vasa recta (88). UT-A1 is present on the apical plasma membrane of the principal cells of the collecting ducts; UT-A2 is expressed within the descending thin limb of the loop of Henle; UT-A3 is localized on the basolateral membrane of the principal cells of the collecting ducts; and UT-A4 is present in the rat kidney medulla (88). Owing to their exclusive localizations in the collecting ducts, UT-A1 and -A3 serve as vital points of regulation of renal medullary urea recycling. Indeed, mice that lack both UT-A1 and -A3 develop severe defects in their urine-concentrating abilities (44) due to the failure to establish a functional interstitial osmotic gradient, resulting in severe urea-induced osmotic diuresis. When maintained on a 20% diet, the urine volume of UT-A1/A3 double knockout mice is almost twice and the urine osmolality is almost half of that of wild type mice (45). Moreover, this basal urine-concentrating defect in UT-A1/A3-null mice is restored when UT-A1 is overexpressed in the mice (92), indicating that UT-A1 is absolutely required for maximal urine-concentrating ability. The membrane abundance and cellular localization of UT-A1 are regulated by endocytosis (186), an EHD4-regulated cellular mechanism (178). Additionally, the diuretic phenotype of UT-A1/A3 mice is very comparable to that of EHD4-KO mice. Also, it has been reported that EHD1 interacts with snapin (204), a common-interacting partner of UT-A1 (122). Although the study focused only on EHD1, and EHD4 has not studied as extensively as EHD1, it is possible that EHD4 may also interact with

snapin and thereby regulate UT-A1 via snapin. Therefore, it is possible that the diuresis in EHD4-KO mice may arise due an increased urea load in the renal tubules resulting from a reduced membrane abundance of UT-A1. **Hence, it is hypothesized that EHD4 regulates the membrane accumulations of UT-A1 of the IMCD, thereby affecting renal urea handling, and regulating the generation of the osmotic gradient in the kidney.**

Methods

Animals

All animal studies were pre-approved by the Institutional Animal Care and Use Committee at the University of Nebraska Medical Center. Male (n = 6-7) and female (n = 5) *Ehd4*$^{-/-}$ (EHD4-KO) mice were bred from heterozygous *Ehd4*$^{+/-}$ parents, which were previously generated on a C57Bl/6 background as described in (56). Age-matched wild-type (WT) C57Bl/6 mice (Jackson Laboratories, Bar Harbor, ME) (male, n = 8-9; female, n = 4) or littermate *Ehd4*$^{+/+}$ (EHD4-HOM) mice (male, n = 7; female, n = 4) were used as control groups. In all experiments, animals were 14-18 weeks old and were housed in cages maintained at room temperature, 60% humidity with a 12/12 hour light/dark cycle. Unless otherwise stated, mice were given free access to regular rodent chow (7012, Harlan Teklad, Madison, WI) and drinking water.

Analysis of urine in mice fed with standard rodent chow

Age-matched WT and EHD4-KO mice were placed in individual metabolic cages for 24 hours to collect urine for analyzing the baseline urinary urea excretion. Animals had free access to standard rodent chow containing 19% protein (7012, Harlan Teklad, Madison, WI) and drinking water, and were returned to their home cage at the end of the experiment for a week. At the end of the week, the animals were sacrificed to collect renal tissues for immunoblotting and histological analyses.

Modified protein diet protocol

To better understand the physiological role of EHD4 in the regulation of renal urea handling, systemic urea load was manipulated by modifying the protein content in the rodent chow. The rationale for this approach was based on the Berliner hypothesis (8), which states that in the absence of functional urea transporters in the kidney epithelium a high protein diet will result in a diuretic phenotype. Subsequently, this diuretic phenotype

can be rescued by restricting protein intake via feeding of a low protein diet. Accordingly, I proceeded with this approach by cycling the feeding routine in mice every 10 days from normal (20%) to high protein (40%) diet, then switching the high protein diet to a low protein (6%) one. To determine the effect of dietary protein intake on renal urea handling, EHD4-HOM and EHD4-KO mice were fed with specialized protein diets were purchased from Harlan Teklad (Madison, WI). These diets are isocaloric (3.8 Kcal/g) and are matched in calcium (0.7%) and phosphorus content (0.54%). The predominant protein source is casein and the calories are matched by adjusting the amount of carbohydrates. Protein diets were divided into the following three categories: low (6% protein; Harlan Teklad cat# TD. 160634), normal (20% protein; Harlan Teklad cat# TD. 160635), and high (40% protein; Harlan Teklad cat# TD. 160636). Mice were cycled through 20% (closest to the animal facility standard rodent chow), then 40%, and then 6%. Mice ate the modified protein diet for 7 days in their home cage and were then placed in individual metabolic cages for 48 hours with access to drinking water and the corresponding protein diet. Mice were allowed to acclimate to the metabolic cage environment for the first 24-h period, and urine was collected over the final 24-h period for baseline urinary analysis. At the end of the entire protein diet protocol, all animals were switched to 20% protein diet for at least 7 days before sacrificing the mice to collect renal tissues for osmolality measurements.

Measurement of tissue osmolality

Renal tissue osmolality was measured using a method described previously in (147, 177). Briefly, kidneys were rapidly excised, de-capsulated, and dissected to collect the total inner medulla and similar-sized cortex and outer medulla. Excised tissue samples were next put in pre-weighed 200 µL tubes and the wet weight of the tissues were measured immediately. Next, the tissues were held at 60 °C in a dry oven. The oven was dried using Drierite (W. A. Hammond Drierite CO. LTD., Xenia, OH) for 48 hours before

the start of tissue collection. The tissues were allowed to dry out for 8 hours before measuring the final dry weight of the tissue samples. Following the dry weight measurement, tissue samples were immersed in 25 µL distilled water and solutes were allowed to diffuse out of the tissues into the water for 24 hours at 4 °C. After the 24-h incubation, tubes were briefly centrifuged and the supernatant were collected for biochemical analyses. Apparent urea concentration in tissue water (C_T) was calculated as follows using the concentration in the supernatant (C_S) and the dilution introduced by adding 25 µL of water to the dry material:

$$C_T = C_S * [25 / (\text{wet weight} – \text{dry weight in mg})]$$

Biochemical assays

Plasma, urine, and tissue urea concentration was measured according to the manufacturer's instructions using the QuantiChrom™ Urea Assay Kit (BioAssay Systems, Hayward, CA). Osmolality of the supernatant collected for tissue osmolality measurement was measured using a vapor pressure osmometer (model 5520, Wescor, Logan, UT).

Quantitative immunoblotting

Renal tissues were homogenized and prepared for Western blotting as described in CHAPTER I (page no. 34). An antibody directed against the C-terminal of UT-A1, previously validated for use in immunoblotting (143), was generously shared by Dr. Janet Klein, Emory University.

Immunofluorescence staining

Immunofluorescent analysis of at least 3 images of the inner medulla of WT and EHD4-KO mice (n = 4 mice per group) were performed using the method described in CHAPTER I (page no. 35). The following primary antibodies were used: rabbit anti-UT-A1 (raised against the C-terminal of rat UT-A1, amino acids 911-929, Catalogue# SPC-406D,

1:200 dilution, StressMarq, Victoria, BC, Canada); goat anti-AQP2 (1:2000 dilution, Santa Cruz Biotechnology, Dallas, TX). Because the above UT-A1 antibody recognizes the C-terminal of UT-A1, it also cross-reacts with UT-A2; however, the antibody would only bind with UT-A1 in the principal cells (marked by AQP2), which does not express any UT-A2.

Statistical analyses

Statistical analyses were performed as described in CHAPTER I (page no. 36).

Results

EHD4-KO mice have a higher urinary urea excretion than WT mice

Urinary urea excretion was significantly higher in both male and female EHD4-KO mice than that in WT mice (Fig. 30) when maintained on a regular rodent chow containing 19% protein. The difference in urinary urea excretion in EHD4-KO was over twice than that in WT mice. Plasma urea concentration was slightly lower (~16% in males and ~10% in females) in EHD4-KO mice than WT mice (Fig. 31), but the difference did not reach statistical significance.

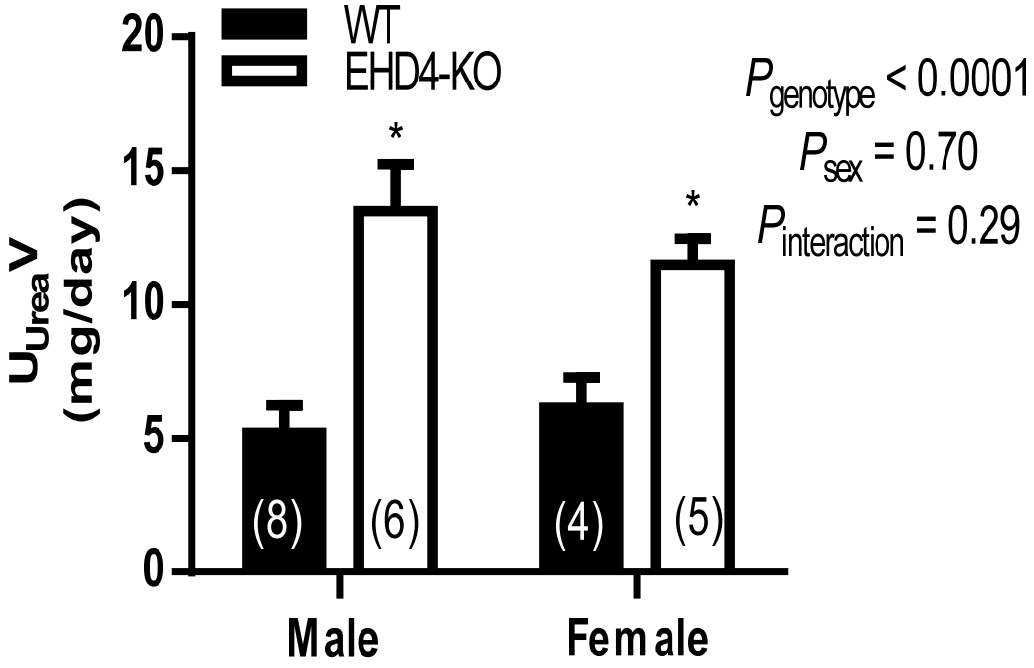

Figure 30: Effect of EHD4 deletion on urinary urea excretion. 24 h urinary urea excretion in male and female WT and EHD4-KO mice during standard rodent chow intake. All values are means ± SEM of n mice (in parentheses). Data were analyzed by 2-factor ANOVA, testing for main effects of genotypes ($P_{genotype}$), sex (P_{sex}), and the interaction between sex and genotype ($P_{interaction}$). * $P < 0.05$ for EHD4-KO vs. WT mice of each sex, by post hoc test.

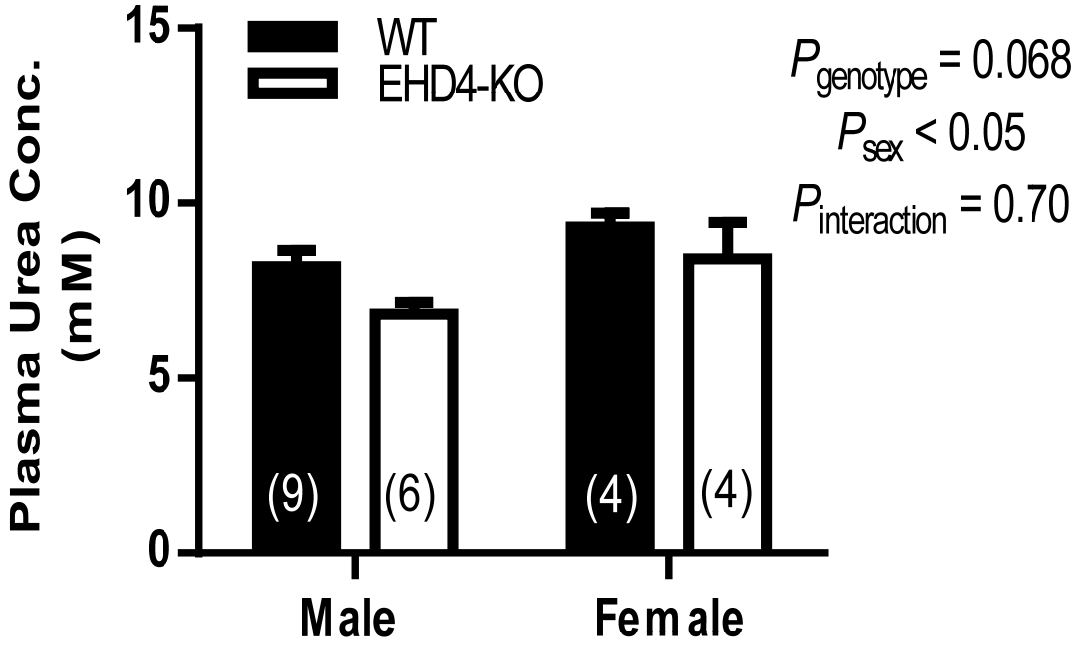

Figure 31: Effect of EHD4 deletion on plasma urea concentration. Plasma urea concentration in male and female WT and EHD4-KO mice during standard rodent chow intake. All values are means ± SEM of n mice (in parentheses). Data were analyzed by 2-factor ANOVA, testing for main effects of genotypes ($P_{genotype}$), sex (P_{sex}), and the interaction between sex and genotype ($P_{interaction}$). * $P < 0.05$ for EHD4-KO vs. WT mice of each sex, by post hoc test.

EHD4-KO mice showed an exaggerated diuretic response to high protein diet compared to EHD4-HOM mice

When fed a 20% protein diet, both male and female EHD4-KO mice had higher urine flow and urinary urea excretion than EHD4-HOM mice (Fig. 32 and 33). In female mice, the differences in the urine flow (Fig. 32A) and urinary urea excretion (Fig. 32B) between EHD4-HOM and EHD4-KO mice were further increased during 40% protein diet intake. In female mice, 6% protein diet reduced the urine flow and urinary urea excretion in both EHD4-HOM and EHD4-KO mice such that these parameters were no longer significantly different (Fig. 32A and B).

Both urine flow and urinary urea excretion remained higher in male EHD4-KO mice than EHD4-HOM mice when fed with 40% protein diet (Figure 33A and B). Moreover, both the urine flow and urinary urea excretion was higher in male EHD4-KO mice than EHD4-HOM mice when fed with 6% protein diet (Figure 33A and 33B).

Although the amount of food intake was similar in both male and female EHD4-HOM and EHD4-KO mice for each particular diet, the total amount of food consumed declined as the protein content of the diet increased (Fig. 34A and 35A). Total protein intake was comparable between the two genotypes for each of the diets, with the exception of the female mice on the high protein diet (Fig. 34B and 35B). Protein content in the diet had a positive effect on the amount of water intake in both the genotypes ($P_{diet} < 0.05$), resulting in an increase in amount of water consumed during high protein diet; however, the difference in the water intake between the EHD4-HOM and EHD4-KO mice remained comparable for each of the diets (Fig. 34C and 35C). The amount of water intake was significantly higher in male EHD4-KO mice than in EHD4-HOM mice when fed with 6% protein diet (Fig. 35C). Changes in body weight in mice during each of the protein diets were comparable between the two genotypes in both the sexes (Fig. 34D and 35D).

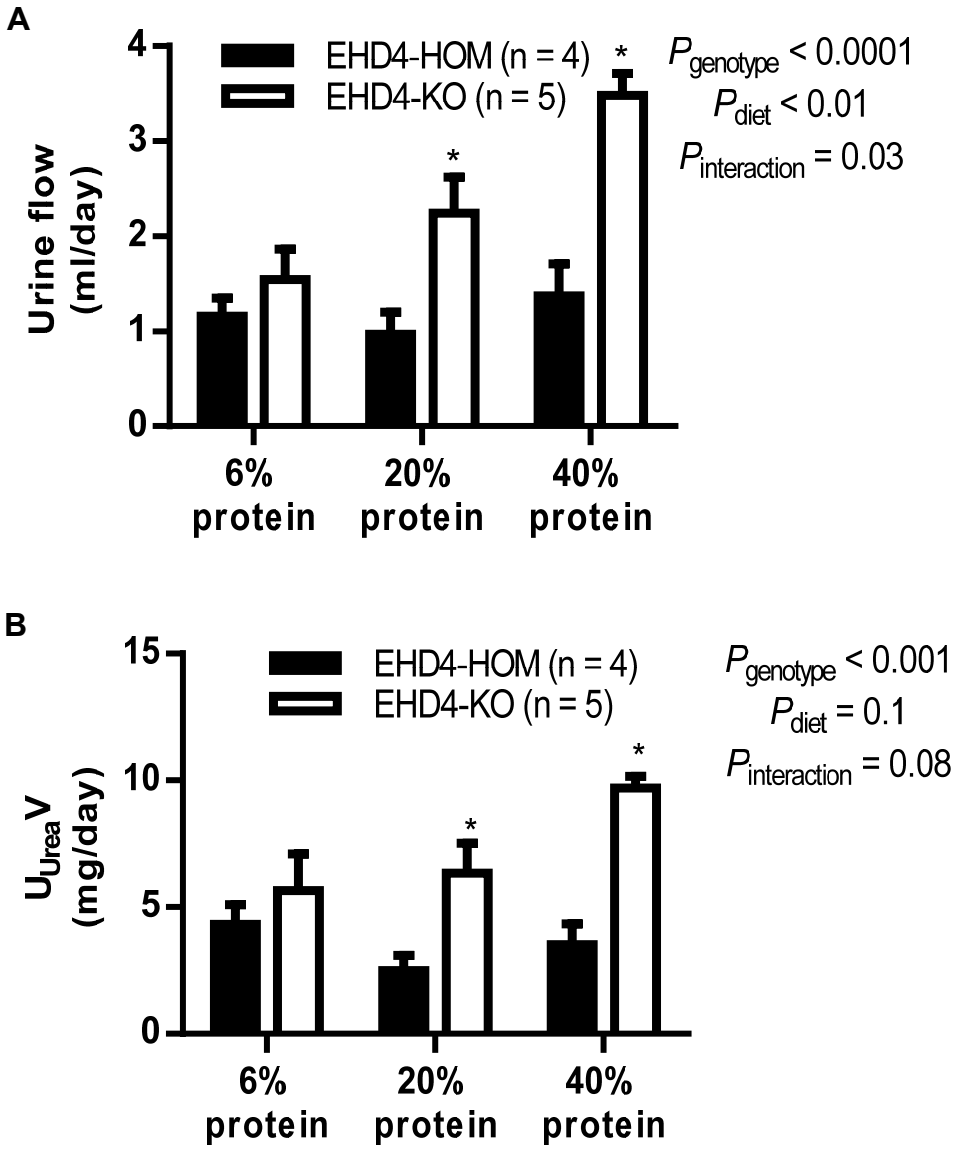

Figure 32: Effect of manipulation of dietary protein on renal urea handling in female mice. Data presented are 24 h urine flow (A) and urinary urea excretion (B) in female EHD4-HOM and EHD4-KO mice fed with 6%, 20%, and 40% protein diets. All values are means ± SEM of n mice (in parentheses). Data were analyzed by 2-factor ANOVA, testing for main effects of genotypes ($P_{genotype}$), diet (P_{diet}), and the interaction between diet and genotype ($P_{interaction}$). * $P < 0.05$ for EHD4-KO vs. EHD4-HOM mice at a particular diet, by post hoc test.

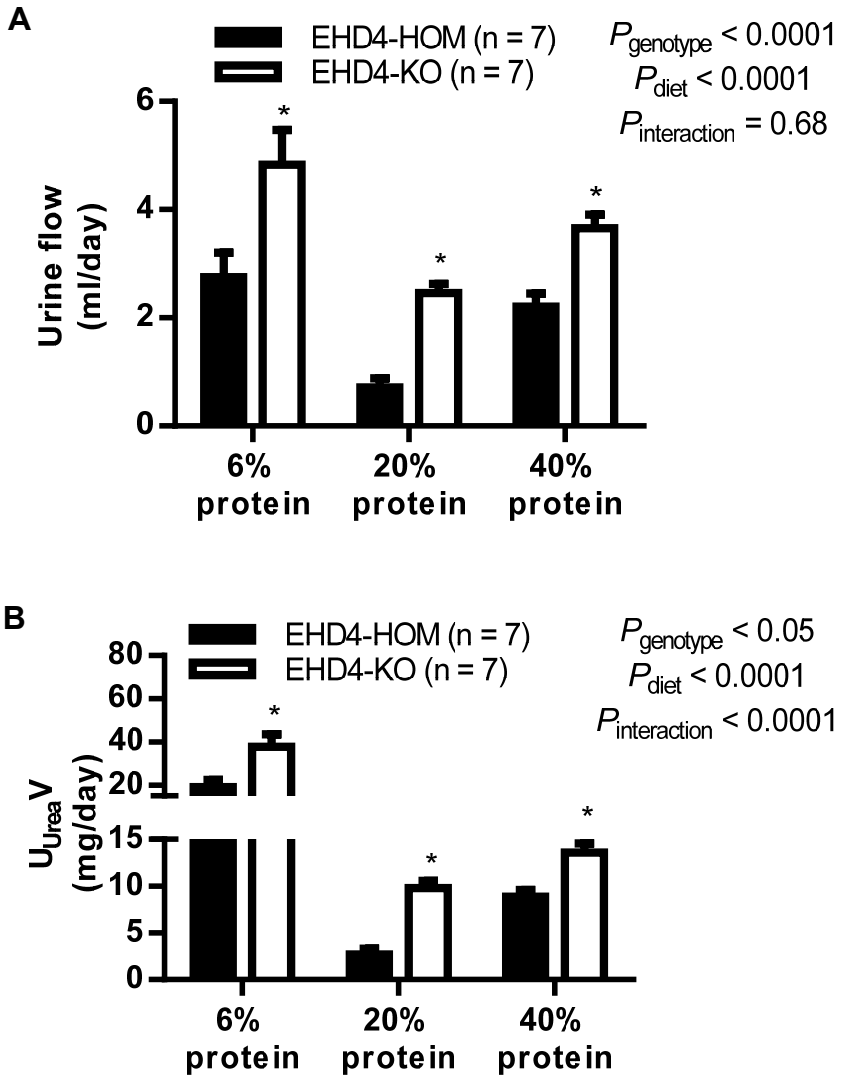

Figure 33: Effect of manipulation of dietary protein on renal urea handling in male mice. Data presented are 24 h urine flow (A) and urinary urea excretion (B) in male EHD4-HOM and EHD4-KO mice fed with 6%, 20%, and 40% protein diets. All values are means ± SEM of n mice (in parentheses). Data were analyzed by 2-factor ANOVA, testing for main effects of genotypes ($P_{genotype}$), diet (P_{diet}), and the interaction between diet and genotype ($P_{interaction}$). * $P < 0.05$ for EHD4-KO vs. EHD4-HOM mice at a particular diet, by post hoc test.

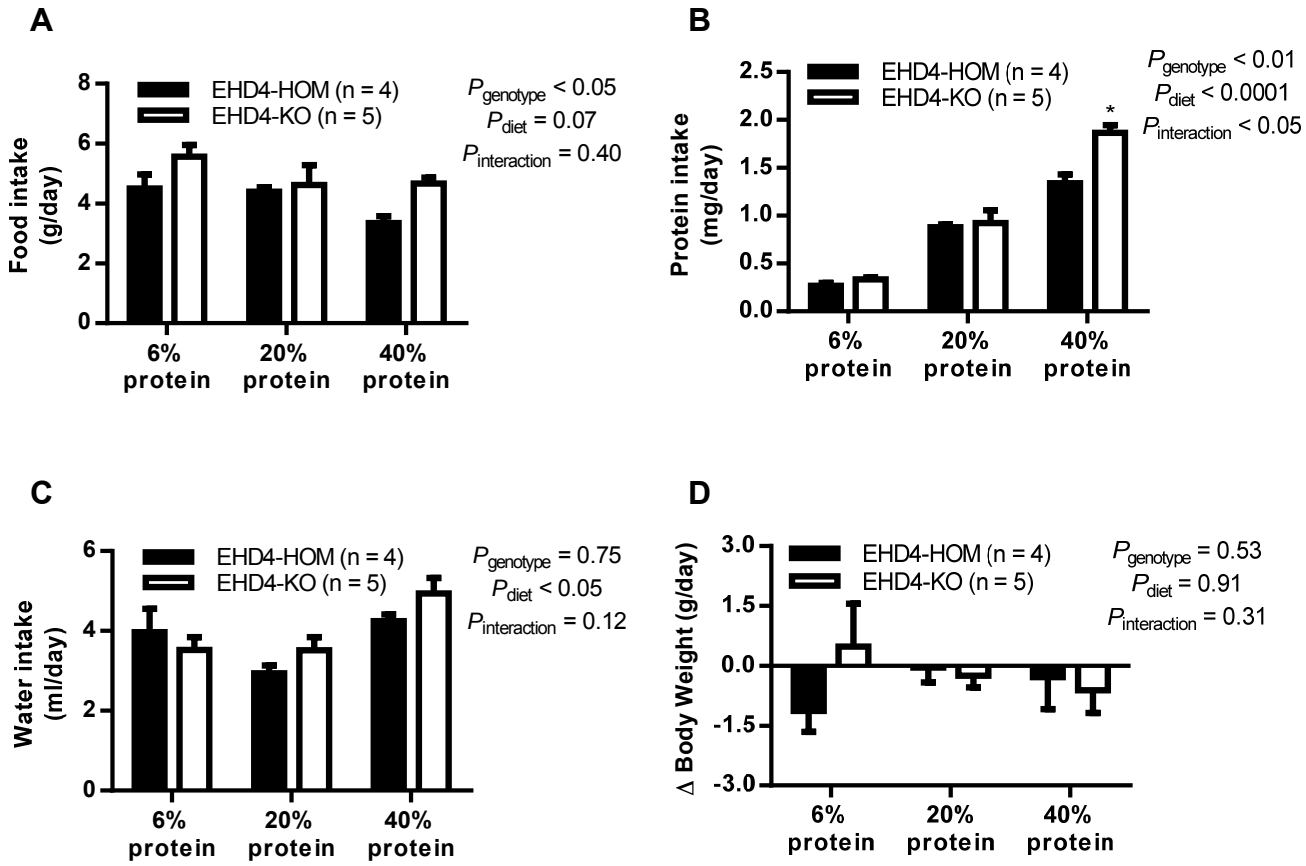

Figure 34: Effect of manipulation of dietary protein on general metabolic parameters in female mice. Data presented are 24 h food intake (A), protein intake (B), water intake (C), and change in body weight in female EHD4-HOM and EHD4-KO mice fed with 6%, 20%, and 40% protein diets. All values are means ± SEM of n mice (in parentheses). Data were analyzed by 2-factor ANOVA, testing for main effects of genotypes ($P_{genotype}$), diet (P_{diet}), and the interaction between diet and genotype ($P_{interaction}$). * $P < 0.05$ for EHD4-KO vs. EHD4-HOM mice at a particular diet, by post hoc test.

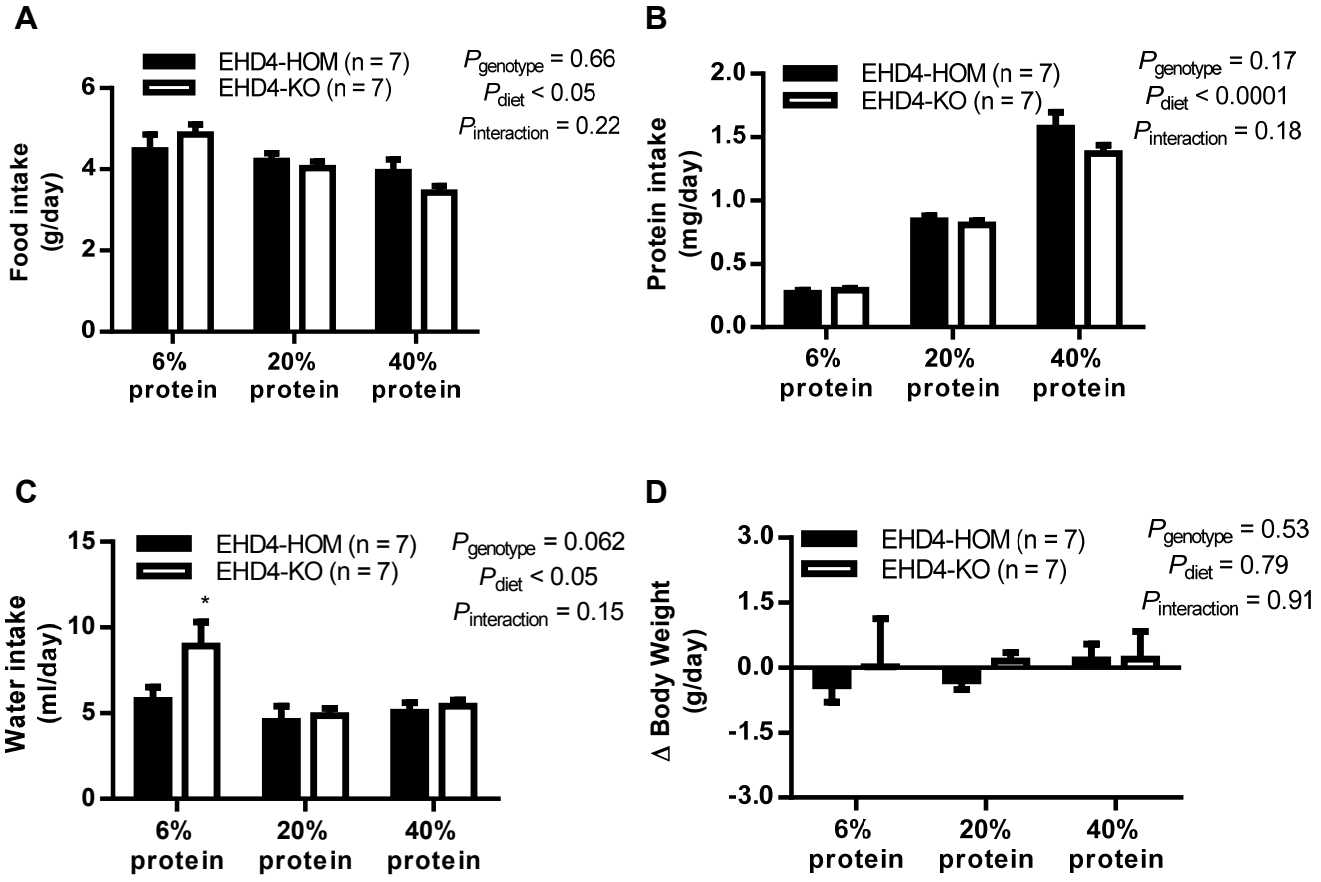

Figure 35: Effect of manipulation of dietary protein on general metabolic parameters in male mice. Data presented are 24 h food intake (A), protein intake (B), water intake (C), and change in body weight in male EHD4-HOM and EHD4-KO mice fed with 6%, 20%, and 40% protein diets. All values are means ± SEM of n mice (in parentheses). Data were analyzed by 2-factor ANOVA, testing for main effects of genotypes ($P_{genotype}$), diet (P_{diet}), and the interaction between diet and genotype ($P_{interaction}$). * $P < 0.05$ for EHD4-KO vs. EHD4-HOM mice at a particular diet, by post hoc test.

Tissue osmolality and tissue urea concentration in EHD4-KO mice were comparable to those in EHD4-HOM mice when fed with 20% protein diet

In mice maintained on a 20% protein diet, there was a gradient of increasing tissue osmolality from renal cortex to the inner medulla in both male and female EHD4-HOM and EHD4-KO mice (Figure 36A and 37A) ($P_{tissue} < 0.0001$). Deletion of EHD4 did not have a significant effect on tissue osmolality in either sex ($P_{genotype} > 0.05$). Tissue urea concentration also exhibited a similar increasing gradient as the tissue osmolality, with the highest concentration present in the inner medulla ($P_{tissue} <0.0001$) (Fig. 36B and 37B). The tissue urea concentration across the three kidney regions were comparable in both the genotypes (Fig. 36B and 37B).

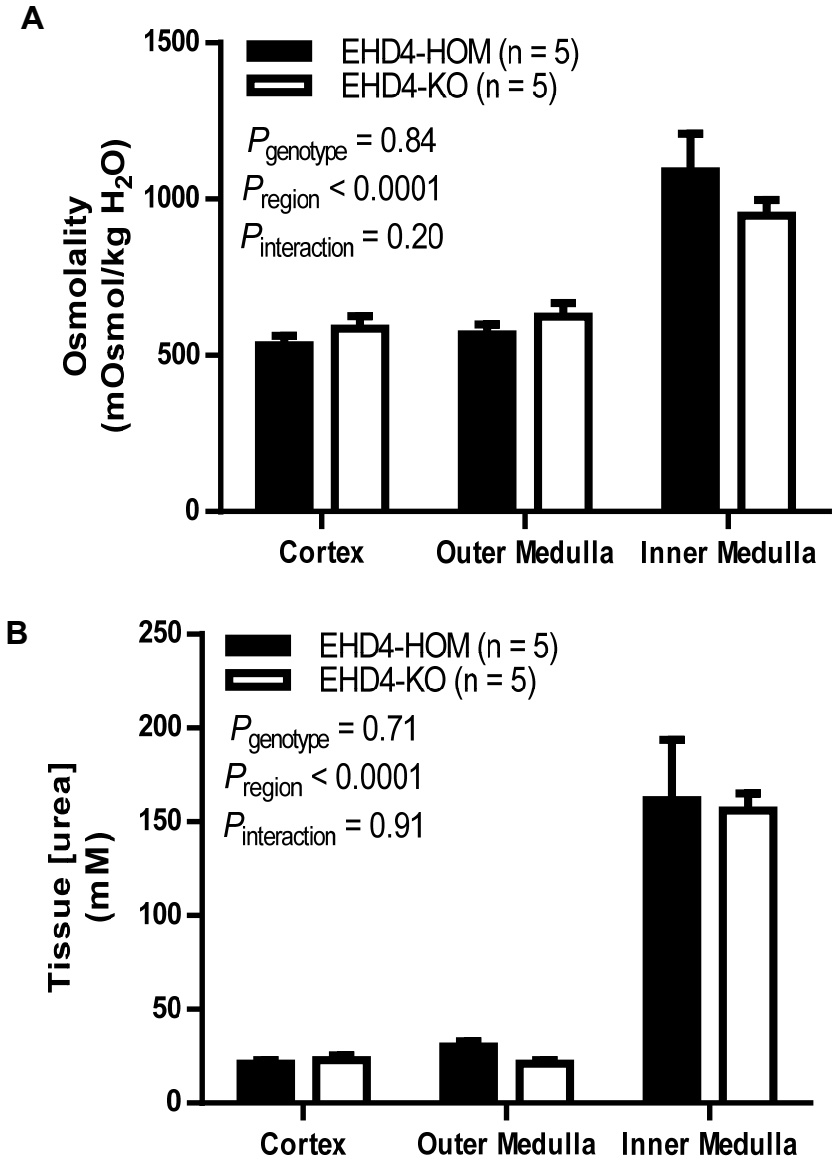

Figure 36: Role of EHD4 in the regulation of renal osmotic gradient in female mice. Data presented are tissue osmolality (A) and tissue urea concentration (B) in female EHD4-HOM and EHD4-KO mice fed with 20% protein diet. All values are means ± SEM of n mice (in parentheses). Data were analyzed by 2-factor ANOVA, testing for main effects of genotypes ($P_{genotype}$), renal region (P_{region}), and the interaction between diet and genotype ($P_{interaction}$).

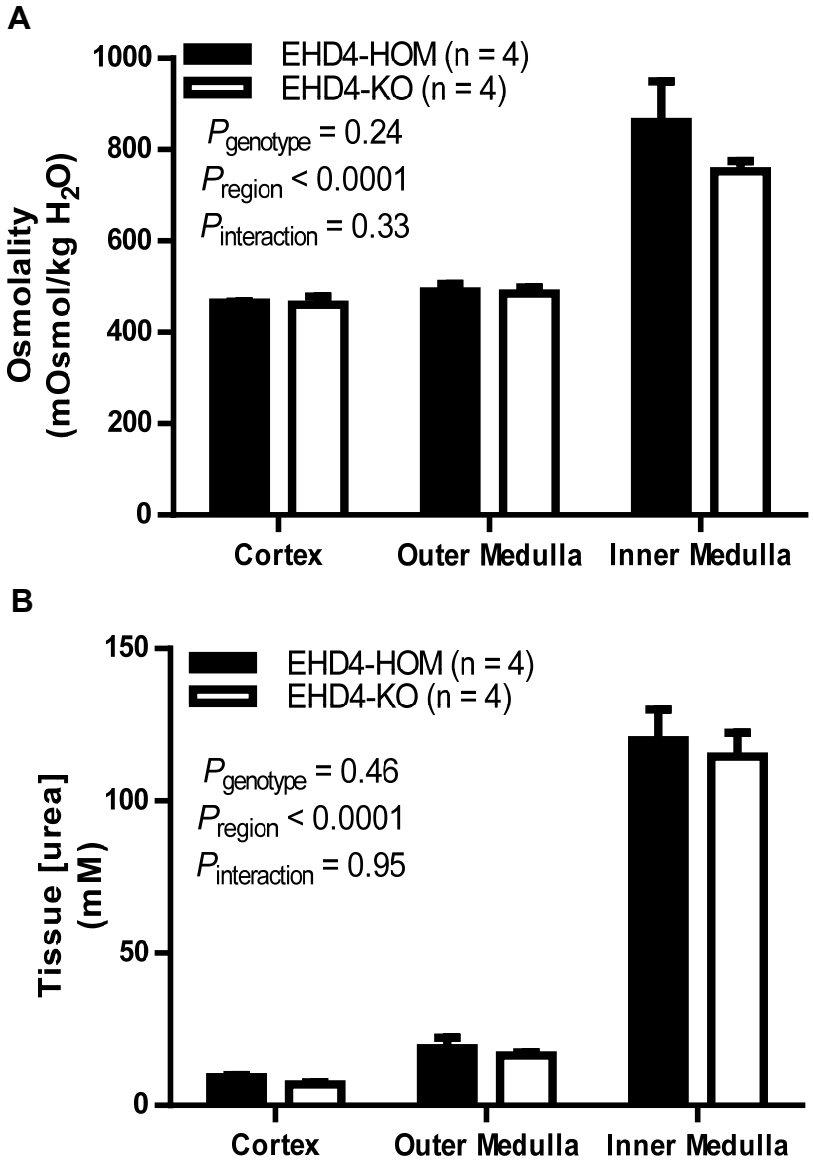

Figure 37: Role of EHD4 in the regulation of renal osmotic gradient in male mice. Data presented are tissue osmolality (A) and tissue urea concentration (B) in male EHD4-HOM and EHD4-KO mice fed with 20% protein diet. All values are means ± SEM of n mice (in parentheses). Data were analyzed by 2-factor ANOVA, testing for main effects of genotypes ($P_{genotype}$), renal region (P_{region}), and the interaction between diet and genotype ($P_{interaction}$).

Cellular distribution of UT-A1 appeared more peri-nuclear in EHD4-KO mice than in WT mice

Higher urea excretion in EHD4-KO mice could arise from a reduced cellular abundance of UT-A1 in the inner medulla. To test if UT-A1 was lower in the EHD4-KO mice than in WT mice, the total abundance of UT-A1 in the inner medulla was examined. Immunoblotting revealed no difference in the overall UT-A1 abundance between the two genotypes (Fig. 38). To investigate if the apical membrane accumulation of UT-A1 was reduced in the EHD4-KO mice, the cellular localization of UT-A1 in principal cells of the IMCD was studied using immunofluorescence staining. Tissues were co-stained with AQP2 antibody to mark principal cells, which express UT-A1 and UT-A3. The antibody used for staining recognizes the C-terminal of UT-A1, which allows for the visualization of only UT-A1 in these principal cells. Qualitative analysis of UT-A1 staining revealed increased staining of UT-A1 in EHD4-KO mice than in WT mice (Fig. 39). Moreover, UT-A1 in EHD4-KO mice appeared to be localized more towards the nucleus, whereas it was more towards the apical membrane in the WT mice.

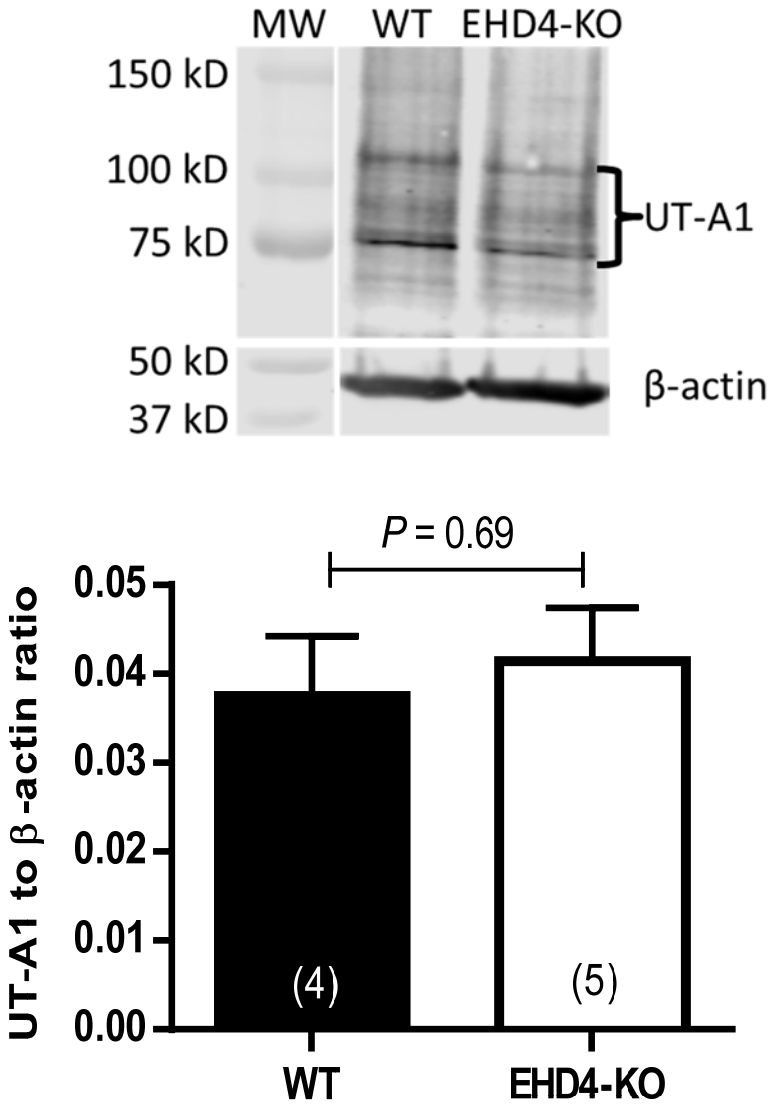

Figure 38: Effect of EHD4 deletion on the total cellular abundance of UT-A1. Representative immunoblot and densitometric quantification of UT-A1 in IM of female WT and EHD4-KO mice. All values are means ± SEM of n mice (in parentheses). Data were analyzed by unpaired *t* test.

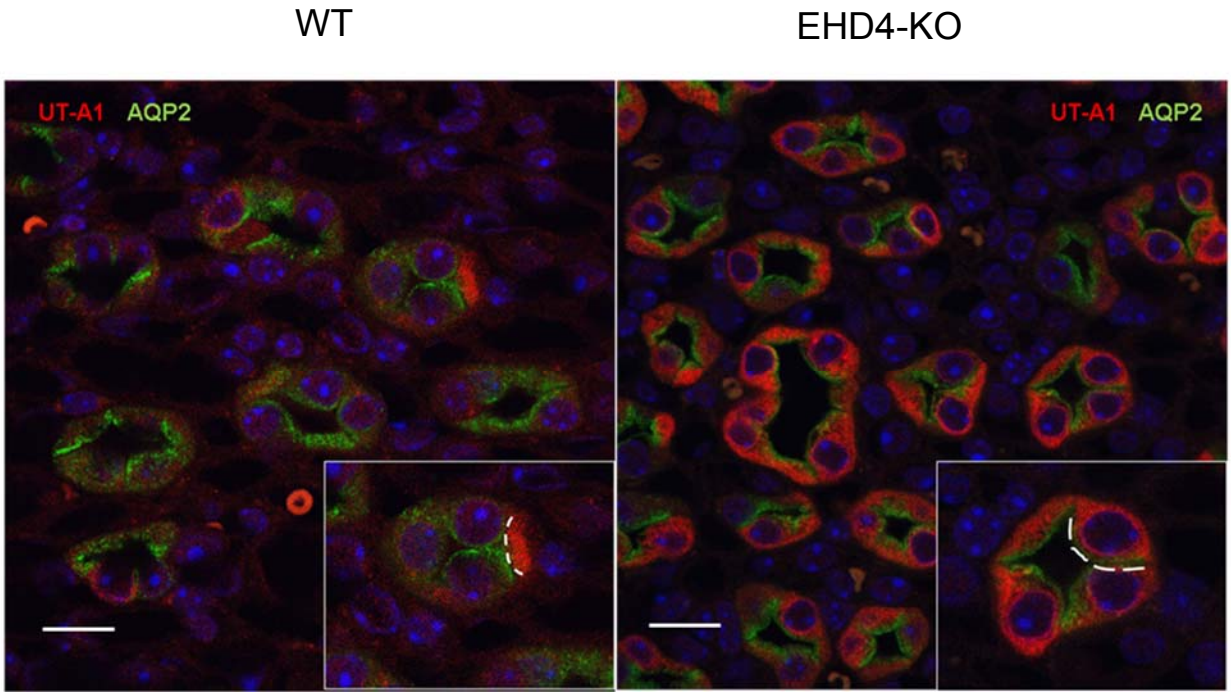

Figure 39: Effect of EHD4 deletion on the cellular localization of UT-A1. Representative immunofluorescent images of UT-A1(red) in IM of female WT and EHD4-KO mice (n = 4 per group; 3 images per animal). Samples were co-stained with AQP2 (green) to identify principal cells in the IM. Gain settings for red channel was intensified to visualize UT-A1 in the WT samples, and was maintained at the same level during analysis of EHD4-KO samples. Enlarged image of a tubule from each genotype is shown in the inset. Scale bar, 10 μm.

Discussion

This study focused on the role of EHD4 in the regulation of renal urea handling. EHD4-KO mice develop a diuretic phenotype that is very similar to that observed in mice lacking UT-A1/A3, including high urine flow and reduced urine osmolality, thereby suggesting a potential role of EHD4 in urea handling. In line with the hypothesis, a significantly higher urea excretion was observed in EHD4-KO mice than both WT and EHD4-HOM mice when fed with rodent chow containing a normal protein content (either 19 or 20%). Increasing protein content in the diet to 40% further increased the urine flow and urinary urea excretion in EHD4-KO mice compared to EHD4-HOM mice, and at least in females, the diuretic phenotype was attenuated in EHD4-KO mice when fed with 6% protein diet. Although EHD4 may not be involved in the generation and preservation of the renal osmotic gradient in mice fed with 20% protein diet, the preliminary data on UT-A1 localization suggest a potential role of EHD4 in the regulation of UT-A1. Thus, I conclude that the diuretic phenotype in EHD4-KO mice may be partially attributable to defective urea handling in the kidney.

Urea handling in the kidney is an important regulator of the urine-concentrating mechanism, allowing the kidney to produce a hyperosmotic urine. Most of the current understanding on the role of urea in urine-concentrating mechanisms derive from the fundamental urea handling model proposed by Berliner in the late 1950s (8). In this elegant model, Berliner described that the urea accumulation in the IMCD does not evoke osmotic diuresis due to the high urea permeability of the IMCD that results from the presence of urea transporters. Indeed, dysregulation of renal urea handling in the IMCD, such as during the absence of functional urea transporters UT-A1/A3, has been shown to impact the ability to properly concentrate urine (44, 45). These studies have reported that UT-A1/A3 double knockout mice develop severe polyuria without any aberrant renal

morphology (159), comparable to what has been observed in EHD4-KO mice. Consistent with these observations, EHD4-KO mice was found to have an increased urinary urea excretion compared to WT mice, almost twice than that in WT mice. Moreover, the plasma urea concentration was also slightly reduced in EHD4-KO mice (~10-16%), which is consistent with urea wasting and also suggests that the increased urea excretion in the EHD4-KO mice is not due to increased production of urea.

The excretion of urea by the kidney is thought to be dependent on two factors: the filtered load of urea and the amount of urea reabsorbed along the nephron. Increased urinary urea excretion in EHD4-KO mice may possibly arise due to a reduced reabsorption of urea in the IMCD, where EHD4 is abundantly expressed. Urea reabsorption in the IMCD occurs in two steps: entry of urea from the luminal fluid into the principal cells via UT-A1 followed by exit into the renal interstitium via the UT-A3 in the basolateral side. The cellular abundances of both UT-A1 and UT-A3 are regulated by various cellular mechanisms, including endocytosis (11, 186). The polyuria observed in EHD4-KO mice is similar to that observed in mice lacking both UT-A1 and UT-A3 (45). In these UT-A1/A3 double knockout mice, transgenic overexpression of UT-A1 restores the diuretic phenotype, suggesting that UT-A1 is necessary for basal maximal urinary concentration (92), a parameter which is also defective in EHD4-KO mice. Therefore, it could be possible that in EHD4-KO mice the amount of UT-A1 may be reduced in the IMCD, causing reduced urea reabsorption in the IMCD. Proteins from the UT-A family share a high degree of sequence homology because they are splice variants derived from the same gene (175), making it quite challenging to accurately identify and quantify these transporters in the renal tissues by immunostaining. An antibody raised against the C-terminal of the parent UT-A protein was used that recognizes UT-A1 (expressed in the IMCD), UT-A2 (expressed in the thin descending limb), and UT-A4 (expressed in the IMCD of rat, not mouse). The bands

around ~97 kD were identified as UT-A1, similar to what has been reported previously (12). Western blotting of inner medulla for total UT-A1 did not show any statistically significant difference in the abundance of UT-A1 between EHD4-KO and WT mice. Because total cellular abundance of a protein does not indicate its abundance in the membrane, immunofluorescence staining was employed to examine the cellular localization of UT-A1. Using a commercially available UT-A1 antibody that recognizes the same epitope of UT-A1, a dramatic and contrasting difference in the staining intensity of UT-A1 between the two genotypes was observed. UT-A1 staining appeared more intense and peri-nuclear in EHD4-KO mice than that in WT mice. These results, albeit conflicting with the Western blot data, suggest a potential role of EHD4 in the regulation of UT-A1 trafficking in the principal cells. Future studies involving UT-A1-transfected principal cell line would be needed to probe further into the role of EHD4 in UT-A1 trafficking. Such a set up would allow us to understand the role of EHD4 in the trafficking of UT-A1 specifically in the principal cells and allow us to identify if and how EHD4 regulates UT-A1.

In the liver, catabolism of amino acids derived from dietary protein generates urea, which is then excreted by the kidney. The filtered load of urea in the kidney is, therefore, in part dictated by the amount of dietary protein. In his urea-handling model (8), Berliner had proposed that in the setting of dysfunctional urea transportation in the IMCD, an increased filtered load of urea would result in a urine-concentrating defect. This urine-concentrating defect would arise because less urea would be reabsorbed from the tubular lumen, which would increase the amount of urea in the lumen and therefore result in urea-induced diuresis. He further described that this urine-concentrating defect would be subsequently reversed when the filtered urea load is reduced. It is currently hypothesized that the high urea excretion in EHD4-KO mice is at least partly due to a defective urea reabsorption in the IMCD. Hence, I proceeded to test this hypothesis further using the

aforementioned model of manipulating filtered urea load with dietary protein. When fed with 40% protein diet, there was a further increase in the urine flow and urinary urea excretion in both male and female EHD4-KO mice. In female mice particularly, the shift from 20% to 40% protein diet resulted in a greater differences in those renal parameters between the EHD4-HOM and EHD4-KO mice. However, the difference in the urine flow and urea excretion between the two female genotypes were comparable when the diet was switched to 6% from 40% protein. The disappearance of differences in these renal parameters in the female mice suggest that EHD4-KO mice could effectively reabsorb enough urea from the tubule via the available UT-A1 in the membrane when urea load is reduced. These findings are in line with Berliner's urea-handling model, and the data strongly suggest that EHD4 regulates urea handling in the kidney. Moreover, the exaggerated diuretic response to high protein diet in EHD4-KO mice is very comparable to that seen in UT-A1/A3 double knockout mice (45). In these UT-A1/A3 double knockout mice, the diuretic phenotype is restored when UT-A1 is transgenically overexpressed in these mice (92), showing that UT-A1, and not UT-A3, is required for basal urine-concentrating ability. Therefore, the current working hypothesis is that in EHD4-KO mice, the accumulation of UT-A1 in the apical membrane of principal cells is reduced. This reduction causes a decrease in the amount of urea that can be reabsorbed in the IMCD, thereby resulting in an accumulation of urea in the tubular lumen. Because of this urea accumulation, EHD4-KO mice develop urea-induced diuresis. Although the immunofluorescence staining of UT-A1 in the kidney sections suggested increased peri-nuclear localization of UT-A1 in EHD4-KO mice, the results are inconclusive. The role of EHD4 in regulating apical UT-A1 localization require further analysis, such in a cell culture model.

Modulation of filtered urea load via modification of dietary protein intake is a model that has been used successfully in many previous studies to understand renal urea handling (44, 45, 47); however, I became aware of the limitations of this model during these experiments. One of the unexpected results of this study was the discovery of a sex difference in the response to 6% protein diet. In male mice, both the urine flow and urinary urea excretion was further elevated in both the genotypes during 6% protein intake. The increased diuresis was matched by an increase in water intake. It has been previously reported by others that low protein diet triggers a urine-concentrating defect in rats (76, 77) and it is proposed that this defect arises in an attempt to conserve nitrogen in the body. It is possible that in the male mice low protein intake triggers a metabolic stress response to allow the urea to be recycled back to the liver to conserve nitrogen. In doing so, the renal urea gradient is compromised and the tissue osmotic gradient is washed out, resulting in a urine-concentrating defect. Recent studies have shed some light on how protein restriction may stimulate the integrated stress response pathways (97-99). A recent study has shown that these pathways are more active in female mice than in males during amino acid-restricted diet (105), providing a better adaptive capacity in females during amino acid restriction. It is possible that female mice can adapt faster to the low protein diet and overcome the nitrogen deficit faster than male mice, thereby not showing the urine-concentrating defect. Another reason for the urine-concentrating defect in male mice could be due to a residual effect of the high protein diet. Because the diets in the mice were switched from 40% to 6%, it is possible that some of the effects of the 40% protein diet could have been retained in the male mice, thereby causing diuresis. In future, a better approach to rule out this residual effect of 40% protein diet would be to step down the protein level gradually to 20% and then to 6% protein. Probing into the role of EHD4 in renal urea handling in mice maintained on 6% protein diet and understanding the effect of sex on renal urea handling are some of the exciting future directions for this work.

Urea undergoes a significant amount of recirculation in the kidney that allows for the sequestration of urea in the renal medulla (102). The disproportional reabsorption of water and urea results in a high concentration of urea in the fluid that arrives in the IMCD. This mechanism allows urea to diffuse into the interstitium via UT-A1 and UT-A3, thereby resulting in an accumulation of urea in the inner medulla of the kidney. This accumulated urea in the inner medulla, however, may escape into the blood via the ascending vasa recta. This risk is overcome by the parallel and close arrangement of the vasa recta and the tubules that allows the urea to be recycled back into the descending vasa recta (via UT-B) and into the descending thin limbs (via UT-A2). Therefore, urea recycling within the renal interstitium helps in the generation and maintenance of the osmotic gradient required for concentrating urine. The current data suggest that the generation and preservation of the renal tissue osmolality and urea concentration is independent of EHD4. Moreover, there was no difference in the amount of tissue urea between EHD4-HOM and EHD4-KO mice, even though the functional data suggests a role of EHD4 in the reabsorption of urea. Previous studies have reported compensatory upregulation of urea transporters in the absence of one or more urea transporters in mice (90). In one particular study (90) with UT-B knockout mice, there was almost a 120% increase in the abundance of UT-A2 in the outer medulla, indicating that mice are capable of an adaptive response to the loss of a urea transporter that may allow them to maintain a functional intrarenal urea recycling pathway. Despite a high urea excretion, EHD4-KO mice may be able to maintain a steady urea concentration possibly by increasing the recycling of urea between the vasculature and tubule. EHD4-KO mice indeed have a slightly reduced plasma urea level than WT mice, suggesting that may be there is an increased recycling of urea via UT-B from the vasa recta into the inner medulla. The expression profiles of other renal urea transporters will need to be assessed in order to fully understand how EHD4-KO mice are able to preserve the osmotic gradient in the kidney despite high urea excretion. One of the major

technical difficulties with studying each of these urea transporters is the lack of specific commercial antibodies for each of the urea transporters. The available antibodies in the market cross-react with the other isoforms, making quantitative analysis difficult to perform.

Most of the current understanding of renal urea handling are based on hypothetical models proposed by various groups, and ongoing studies have helped shed light on the complexity of the process. These data strongly suggest a role of EHD4 in the regulation of renal urea handling. In the light of the current data, wherein high levels of EHD4 expression are found in the IMCD, it is hypothesized that EHD4 is most likely to regulate the reabsorption of urea in the IMCD; however, the exact role of EHD4 in the regulation renal urea handling remains unclear. As mentioned before, RNA sequencing data has shown that EHD4 is also expressed in the thin limbs, so it is also possible that EHD4 may regulate UT-A2 in the thin limbs. **The working hypothesis is that EHD4 regulates the membrane accumulation of UT-A1 in the IMCD. A lack of EHD4 in mice reduces the membrane accumulation of these urea transporters in the IMCD, thereby reducing urea reabsorption and causing a urea-induced osmotic diuresis.**

DISCUSSION

Major findings of the dissertation

The experiments performed in this dissertation have provided novel insights into the physiological and cellular role of a regulator of endocytic recycling. Endocytic recycling is an important cellular mechanism that is involved in the regulation of extracellular fluid osmolality (46, 75). EHD4 regulates endocytic recycling, but the specific role of EHD4 pertaining to renal water and solute handling remains largely unknown. The overall aim of this dissertation was to elucidate the role of EHD4 in the kidney in order to bridge some of the gap in the knowledge of cellular machinery involved in the regulation of renal channels and transporters. This dissertation described for the first time a role of EHD4 in the regulation of trafficking of AQP2 and AQP4 in principal cells, and recycling of urea in the kidney. This study provides important insights on the cellular machineries of the endocytic recycling process in the kidney, and shows how the lack of a regulator of endocytic recycling can have a profound effect on the kidney's ability to handle water and urea.

This study has shown for the first time that EHD4 is an important regulator of urine formation and composition. A major finding of this study has been the discovery that EHD4 regulates renal water handling, and in its absence EHD4-KO mice were found to develop a diuretic phenotype. Experiments from Chapter I revealed that EHD4 is required for the control of basal and maximal urine concentration, and anti-diuretic responses during 24-h water restriction is independent of EHD4. Data gathered in Chapter I also revealed that EHD4 might not regulate the central release of AVP in mice. Additionally, in Chapter III EHD4 was discovered to be involved in the regulation of renal urea handling, a complex physiological process that is crucial for concentrating urine. Albeit weak, current data suggest a potential role of EHD4 in the regulation of UT-A1 cellular localization in principal cells.

Investigations in Chapter II revealed that EHD4 regulates the membrane abundance of both AQP2 and AQP4 in their respective membranes in principal cells. Although several studies have identified and isolated protein complexes found within AQP2-containing vesicles in principal cells, very limited information is available regarding the exact role of these proteins in the actual trafficking event. Studies in Chapter II of this dissertation have addressed how EHD4 may regulate AQP2 trafficking, and shown that EHD4 reduces the accumulation of glycosylated AQP2 in the apical membrane of principal cells. Both Chapters I and II strongly indicate that EHD4 may not be involved in the classical AVP-mediated regulation of AQP2 trafficking, and may regulate the constitutive recycling of AQP2, an avenue that currently remains largely unexplored in the scientific world. Moreover, almost no information is currently present regarding the trafficking of AQP4 in the kidney. A novel and valuable finding of Chapter II of this dissertation has been the discovery of the role of EHD4 in the regulation of AQP4 trafficking to the basolateral membrane in principal cells. Deletion of EHD4 reduces the membrane abundance of AQP4 in the basolateral membrane of principal cells, which possibly contributes to the diuretic phenotype of the EHD4-KO mice.

In addition, this work also provided evidences supporting the role of EHD4 in the regulation of synthesis of PGE2. This finding provides a possible mechanism of regulation of AQP2 and/or UT-A1 trafficking in the principal cells via EHD4. Moreover, there was a lack of evidence to support a role of EHD4 in the regulation of renal sodium handling. Taken together, these findings indicate that **EHD4 regulates renal water handling, and therefore plays an important role in the formation of urine and its composition. My current working hypothesis is that EHD4 regulates urine formation and composition by regulating the cellular trafficking of AQP2, AQP4, and UT-A1.** Figure 40 summarizes these major findings.

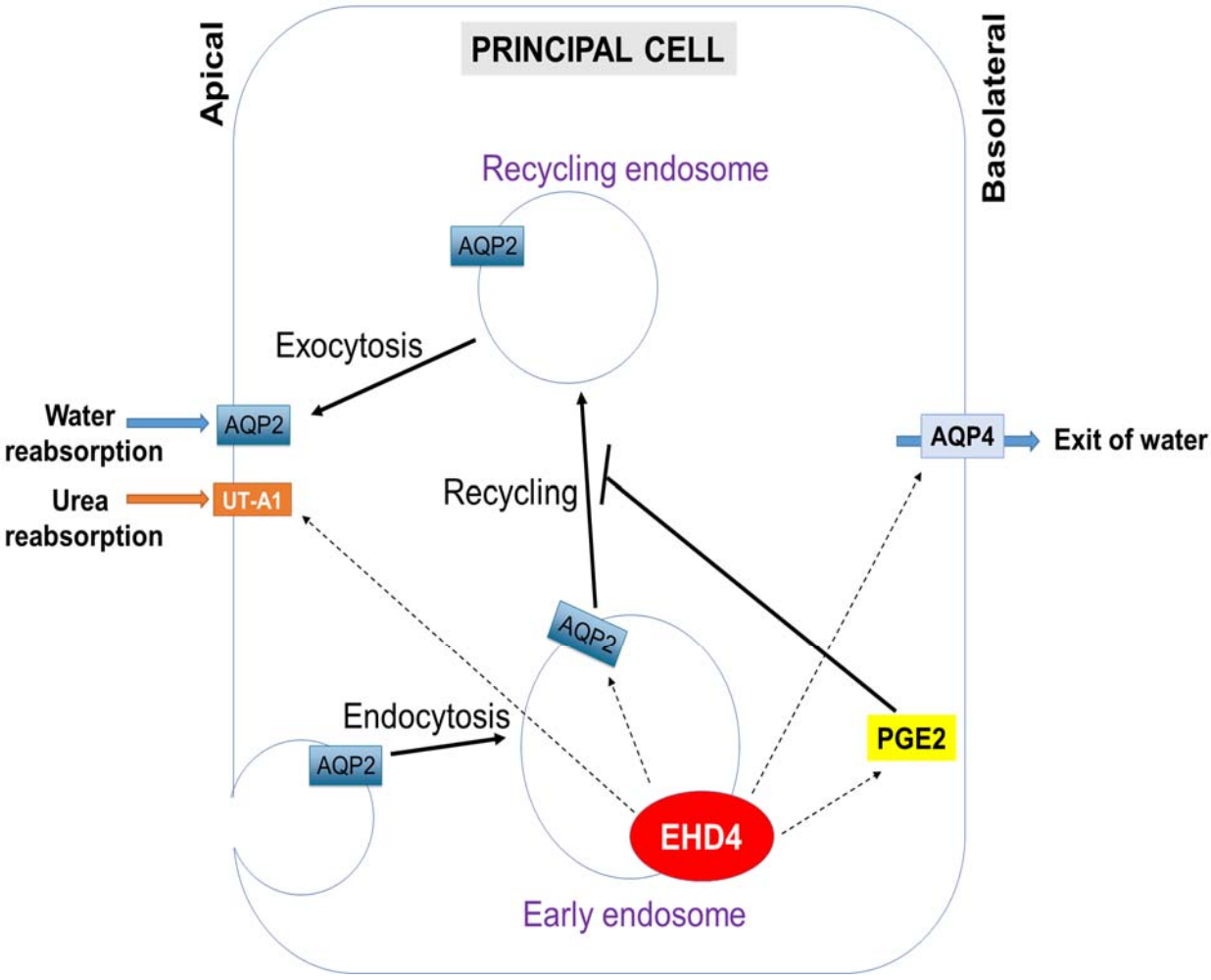

Figure 40: Representative figure of the major findings of this study. Global deletion of EHD4 in mice results in increased urine flow, reduced urine osmolality, and increased urea excretion. Data generated during this study (dashed lines) has shown the role of EHD4 in the regulation of membrane accumulation of AQP2, AQP4, and UT-A1, and the generation of PGE2 in principal cells. EHD4 has also been found to co-localize with AQP2 in cultured principal cells, but immunoprecipitation data suggest a lack of direct physical interaction between the two proteins. Deletion of EHD4 increases the production of PGE2 both in vivo and in vitro. One way PGE2 reduces membrane accumulation of AQP2 in principal cells is via the inhibition of AQP2 recycling (solid line), which has been reported in previous studies (148). Therefore, it is hypothesized that EHD4 deletion results in an increase in PGE2, which in turn may stall the recycling of AQP2 in principal cells.

Potential mechanisms underlying the effect of EHD4 on the subcellular localization of AQP2

A defect in urine-concentrating mechanism may arise due a faulty renal water handling. Fine-tuning of water reabsorption occurs exclusively in the collecting duct, where membrane abundance of the aquaporin water channels of the principal cells determine the water permeability of the collecting duct. The role of EHD4 in the regulation of the cellular localization of the aquaporin channels of the IMCD are discussed in the following section.

Role of EHD4 in the regulation of post-translational modifications of aquaporins of the principal cells

The aquaporin water channels of the principal cells, namely AQP2, -3, and -4, regulate the water permeability of the collecting duct. AQP3 and -4 are constitutively expressed in the basolateral membrane of principal cells, whereas expression of AQP2 in the apical membrane is regulated. It was found that EHD4 deletion reduces the amount of AQP2 in the apical membrane of principal cells of IM in mice (Fig. 16). Additionally, using a cultured principal cell line, it was also found that EHD4 regulates the accumulation of glycosylated AQP2 in the apical membrane of principal cells (Fig. 22), indicating a potential role of EHD4 in regulating the glycosylation process of AQP2. EHD4 does not appear to influence the abundance and localization of non-glycosylated-AQP2. Glycosylation of membrane proteins occur in the rough ER (197) and a distinct peri-nuclear localization of EHD4 was observed in the cultured principal cells (Fig. 24 and 25), thereby raising the possibility that EHD4 to regulate the glycosylation process of AQP2. Additional evidence supporting this notion comes from the data on AQP4 expression in EHD4-KO mice. In the absence of EHD4, the amount of AQP4 is significantly reduced in the basolateral membrane (Fig. 18), and immunoblotting revealed a reduced expression

of glycosylated-AQP4, and not the non-glycosylated form. Together, these data on AQP2 and AQP4 suggest a role of EHD4 in the glycosylation of these membrane proteins, and the specific role of EHD4 in the regulation of glycosylation of membrane proteins remains to be tested in future.

Potential cellular mechanisms by which EHD4 regulates apical membrane abundance of AQP2

EHD proteins usually interact with their partner proteins via an interaction between EH-NPF motifs (135). AQP2 lacks an NPF motif, therefore the chances of a direct physical interaction between AQP2 and EHD4 is small. Moreover, EHD4 was not found in the immunoprecipitate complex containing AQP2 (Fig. 26), suggesting a lack of direct physical interaction between the two proteins. However, EHD4 was found to co-localize with AQP2 (Fig. 25), thereby providing a high possibility for these proteins to interact in some indirect way. A better approach in understanding the exact nature of the interaction between EHD4 and AQP2 would be to transfect principal cells with constructs containing specific domains of EHD4 and then testing to see if AQP2 can be found in the pulled down complexes.

Data from both in vivo and in vitro models show that EHD4 deletion reduces the accumulation of AQP2 in the apical membrane of principal cells. EHD4 is known to regulate the early endosomal trafficking of membrane proteins (178) and in principal cells, it was observed that EHD4 localized near the plasma membrane (Fig. 24 and 25), where early endosomes would be found. These data indicate that one way EHD4 possibly regulates the membrane activity of channels and transporters in principal cells is by regulating the early endosomal trafficking. The protein-protein interaction profile predicts that EHD4 interacts with early endosomal proteins called Rab5 (Fig. 23). It has been reported previously that when EHD4 is absent, the activity of Rab5 increases (178), which in turn may increase early endosomal traffic. Therefore, it is possible that the reduced

membrane abundance of AQP2 in the absence of EHD4 could arise due to increased uptake into the early endosome combined with a reduced entry to the recycling endosome. Sorting of proteins in the early endosome is a highly dynamic process and involves coordinated activity of several proteins, including EHD4 (81). Because early endosomal sorting is dynamic, it would require a robust live-cell imaging technique involving pulse-chase experiments with labelled compounds to follow the dynamics of the traffic of AQP2 through the endosomal system in the principal cell when EHD4 is absent. Such an approach in the future would certainly allow accurate identification of the role of EHD4 in the regulation of AQP2 trafficking, but it was beyond the scope of the current project.

Another possible reason behind the reduced membrane accumulation of AQP2 in EHD4-depleted cells could be due to reduced entry of AQP2 into the recycling endosome. Under basal conditions, AQP2 is known to undergo constitutive recycling (112) and one of the major proteins that regulate the shuttling of AQP2 to and from the recycling endosome is Rab11-Fip2 (137). Rab11-Fip2 is known to interact with EHD proteins (136), therefore it is possible that Rab11-Fip2 may be a common interacting partner between AQP2 and EHD4. Studies with EHD3 have shown that the interaction between EHD3 and Rab11-Fip2 is required for the entry of internalized cargo into the recycling endosome (136). Although interaction between EHD4 and Rab11-Fip2 has not been studied, it is possible that, in the absence of EHD4, the interaction between AQP2 and Rab11-Fip2 may be lost, thereby resulting in reduced entry of AQP2 into the recycling endosome. Due to the lack of a Rab11-Fip2 antibody that works with co-immunoprecipation, this hypothesis remains to be tested using alternative techniques such as yeast-two hybrid binding assay in the future.

Although it is possible that the effect of EHD4 on AQP2 is mediated by physical interactions, it is also very likely that some alternative mechanisms that regulates AQP2

is altered in EHD4-depleted cells. One pathway that was found to be upregulated in EHD4-depleted cells was the synthesis of PGE2 (Fig. 27 and 29). The recycling of AQP2 is negatively regulated by PGE2, so it is quite possible that EHD4 regulates AQP2 recycling in a PGE2-dependent manner.

Physiological roles of EHD4 in the regulation of renal function

Studies performed over several decades have already established the importance of endocytic recycling in the regulation of renal function (75). It was, therefore, not surprising when expression profiling of EHD proteins across tissues revealed the presence of EHD4 in the kidney (58). However, the specific role of EHD4 in the kidney remained unknown, and only very recently a role for EHD proteins in the glomerular microvasculature had been reported (56), but nothing is known regarding the functional role of EHD4 or other EHDs in the tubular system. The overall objective of the work contained in this dissertation has been to elucidate the physiological roles of EHD4 in the regulation of renal function, and to shed some light on to the cellular processes regulated by EHD4 in the kidney.

In order to better understand the exact role of EHD4 in the kidney, it was important to identify the sections of the kidney where EHD4 is expressed. It was found that, among all the nephron sections that could be isolated, EHD4 is expressed the most in the IMCD (Fig. 1). This part of the kidney is exquisitely involved in the fine-tuning of urine formation and its final composition. Consistent with this expression profile, it was found that EHD4-KO mice have a higher urine flow and lower urine osmolality than WT mice (Fig. 5). This diuretic phenotype in EHD4-KO mice suggests that EHD4 is important for regulating urinary water homeostasis. At the level of the kidney, water homeostasis is maintained by two major urine-concentrating mechanisms-

1. Increased permeability of the collecting duct to water, which depends on a functional AVP-AQP2 axis between the hypothalamus and the kidney.
2. High osmolality of the renal medullary interstitial fluid, which depends on effective renal water, sodium, and urea handling mechanisms.

I explored the roles of EHD4 in the regulation of both of these major physiological processes.

Role of EHD4 in the regulation of the hypothalamic-renal feedback mechanisms

Formation and concentration of urine in the kidney depends on the feedback mechanisms involving the hypothalamus (central component) and the kidney (renal component) (75). These central and renal components form the regulatory axis that maintains water balance during variations of water intake and water loss. Along with being expressed in the IMCD, EHD4 was also found to be expressed in the hypothalamus (Fig. 11); however, the exact cell type that expresses EHD4 is not currently known and this was a crude attempt to investigate whether EHD4 is expressed in the hypothalamus. These data suggest that EHD4 could be involved in the regulation of the central and/or renal components of water balance. The interpretation that the diuretic phenotype is due to defective renal water handling rather than primary polydipsia derives primarily from the observations made during the acute water loading experiments (Fig. 6) as well as the subcellular localization of AQP2 (Fig. 16). An i.p. injection of water allowed us to bypass the oral route of water intake. This approach provided a way to assess the role of EHD4 in eliminating a water load without the influence of the thirst mechanism mediated via the central regulatory component of water homeostasis. As shown in figure 6, the diuretic response to an acute water load in EHD4-KO mice was significantly larger than that in WT mice. The exaggeration of the diuretic phenotype in EHD4-KO mice after the water load suggested that the renal component of water homeostasis may be compromised in EHD4-KO mice.

It has been long known that an increase in plasma osmolality is a strong stimulation for the secretion of AVP from the hypothalamus (35). Secreted AVP from the hypothalamus enters the blood circulation and increases the water permeability of the

collecting duct of the kidney to allow concentration of urine (93, 139). A series of observations in EHD4-KO mice so far has led us to believe that the diuretic phenotype of the EHD4-KO mice is not attributable to a central effect of loss of EHD4, given that the role of EHD4 in the hypothalamus is unclear at this point. Firstly, the plasma osmolality of EHD4-KO mice was similar to that in WT mice (Fig. 12A), indicating an ability to conserve water balance even in the light of the diuresis. Secondly, it was also found urinary AVP excretion to be similar between the two genotypes (Fig. 12B). Urinary AVP excretion is not a direct measurement of the circulating AVP, but it has been successfully used before (53, 69) as a surrogate marker for circulating AVP. Similarity of AVP excretion between the two groups indicate that the effect of EHD4 deletion on the regulation of AVP release from the hypothalamus is either negligible or masked by another compensatory mechanism. Indeed, the expression of EHD1 in the hypothalamus increases significantly in EHD4-KO mice (Fig. 11B). EHD proteins possess a high degree of homology with each other (134) and have been reported to compensate for each other in previous studies (56). Therefore, it is possible that the effect of EHD4 deletion on the central component remains masked due to EHD1, which allows keeping AVP secretion, and in turn plasma osmolality, constant despite the diuresis. The upregulation of EHD1 in the hypothalamus of EHD4-KO mice suggests that EHD4 has a necessary functional role in the hypothalamus, which remains to be tested. Thirdly, the mismatch between water intake and urine volume in EHD4-KO mice was greater than WT mice (Fig. 4A and 5A), suggesting that polydipsia may not be the primary cause of this diuretic phenotype in EHD4-KO mice. This observation further provides more evidence for a renal defect rather than a defect in the central component; however, more experiments, such as studying the response of EHD4-KO mice to dipsogenic agents, will be needed to elucidate the exact role of EHD4 in the thirst mechanism.

Role of EHD4 in the regulation of renal AVP-AQP2 axis

Multiple lines of evidence suggest that the AVP-AQP2 axis remains functional in EHD4-KO mice. No difference in the cellular abundance of pAQP2 was found between WT and EHD4-KO mice under baseline conditions (Fig. 17A), which indicates a functional AVP-AQP2 axis in EHD4-KO mice. Moreover, EHD4-KO mice were found to exhibit similar anti-diuretic responses as WT mice during 24-h water restriction (Fig. 7). AVP is the major anti-diuretic agent released during water deprivation (49) and allows conservation of water by increasing water permeability of the collecting duct. AVP increases the phosphorylation of AQP2 (144), resulting in an increase in the membrane accumulation of AQP2. Both the abundance and the membrane availability of AQP2 increased in a similar way in both WT and EHD4-KO mice post-water restriction (Fig. 8). These observations strongly indicate that the AVP-AQP2 axis in the kidney remains intact even in the absence of EHD4.

The role of the AVP-AQP2 axis in the regulation of water permeability of the IMCD comes into play when plasma osmolality increases, such as during water restriction. EHD4-KO mice showed a similar anti-diuretic response to 24-h water restriction as WT mice. This data, along with the other observations discussed in the previous section, suggest that this AVP-AQP2 axis is functional in the absence of EHD4. Moreover, the diuresis in EHD4-KO mice is more prominent under baseline conditions, and urine-concentrating abilities seemed to be functional during water restriction. Although EHD4-KO mice were able to concentrate their urine post water restriction, the urine osmolality of EHD4-KO mice remained significantly lower compared to WT mice (Fig. 7B). This suggests that EHD4 is required for maximal urine-concentrating ability. Therefore, it is possible that the diuretic phenotype in EHD4-KO mice is more of a baseline defect, which can be overcome during anti-diuresis.

EHD proteins have been reported previously to exhibit compensatory roles for one another when one of the members is absent (56). Consistent with this, there was an increased expression of EHD1 in the hypothalamus in the absence of EHD4 in mice (Fig. 11B). Hence, it is possible that the urine-concentrating ability in EHD4-KO remains functional due a compensatory upregulation of other EHD proteins. No such increase in the expressions of EHD1, -2, and -3 in the renal tissues of EHD4-KO mice after 24-h water restriction was observed (Fig. 10), suggesting that the anti-diuretic response to water restriction occurs in an EHD-independent manner. All these observations suggest that EHD4 has a role in the regulation of renal water reabsorption during baseline conditions, whereas key physiological mechanisms allowing for increases of urinary concentration under conditions of water restriction remain intact.

Role of EHD4 in the regulation of renal osmotic gradient

In order for the kidney to generate a hyperosmotic urine, it needs to maintain a hyperosmolar environment in the renal medulla. Two major processes in the renal medulla contribute to the generation of the osmotic gradient: active transport of sodium ions via the NKCC2 in the MTAL, and the facilitated diffusion of urea through the urea transporters of the IMCD. It was found that both MTAL and IMCD expresses EHD4 (Fig. 1), and therefore, it is possible that EHD4 regulates the generation of the osmotic gradient by influencing either or both of these two processes at these sites. The data on the NKCC2 expression and responses to acute furosemide injection suggest that EHD4 may not be involved in the regulation of sodium transport via NKCC2 (Fig. 15). However, it is possible that the effect of EHD4 deletion on sodium reabsorption via NKCC2 may be masked by the compensatory upregulation of the activities of other medullary sodium channels/transporters, such as ENaC activity in principal cells. It has been previously reported that a chronic administration of furosemide in rats result in an increases in ENaC

abundance (131) that results in the generation of tolerance to diuretics. My attempt to understand this phenomenon remained largely unsuccessful and inconclusive because of the failure of amiloride to generate a natriuretic effect (Fig. 14). ENaC is responsible for only a small percentage of total Na reabsorption, perhaps contributing to the difficulty in detecting an effect in conscious mice Although the abundance of αENaC was not different between WT and EHD4-KO mice, it is still possible that the activity or membrane abundance of ENaC, as well as NKCC2, may be compromised in EHD4-KO mice. Endocytic recycling is known to regulate the membrane abundance of both ENaC (19, 20, 37) and NKCC2 (1, 21). Indeed, SNAP29, one of the predicted interacting partners of EHD4 (found through STRING analysis) (Fig. 23), has been identified in vesicles involved in NKCC2 trafficking (21). Despite the expression of EHD4 in these segments where NKCC2 and ENaC are expressed, the exact role of EHD4 in the regulation of these channels and transporters remain unclear. One way to understand if EHD4 regulates either or both NKCC2 and ENaC would be to study the effect of EHD4 deletion on the membrane accumulation of these channels and transporters in appropriate cultured cells.

The renal osmotic gradient is generated by the buildup of solute concentration, particularly sodium and urea. It was found that the osmotic gradient across the renal interstitium was similar between EHD4-HOM and EHD4-KO mice (Fig. 36A and 37A). On a first glance, this data would seem to indicate that the maintenance of the renal osmotic gradient is independent of EHD4, which may be true. However, the generation and preservation of this osmotic gradient is a complex process, and EHD4 may be involved in the regulation of this process in a way that may not be readily apparent from the current data. Urea reabsorption and recycling within the IM are important factors for maintaining the renal osmotic gradient. Tissue urea concentration of EHD4-KO mice was found to be similar to that in EHD4-HOM mice (Fig. 36B and 37B). These data indicate that, along with

tissue osmolality, preservation of tissue urea gradient may also be EHD4-independent. However, it was also found that in the absence of EHD4, urinary urea excretion is increased and plasma urea level is slightly reduced (Fig. 30 and 31). These findings present an interesting view on the role of EHD4 in the regulation of renal urea handling and urea gradient. EHD4-KO mice seem able to conserve the tissue urea gradient despite an apparent urea-wasting phenotype, at least when maintained on a normal protein diet. One possible explanation for this paradoxical finding between urea excretion and tissue urea gradient could be a reduced reabsorption of urea in the IMCD, where EHD4 is highly expressed, and an increased re-entry of urea from the vasculature into the interstitium.

Principal cells of the IMCD express two urea transporters: UT-A1 in the apical membrane that transports urea from the luminal fluid into the principal cell, and UT-A3 in the basolateral membrane that transports urea from the inside of the principal cell to the renal interstitium (88). Absence of both UT-A1 and UT-A3 can result in a urine-concentrating defect in mice (45), but only UT-A1, and not UT-A3, is required for basal urea permeability and a maximal urine-concentrating ability (92). Although some studies have highlighted the importance of endocytosis in the regulation of UT-A1 and -A3, there is no current report on the role of EHD proteins in the regulation of trafficking of these transporters. In the water restriction experiment, EHD4-KO mice was found to increase urine osmolality when water was restricted, but the urine osmolality remained lower than that in WT mice (Fig. 7B). This observation indicates that EHD4 is required for maximal urine-concentrating ability in mice. Moreover, an EHD-interacting protein, called Snapin (119), also interacts with UT-A1 (122). Combining these observations, it seems very likely that EHD4 may regulate the maximal urine-concentrating ability by regulating UT-A1 in the IMCD. Although the current results on the localization of UT-A1 in the principal cells needs further verification, it appears that EHD4 may regulate the accumulation of UT-A1

in the apical membrane of principal cells. In EHD4-KO mice, there seems to be a lack of UT-A1 in the apical membrane (Fig. 39) and this in turn might result in reduced urea reabsorption within the IMCD.

It is also quite possible that the increased urea excretion in EHD4-KO mice may result due to the high urine flow in these mice. The high urine flow would allow less time for proper urea reabsorption in EHD4-KO mice, thereby increasing urea excretion. However, I would argue against this flow-induced increase in urea excretion in EHD4-KO mice. The data from the experiments involving modified protein diets showed that, at least in female mice, a high protein diet exacerbated the diuretic phenotype and further increased the urea excretion (Fig. 32), which was reversed by a low protein diet. These observations point more toward a defect in renal urea reabsorption in the absence of EHD4; however, it is also possible that EHD4 regulates the activity of UT-A2 in the thin descending limb. Data generated by Lee et. al. (104) from RNA sequencing of single tubules, shows that the expression of EHD4 mRNA is actually the highest in the thin limbs, which makes it possible for EHD4 to regulate UT-A2 as well. Therefore, a comprehensive profiling of the status of all arms of renal urea handling will be needed to confirm the exact role of EHD4 in this physiological process.

Conclusion and perspectives

The functional data presented in this dissertation indicate an important regulatory role of EHD4 in the renal handling of both water and urea. The findings of these studies indicate that EHD4 does this, at least in part, through regulation of the subcellular localization of AQP2 and AQP4 in the collecting duct. Future studies are needed to fully elucidate the identity and cellular site of the urea transporter(s) regulated by EHD4, although UT-A1 appears to be a likely candidate.

This study highlighted the potential impact on renal function of proteins involved in endocytic trafficking, which has received little attention so far. This study provides an insight into the cellular machineries that are involved in the regulation of water homeostasis. The exact roles of EHD proteins in humans and any pathophysiology associated with the lack of these proteins in humans has not been explored yet. This work has clinical relevance because an imbalance in body water can be fatal. In many clinical conditions, such as during nephrogenic diabetes insipidus, the water permeability is significantly reduced, resulting in a reduced reabsorption of water. EHD4-KO mice demonstrated a phenotype very similar to that seen during nephrogenic diabetes insipidus. One form of this disease occurs due a dysfunctional recycling of AQP2 in the principal cells. These findings shed an important light on the cellular processes involved in the trafficking of AQP2, as well as AQP4, that may be used in designing appropriate therapeutic agents. Targeted therapy is absolutely necessary for patients suffering from this disease because there are no treatment strategies available right now, and the only way to manage this condition is by monitoring fluid intake. Unresolved polyuria, such as during nephrogenic diabetes insipidus or acute renal failure, can raise the solute levels in the circulation and, thereby, can be fatal. In addition to polyuria, imbalance in body water can also occur during improper water retention, such as during congestive heart failure

(75). Increased expression and membrane accumulation of AQP2 has been shown to be one of the driving forces in the development of congestive heart failure (142). This work showed that EHD4 regulates AQP2 trafficking, thereby, providing a novel target for future work focusing on the designing of therapeutic agents to treat water imbalance and will likely prompt investigators in the future to explore whether reduced EHD4 expression or function might contribute to fluid imbalance in humans.

REFERENCES

1. **Ares GR, and Ortiz PA**. Constitutive endocytosis and recycling of NKCC2 in rat thick ascending limbs. *Am J Physiol Renal Physiol* 299: F1193-F1202, 2010.

2. **Arima H, Azuma Y, Morishita Y, and Hagiwara D**. Central diabetes insipidus. *Nagoya J Med Sci* 78: 349, 2016.

3. **Arnspang EC, Sundbye S, Nelson WJ, and Nejsum LN**. Aquaporin-3 and aquaporin-4 are sorted differently and separately in the trans-Golgi network. *PLoS One* 8: e73977, 2013.

4. **Arya P, Rainey MA, Bhattacharyya S, Mohapatra BC, George M, Kuracha MR, Storck MD, Band V, Govindarajan V, and Band H**. The endocytic recycling regulatory protein EHD1 Is required for ocular lens development. *Dev Biol* 408: 41-55, 2015.

5. **Barile M, Pisitkun T, Yu M-J, Chou C-L, Verbalis MJ, Shen R-F, and Knepper MA**. Large scale protein identification in intracellular aquaporin-2 vesicles from renal inner medullary collecting duct. *Mol Cell Proteomics* 4: 1095-1106, 2005.

6. **Båtshake B, Nilsson C, and Sundelin J**. Molecular characterization of the mouse prostanoid EP1 receptor gene. *The FEBS Journal* 231: 809-814, 1995.

7. **Baumgarten R, Van De Pol M, Wetzels J, Van Os CH, and Deen P**. Glycosylation is not essential for vasopressin-dependent routing of aquaporin-2 in transfected Madin-Darby canine kidney cells. *J Am Soc Nephrol* 9: 1553-1559, 1998.

8. **Berliner RW, Levinsky NG, Davidson DG, and Eden M**. Dilution and concentration of the urine and the action of antidiuretic hormone. *The Am J Med* 24: 730-744, 1958.

9. **Blount MA, Cipriani P, Redd SK, Ordas RJ, Black LN, Gumina DL, Hoban CA, Klein JD, and Sands JM**. Activation of protein kinase Cα increases phosphorylation of the UT-A1 urea transporter at serine 494 in the inner medullary collecting duct. *Am J Physiol Cell Physiol* 309: C608-C615, 2015.

10. **Blount MA, Klein JD, Martin CF, Tchapyjnikov D, and Sands JM**. Forskolin stimulates phosphorylation and membrane accumulation of UT-A3. *Am J Physiol Renal Physiol* 293: F1308-F1313, 2007.

11. **Blount MA, Mistry AC, Fröhlich O, Price SR, Chen G, Sands JM, and Klein JD**. Phosphorylation of UT-A1 urea transporter at serines 486 and 499 is important for vasopressin-regulated activity and membrane accumulation. *Am J Physiol Renal Physiol* 295: F295-F299, 2008.

12. **Bradford AD, Terris JM, Ecelbarger CA, Klein JD, Sands JM, Chou C-L, and Knepper MA**. 97-and 117-kDa forms of collecting duct urea transporter UT-A1 are due to different states of glycosylation. *Am J Physiol Renal Physiol* 281: F133-F143, 2001.

13. **Braun A, Pinyol R, Dahlhaus R, Koch D, Fonarev P, Grant BD, Kessels MM, and Qualmann B**. EHD proteins associate with syndapin I and II and such interactions play a crucial role in endosomal recycling. *Mol Biol Cell* 16: 3642-3658, 2005.

14. **Breyer MD, and Breyer RM**. Prostaglandin E receptors and the kidney. *Am J Physiol Renal Physiol* 279: F12-F23, 2000.

15. **Breyer MD, Jacobson HR, Davis LS, and Breyer RM**. In situ hybridization and localization of mRNA for the rabbit prostaglandin EP3 receptor. *Kidney Int* 44: 1372-1378, 1993.

16. **Breyer RM, Davis LS, Nian C, Redha R, Stillman B, Jacobson HR, and Breyer MD**. Cloning and expression of the rabbit prostaglandin EP4 receptor. *Am J Physiol Renal Physiol* 270: F485-F493, 1996.

17. **Brimble M, and Dyball R**. Characterization of the responses of oxytocin-and vasopressin-secreting neurones in the supraoptic nucleus to osmotic stimulation. *The Journal of physiology* 271: 253-271, 1977.

18. **Brown D**. The ins and outs of aquaporin-2 trafficking. *Am J Physiol Renal Physiol* 284: F893-F901, 2003.

19. **Bugaj V, Pochynyuk O, and Stockand JD**. Activation of the epithelial Na+ channel in the collecting duct by vasopressin contributes to water reabsorption. *Am J Physiol Renal Physiol* 297: F1411-F1418, 2009.

20. **Butterworth MB, Edinger RS, Silvis MR, Gallo LI, Liang X, Apodaca G, Fizzell RA, and Johnson JP**. Rab11b regulates the trafficking and recycling of the epithelial sodium channel (ENaC). *Am J Physiol Renal Physiol* 302: F581-F590, 2012.

21. **Caceres PS, Mendez M, and Ortiz PA**. Vesicle-associated membrane protein 2 (VAMP2) but Not VAMP3 mediates cAMP-stimulated trafficking of the renal Na+-K+-2Cl− co-transporter NKCC2 in thick ascending limbs. *J Biol Chem* 289: 23951-23962, 2014.

22. **Chou C-L, Hwang G, Hageman DJ, Han L, Agrawal P, Pisitkun T, and Knepper MA**. Identification of UT-A1 and AQP2 interacting proteins in rat inner medullary collecting duct. *Am J Physiol Cell Physiol* ajpcell. 00082.02017, 2017.

23. **Chou C-L, Knepper MA, van Hoek AN, Brown D, Yang B, Ma T, and Verkman A**. Reduced water permeability and altered ultrastructure in thin descending limb of Henle in aquaporin-1 null mice. *J Clin Invest* 103: 491, 1999.

24. **Chou C-L, Yip K-P, Michea L, Kador K, Ferraris JD, Wade JB, and Knepper MA**. Regulation of Aquaporin-2 Trafficking by Vasopressin in the Renal Collecting Duct ROLES OF RYANODINE-SENSITIVE Ca2+ STORES AND CALMODULIN. *J Biol Chem* 275: 36839-36846, 2000.

25. **Chou C, Ma T, Yang B, Knepper MA, and Verkman A**. Fourfold reduction of water permeability in inner medullary collecting duct of aquaporin-4 knockout mice. *Am J Physiol Cell Physiol* 274: C549-C554, 1998.

26. **Chukkapalli S, Amessou M, Dekhil H, Dilly AK, Liu Q, Bandyopadhyay S, Thomas RD, Bejna A, Batist G, and Kandouz M**. Ehd3, a regulator of vesicular trafficking, is silenced in gliomas and functions as a tumor suppressor by controlling cell cycle arrest and apoptosis. *Carcinogenesis* 35: 877-885, 2014.

27. **Ciura S, and Bourque CW**. Transient receptor potential vanilloid 1 is required for intrinsic osmoreception in organum vasculosum lamina terminalis neurons and for normal thirst responses to systemic hyperosmolality. *J Neurosci* 26: 9069-9075, 2006.

28. **Conner SD, and Schmid SL**. Regulated portals of entry into the cell. *Nature* 422: 37-44, 2003.

29. **Corbeel L, and Freson K**. Rab proteins and Rab-associated proteins: major actors in the mechanism of protein-trafficking disorders. *Eur J Pediatr* 167: 723, 2008.

30. **Cullis DN, Philip B, Baleja JD, and Feig LA**. Rab11-FIP2, an adaptor protein connecting cellular components involved in internalization and recycling of epidermal growth factor receptors. *J Biol Chem* 277: 49158-49166, 2002.

31. **Curran J, Makara MA, Little SC, Musa H, Liu B, Wu X, Polina I, Alecusan JS, Wright P, and Li J**. EHD3-dependent endosome pathway regulates cardiac membrane excitability and physiology. *Circ Res* 115: 68-78, 2014.

32. **Curran J, Musa H, Kline CF, Makara MA, Little SC, Higgins JD, Hund TJ, Band H, and Mohler PJ**. Eps15 homology domain-containing protein 3 regulates cardiac T-type Ca2+ channel targeting and function in the atria. *J Biol Chem* 290: 12210-12221, 2015.

33. **Danziger J, and Zeidel ML**. Osmotic homeostasis. *Clin J Am Soc Nephrol* CJN. 10741013, 2014.

34. **Deen PM, Verdijk MA, Knoers N, Wieringa B, Monnens LA, Os Cv, and Oost Bv**. Requirement of human renal water channel aquaporin-2 for vasopressin-dependent

concentration of urine. *Science-AAAS-Weekly Paper Edition-including Guide to Scientific Information* 264: 92-94, 1994.

35. **Dunn FL, Brennan TJ, Nelson AE, and Robertson GL**. The role of blood osmolality and volume in regulating vasopressin secretion in the rat. *J Clin Invest* 52: 3212, 1973.

36. **Ecelbarger CA, Terris J, Frindt G, Echevarria M, Marples D, Nielsen S, and Knepper M**. Aquaporin-3 water channel localization and regulation in rat kidney. *Am J Physiol Renal Physiol* 269: F663-F672, 1995.

37. **Edinger RS, Bertrand CA, Rondandino C, Apodaca GA, Johnson JP, and Butterworth MB**. The epithelial sodium channel (ENaC) establishes a trafficking vesicle pool responsible for its regulation. *PLoS One* 7: e46593, 2012.

38. **Egan G, Silk T, Zamarripa F, Williams J, Federico P, Cunnington R, Carabott L, Blair-West J, Shade R, and McKinley M**. Neural correlates of the emergence of consciousness of thirst. *Proc Nat Acad Sci* 100: 15241-15246, 2003.

39. **Evans JH, Fergus DJ, and Leslie CC**. Regulation of cytosolic phospholipase A2 translocation. *Adv Enzyme Regul* 43: 229-244, 2003.

40. **Faergeman NJ, and Knudsen J**. Role of long-chain fatty acyl-CoA esters in the regulation of metabolism and in cell signalling. *Biochem J* 323: 1-12, 1997.

41. **Feng X, Li Z, Du Y, Fu H, Klein JD, Cai H, Sands JM, and Chen G**. Downregulation of urea transporter UT-A1 activity by 14-3-3 protein. *Am J Physiol Renal Physiol* 309: F71-F78, 2015.

42. **Fenton R, Howorth A, Cooper G, Meccariello R, Morris I, and Smith C**. Molecular characterization of a novel UT-A urea transporter isoform (UT-A5) in testis. *Am J Physiol Cell Physiol* 279: C1425-C1431, 2000.

43. **Fenton RA**. Essential role of vasopressin-regulated urea transport processes in the mammalian kidney. *Pflügers Archiv-European Journal of Physiology* 458: 169-177, 2009.

44. **Fenton RA, Chou C-L, Stewart GS, Smith CP, and Knepper MA**. Urinary concentrating defect in mice with selective deletion of phloretin-sensitive urea transporters in the renal collecting duct. *Proc Natl Acad Sci U S A* 101: 7469-7474, 2004.

45. **Fenton RA, Flynn A, Shodeinde A, Smith CP, Schnermann J, and Knepper MA**. Renal phenotype of UT-A urea transporter knockout mice. *J Am Soc Nephrol* 16: 1583-1592, 2005.

46. **Fenton RA, and Knepper MA**. Mouse models and the urinary concentrating mechanism in the new millennium. *Physiol Rev* 87: 1083-1112, 2007.

47. **Fenton RA, and Knepper MA**. Urea and renal function in the 21st century: insights from knockout mice. *J Am Soc Nephrol* 18: 679-688, 2007.

48. **Fenton RA, Moeller HB, Hoffert JD, Yu M-J, Nielsen S, and Knepper MA**. Acute regulation of aquaporin-2 phosphorylation at Ser-264 by vasopressin. *Proc Nat Acad Sci* 105: 3134-3139, 2008.

49. **Franchini KG, and Cowley A**. Renal cortical and medullary blood flow responses during water restriction: role of vasopressin. *Am J Physiol Reg Integ Comp Physiol* 270: R1257-R1264, 1996.

50. **Fushimi K, Sasaki S, and Marumo F**. Phosphorylation of serine 256 is required for cAMP-dependent regulatory exocytosis of the aquaporin-2 water channel. *J Biol Chem* 272: 14800-14804, 1997.

51. **Fushimi K, Uchida S, Harat Y, Hirata Y, Marumo F, and Sasaki S**. Cloning and expression of apical membrane water channel of rat kidney collecting tubule. *Nature* 361: 549-552, 1993.

52. **Gamba G, Saltzberg SN, Lombardi M, Miyanoshita A, Lytton J, Hediger MA, Brenner BM, and Hebert SC**. Primary structure and functional expression of a cDNA encoding the thiazide-sensitive, electroneutral sodium-chloride cotransporter. *Proc Nat Acad Sci* 90: 2749-2753, 1993.

53. **Gao Y, Stuart D, Pollock JS, Takahishi T, and Kohan DE**. Collecting duct-specific knockout of nitric oxide synthase 3 impairs water excretion in a sex-dependent manner. *Am J Physiol Renal Physiol* 311: F1074-F1083, 2016.

54. **Garty H, and Palmer LG**. Epithelial sodium channels: function, structure, and regulation. *Physiol Rev* 77: 359-396, 1997.

55. **Ge Y, Ahn D, Stricklett PK, Hughes AK, Yanagisawa M, Verbalis JG, and Kohan DE**. Collecting duct-specific knockout of endothelin-1 alters vasopressin regulation of urine osmolality. *Am J Physiol Renal Physiol* 288: F912-F920, 2005.

56. **George M, Rainey MA, Naramura M, Foster KW, Holzapfel MS, Willoughby LL, Ying G, Goswami RM, Gurumurthy CB, Band V, Satchell SC, and Band H**. Renal thrombotic microangiopathy in mice with combined deletion of endocytic recycling regulators EHD3 and EHD4. *PLoS One* 6: e17838, 2011.

57. **George M, Rainey MA, Naramura M, Ying G, Harms DW, Vitaterna MH, Doglio L, Crawford SE, Hess RA, Band V, and Band H**. Ehd4 is required to attain normal prepubertal testis size but dispensable for fertility in male mice. *genesis* 48: 328-342, 2010.

58. **George M, Ying G, Rainey MA, Solomon A, Parikh PT, Gao Q, Band V, and Band H**. Shared as well as distinct roles of EHD proteins revealed by biochemical and functional comparisons in mammalian cells and C. elegans. *BMC Cell Biol* 8: 3, 2007.

59. **Gonen T, and Walz T**. The structure of aquaporins. *Q Rev Biophys* 39: 361-396, 2006.

60. **Grant BD, and Caplan S**. Mechanisms of EHD/RME-1 Protein Function in Endocytic Transport. *Traffic* 9: 2043-2052, 2008.

61. **Grant BD, and Donaldson JG**. Pathways and mechanisms of endocytic recycling. *Nat Rev Mol Cell Biol* 10: 597-608, 2009.

62. **Greger R**. Ion transport mechanisms in thick ascending limb of Henle's loop of mammalian nephron. *Physiol Rev* 65: 760-797, 1985.

63. **Gudmundsson H, Hund TJ, Wright PJ, Kline CF, Snyder JS, Qian L, Koval OM, Cunha SR, George M, and Rainey MA**. EH domain proteins regulate cardiac membrane protein targeting. *Circ Res* 107: 84-95, 2010.

64. **Gustafson CE, Katsura T, McKee M, Bouley R, Casanova JE, and Brown D**. Recycling of AQP2 occurs through a temperature-and bafilomycin-sensitive trans-Golgi-associated compartment. *Am J Physiol Renal Physiol* 278: F317-F326, 2000.

65. **Hall JE**. *Guyton and Hall Textbook of Medical Physiology E-Book*. Elsevier Health Sciences, 2015.

66. **Hasler U, Leroy V, Martin P-Y, and Féraille E**. Aquaporin-2 abundance in the renal collecting duct: new insights from cultured cell models. *Am J Physiol Renal Physiol* 297: F10-F18, 2009.

67. **Hasler U, Mordasini D, Bens M, Bianchi M, Cluzeaud F, Rousselot M, Vandewalle A, Féraille E, and Martin P-Y**. Long term regulation of aquaporin-2 expression in vasopressin-responsive renal collecting duct principal cells. *J Biol Chem* 277: 10379-10386, 2002.

68. **Hendriks G, Koudijs M, van Balkom BW, Oorschot V, Klumperman J, Deen PM, and van der Sluijs P**. Glycosylation is important for cell surface expression of the water channel aquaporin-2 but is not essential for tetramerization in the endoplasmic reticulum. *J Biol Chem* 279: 2975-2983, 2004.

69. **Ho HT, Chung SK, Law JW, Ko BC, Tam SC, Brooks HL, Knepper MA, and Chung SS**. Aldose reductase-deficient mice develop nephrogenic diabetes insipidus. *Mol Cell Biol* 20: 5840-5846, 2000.

70. **Hoffert JD, Fenton RA, Moeller HB, Simons B, Tchapyjnikov D, McDill BW, Yu M-J, Pisitkun T, Chen F, and Knepper MA**. Vasopressin-stimulated increase in phosphorylation at Ser269 potentiates plasma membrane retention of aquaporin-2. *J Biol Chem* 283: 24617-24627, 2008.

71. **Hoffert JD, Nielsen J, Yu M-J, Pisitkun T, Schleicher SM, Nielsen S, and Knepper MA**. Dynamics of aquaporin-2 serine-261 phosphorylation in response to short-term vasopressin treatment in collecting duct. *Am J Physiol Renal Physiol* 292: F691-F700, 2007.

72. **Hollis JH, McKinley MJ, D'Souza M, Kampe J, and Oldfield BJ**. The trajectory of sensory pathways from the lamina terminalis to the insular and cingulate cortex: a neuroanatomical framework for the generation of thirst. *Am J Physiol Reg Integ Comp Physiol* 294: R1390-R1401, 2008.

73. **Hou J, Rajagopal M, and Yu AS**. Claudins and the kidney. *Annu Rev Physiol* 75: 479-501, 2013.

74. **Imai M, and Kokko J**. Sodium chloride, urea, and water transport in the thin ascending limb of Henle. Generation of osmotic gradients by passive diffusion of solutes. *J Clin Invest* 53: 393, 1974.

75. **Ingelfinger JR, Knepper MA, Kwon T-H, and Nielsen S**. Molecular Physiology of Water Balance. *N Engl J Med* 372: 1349-1358, 2015.

76. **Isozaki T, Gillin AG, Swanson CE, and Sands JM**. Protein restriction sequentially induces new urea transport processes in rat initial IMCD. *Am J Physiol Renal Physiol* 266: F756-F761, 1994.

77. **Isozaki T, Verlander JW, and Sands JM**. Low protein diet alters urea transport and cell structure in rat initial inner medullary collecting duct. *J Clin Invest* 92: 2448, 1993.

78. **Jackson BA**. Prostaglandin E2 synthesis in the inner medullary collecting duct of the rat: Implications for vasopressin-dependent cyclic AMP formation. *J Cell Physiol* 129: 60-64, 1986.

79. **Janaky T, Laszlo F, Sirokman F, and Morgat J-L**. Biological half-life and organ distribution of [3H] 8-arginine-vasopressin in the rat. *J Endocrinol* 93: 295-303, 1982.

80. **Jang EJ, Jeong H, Han KH, Kwon HM, Hong J-H, and Hwang ES**. TAZ suppresses NFAT5 activity through tyrosine phosphorylation. *Mol Cell Biol* 32: 4925-4932, 2012.

81. **Jovic M, Sharma M, Rahajeng J, and Caplan S**. The early endosome: a busy sorting station for proteins at the crossroads. *Histol Histopathol* 25: 99, 2010.

82. **Kamsteeg E-J, Hendriks G, Boone M, Konings IB, Oorschot V, van der Sluijs P, Klumperman J, and Deen PM**. Short-chain ubiquitination mediates the regulated endocytosis of the aquaporin-2 water channel. *Proc Nat Acad Sci* 103: 18344-18349, 2006.

83. **Karakashian A, Timmer RT, Klein JD, Gunn RB, Sands JM, and Bagnasco SM**. Cloning and characterization of two new isoforms of the rat kidney urea transporter UT-A3 and UT-A4. *J Am Soc Nephrol* 10: 230-237, 1999.

84. **Katsuyama M, Nishigaki N, Sugimoto Y, Morimoto K, Negishi M, Narumiya S, and Ichikawa A**. The mouse prostaglandin E receptor EP2 subtype: cloning, expression, and northern blot analysis. *FEBS Lett* 372: 151-156, 1995.

85. **Khanna A**. Acquired nephrogenic diabetes insipidus. In: *Semin Nephrol*Elsevier, 2006, p. 244-248.

86. **Kim SM, Chen L, Mizel D, Huang YG, Briggs JP, and Schnermann J**. Low plasma renin and reduced renin secretory responses to acute stimuli in conscious COX-2-deficient mice. *Am J Physiol Renal Physiol* 292: F415-F422, 2007.

87. **Klein JD, Blount MA, and Sands JM**. Molecular mechanisms of urea transport in health and disease. *Pflügers Archiv-European Journal of Physiology* 464: 561-572, 2012.

88. **Klein JD, Blount MA, and Sands JM**. Urea transport in the kidney. *Comprehensive Physiology* 2011.

89. **Klein JD, Fröhlich O, Blount MA, Martin CF, Smith TD, and Sands JM**. Vasopressin increases plasma membrane accumulation of urea transporter UT-A1 in rat inner medullary collecting ducts. *J Am Soc Nephrol* 17: 2680-2686, 2006.

90. **Klein JD, Sands JM, Qian L, Wang X, and Yang B**. Upregulation of urea transporter UT-A2 and water channels AQP2 and AQP3 in mice lacking urea transporter UT-B. *J Am Soc Nephrol* 15: 1161-1167, 2004.

91. **Klein JD, Wang Y, Blount MA, Molina PA, LaRocque LM, Ruiz JA, and Sands JM**. Metformin, an AMPK activator, stimulates the phosphorylation of aquaporin 2 and urea transporter A1 in inner medullary collecting ducts. *Am J Physiol Renal Physiol* 310: F1008-F1012, 2016.

92. **Klein JD, Wang Y, Mistry A, LaRocque LM, Molina PA, Rogers RT, Blount MA, and Sands JM**. Transgenic restoration of urea transporter A1 confers maximal urinary concentration in the absence of urea transporter A3. *J Am Soc Nephrol* ASN. 2014121267, 2015.

93. **Knepper M, and Nielsen S**. Kinetic model of water and urea permeability regulation by vasopressin in collecting duct. *Am J Physiol Renal Physiol* 265: F214-F224, 1993.

94. **Kohan DE, Padilla E, and Hughes AK**. Endothelin B receptor mediates ET-1 effects on cAMP and PGE2 accumulation in rat IMCD. *Am J Physiol Renal Physiol* 265: F670-F676, 1993.

95. **Kokko JP**. Sodium chloride and water transport in the descending limb of Henle. *J Clin Invest* 49: 1838, 1970.

96. **Kwon T-H, Hager H, Nejsum LN, Andersen M, Frøkiaer J, and Nielsen S**. Physiology and pathophysiology of renal aquaporins. In: *Semin Nephrol*2001, p. 231-238.

97. **Laeger T, Albarado D, Trosclair L, Hedgepeth J, and Morrison C**. Role of FGF21 and GCN2 in mediating the metabolic response to dietary protein restriction. *Diabetologie und Stoffwechsel* 11: FV24, 2016.

98. **Laeger T, Albarado DC, Burke SJ, Trosclair L, Hedgepeth JW, Berthoud H-R, Gettys TW, Collier JJ, Münzberg H, and Morrison CD**. Metabolic responses to dietary protein restriction require an increase in FGF21 that is delayed by the absence of GCN2. *Cell reports* 16: 707-716, 2016.

99. **Laeger T, Henagan TM, Albarado DC, Redman LM, Bray GA, Noland RC, Münzberg H, Hutson SM, Gettys TW, and Schwartz MW**. FGF21 is an endocrine signal of protein restriction. *J Clin Inves* 124: 3913, 2014.

100. **Land H, Schütz G, Schmale H, and Richter D**. Nucleotide sequence of cloned cDNA encoding bovine arginine vasopressin–neurophysin II precursor. *Nature* 295: 299-303, 1982.

101. **Langaa S, Bloksgaard M, Bek S, Neess D, Nørregaard R, Hansen PB, Marcher AB, Frøkiær J, Mandrup S, and Jensen BL**. Mice with targeted disruption of the acyl-CoA binding protein display attenuated urine concentrating ability and diminished renal aquaporin-3 abundance. *Am J Physiol Renal Physiol* 302: F1034-F1044, 2012.

102. **Lassiter WE, Gottschalk CW, and Mylle M**. Micropuncture study of net transtubular movement of water and urea in nondiuretic mammalian kidney. *Am J Physiol Leg Cont* 200: 1139-1147, 1961.

103. **Lechner SG, Markworth S, Poole K, Smith ESJ, Lapatsina L, Frahm S, May M, Pischke S, Suzuki M, and Ibañez-Tallon I**. The molecular and cellular identity of peripheral osmoreceptors. *Neuron* 69: 332-344, 2011.

104. **Lee JW, Chou C-L, and Knepper MA**. Deep Sequencing in Microdissected Renal Tubules Identifies Nephron Segment–Specific Transcriptomes. *J Am Soc Nephrol* ASN. 2014111067, 2015.

105. **Lee Y-H, Kim SH, Kim S-N, Kwon H-J, Kim J-D, Oh JY, and Jung Y-S**. Sex-specific metabolic interactions between liver and adipose tissue in MCD diet-induced non-alcoholic fatty liver disease. *Oncotarget* 7: 46959, 2016.

106. **Leng G, Brown CH, and Russell JA**. Physiological pathways regulating the activity of magnocellular neurosecretory cells. *Prog Neurobiol* 57: 625-655, 1999.

107. **Leng G, Mason W, and Dyer R**. The supraoptic nucleus as an osmoreceptor. *Neuroendocrinology* 34: 75-82, 1982.

108. **Levin EJ, and Zhou M**. Structure of urea transporters. In: *Urea Transporters*Springer, 2014, p. 65-78.

109. **Li S-Z, McDill BW, Kovach PA, Ding L, Go WY, Ho SN, and Chen F**. Calcineurin-NFATc signaling pathway regulates AQP2 expression in response to calcium signals and osmotic stress. *Am J Physiol Cell Physiol* 292: C1606-C1616, 2007.

110. **Liedtke W, Choe Y, Martí-Renom MA, Bell AM, Denis CS, Hudspeth A, Friedman JM, and Heller S**. Vanilloid receptor–related osmotically activated channel (VR-OAC), a candidate vertebrate osmoreceptor. *Cell* 103: 525-535, 2000.

111. **Linshaw MA**. Congenital nephrogenic diabetes insipidus. *Pediatr Rev* 28: 372-380, 2007.

112. **Lu H, Sun T-X, Bouley R, Blackburn K, McLaughlin M, and Brown D**. Inhibition of endocytosis causes phosphorylation (S256)-independent plasma membrane accumulation of AQP2. *Am J Physiol Renal Physiol* 286: F233-F243, 2004.

113. **Lu HJ, Matsuzaki T, Bouley R, Hasler U, Qin Q-H, and Brown D**. The phosphorylation state of serine 256 is dominant over that of serine 261 in the regulation of AQP2 trafficking in renal epithelial cells. *Am J Physiol Renal Physiol* 295: F290-F294, 2008.

114. **Ma T, Song Y, Yang B, Gillespie A, Carlson EJ, Epstein CJ, and Verkman A**. Nephrogenic diabetes insipidus in mice lacking aquaporin-3 water channels. *Proc Nat Acad Sci* 97: 4386-4391, 2000.

115. **Mahnensmith RL, and Aronson PS**. The plasma membrane sodium-hydrogen exchanger and its role in physiological and pathophysiological processes. *Circ Res* 56: 773-788, 1985.

116. **Marr N, Kamsteeg E, van Raak M, Van Os C, and Deen P**. Functionality of aquaporin-2 missense mutants in recessive nephrogenic diabetes insipidus. *Pflügers Archiv European Journal of Physiology* 442: 73-77, 2001.

117. **Marsh DJ, and Knepper MA**. Renal handling of urea. *Comprehensive Physiology* 2011.

118. **Mason W**. Supraoptic neurones of rat hypothalamus are osmosensitive. *Nature* 287: 154-157, 1980.

119. **Mate SE, Van Der Meulen JH, Arya P, Bhattacharyya S, Band H, and Hoffman EP**. Eps homology domain endosomal transport proteins differentially localize to the neuromuscular junction. *Skeletal muscle* 2: 19, 2012.

120. **Matsumura Y, Uchida S, Rai T, Sasaki S, and Marumo F**. Transcriptional regulation of aquaporin-2 water channel gene by cAMP. *J Am Soc Nephrol* 8: 861-867, 1997.

121. **Maxfield FR, and McGraw TE**. Endocytic recycling. *Nat Rev Mol Cell Biol* 5: 121-132, 2004.

122. **Mistry AC, Mallick R, Fröhlich O, Klein JD, Rehm A, Chen G, and Sands JM**. The UT-A1 urea transporter interacts with snapin, a SNARE-associated protein. *J Biol Chem* 282: 30097-30106, 2007.

123. **Moeller HB, Aroankins TS, Slengerik-Hansen J, Pisitkun T, and Fenton RA**. Phosphorylation and ubiquitylation are opposing players in regulating endocytosis of the water channel Aquaporin-2. *J Cell Sci* jcs. 150680, 2014.

124. **Moeller HB, Knepper MA, and Fenton RA**. Serine 269 phosphorylated aquaporin-2 is targeted to the apical membrane of collecting duct principal cells. *Kidney Int* 75: 295-303, 2009.

125. **Moeller HB, Olesen ET, and Fenton RA**. Regulation of the water channel aquaporin-2 by posttranslational modification. *Am J Physiol Renal Physiol* 300: F1062-F1073, 2011.

126. **Moeller HB, Praetorius J, Rützler MR, and Fenton RA**. Phosphorylation of aquaporin-2 regulates its endocytosis and protein–protein interactions. *Proc Nat Acad Sci* 107: 424-429, 2010.

127. **Moffat D, and Fourman J**. The vascular pattern of the rat kidney. *J Anat* 97: 543, 1963.

128. **Morello J-P, and Bichet DG**. Nephrogenic diabetes insipidus. *Annu Rev Physiol* 63: 607-630, 2001.

129. **Morello J-P, Salahpour A, Laperrière A, Bernier V, Arthus M-F, Lonergan M, Petäjä-Repo U, Angers S, Morin D, and Bichet DG**. Pharmacological chaperones rescue cell-surface expression and function of misfolded V2 vasopressin receptor mutants. *J Clin Invest* 105: 887, 2000.

130. **Morgan T, and Berliner RW**. Permeability of the loop of Henle, vasa recta, and collecting duct to water, urea, and sodium. *Am J Physiol Leg Cont* 215: 108-115, 1968.

131. **Na KY, Oh YK, Han JS, Joo KW, Lee JS, Earm J-H, Knepper MA, and Kim G-H**. Upregulation of Na+ transporter abundances in response to chronic thiazide or loop diuretic treatment in rats. *Am J Physiol Renal Physiol* 284: F133-F143, 2003.

132. **Nadler SP, Zimpelmann J, and Hebert R**. PGE2 inhibits water permeability at a post-cAMP site in rat terminal inner medullary collecting duct. *Am J Physiol Renal Physiol* 262: F229-F235, 1992.

133. **Nakayama Y, Naruse M, Karakashian A, Peng T, Sands JM, and Bagnasco SM**. Cloning of the rat Slc14a2 gene and genomic organization of the UT-A urea transporter. *Biochimica et Biophysica Acta (BBA)-Gene Structure and Expression* 1518: 19-26, 2001.

134. **Naslavsky N, and Caplan S**. C-terminal EH-domain-containing proteins: consensus for a role in endocytic trafficking, EH? *J Cell Sci* 118: 4093-4101, 2005.

135. **Naslavsky N, and Caplan S**. EHD proteins: key conductors of endocytic transport. *Trends Cell Biol* 21: 122-131, 2011.

136. **Naslavsky N, Rahajeng J, Sharma M, Jović M, and Caplan S**. Interactions between EHD proteins and Rab11-FIP2: a role for EHD3 in early endosomal transport. *Mol Biol Cell* 17: 163-177, 2006.

137. **Nedvetsky PI, Stefan E, Frische S, Santamaria K, Wiesner B, Valenti G, Hammer JA, Nielsen S, Goldenring JR, and Rosenthal W**. A Role of Myosin Vb and Rab11-FIP2 in the Aquaporin-2 Shuttle. *Traffic* 8: 110-123, 2007.

138. **Nejsum LN, Zelenina M, Aperia A, Frøkiær J, and Nielsen S**. Bidirectional regulation of AQP2 trafficking and recycling: involvement of AQP2-S256 phosphorylation. *Am J Physiol Renal Physiol* 288: F930-F938, 2005.

139. **Nielsen S, Chou C-L, Marples D, Christensen EI, Kishore BK, and Knepper MA**. Vasopressin increases water permeability of kidney collecting duct by inducing translocation of aquaporin-CD water channels to plasma membrane. *Proc Nat Acad Sci* 92: 1013-1017, 1995.

140. **Nielsen S, Frøkiær J, Marples D, Kwon T-H, Agre P, and Knepper MA**. Aquaporins in the kidney: from molecules to medicine. *Physiol Rev* 82: 205-244, 2002.

141. **Nielsen S, and Knepper MA**. Vasopressin activates collecting duct urea transporters and water channels by distinct physical processes. *Am J Physiol Renal Physiol* 265: F204-F213, 1993.

142. **Nielsen S, Terris J, Andersen D, Ecelbarger C, Frøkiær J, Jonassen T, Marples D, Knepper MA, and Petersen JS**. Congestive heart failure in rats is associated with increased expression and targeting of aquaporin-2 water channel in collecting duct. *Proc Nat Acad Sci* 94: 5450-5455, 1997.

143. **Nielsen S, Terris J, Smith CP, Hediger MA, Ecelbarger CA, and Knepper MA**. Cellular and subcellular localization of the vasopressin-regulated urea transporter in rat kidney. *Proc Nat Acad Sci* 93: 5495-5500, 1996.

144. **Nishimoto G, Zelenina M, Li D, Yasui M, Aperia A, Nielsen S, and Nairn AC**. Arginine vasopressin stimulates phosphorylation of aquaporin-2 in rat renal tissue. *Am J Physiol Renal Physiol* 276: F254-F259, 1999.

145. **Noda Y, Horikawa S, Kanda E, Yamashita M, Meng H, Eto K, Li Y, Kuwahara M, Hirai K, and Pack C**. Reciprocal interaction with G-actin and tropomyosin is essential for aquaporin-2 trafficking. *J Cell Biol* 182: 587-601, 2008.

146. **Noda Y, and Sasaki S**. Regulation of aquaporin-2 trafficking and its binding protein complex. *Biochimica et Biophysica Acta (BBA)-Biomembranes* 1758: 1117-1125, 2006.

147. **Nørregaard R, Madsen K, Hansen PB, Bie P, Thavalingam S, Frøkiær J, and Jensen BL**. COX-2 disruption leads to increased central vasopressin stores and impaired urine concentrating ability in mice. *Am J Physiol Renal Physiol* 301: F1303-F1313, 2011.

148. **Olesen ET, and Fenton RA**. Is there a role for PGE2 in urinary concentration? *J Am Soc Nephrol* ASN. 2012020217, 2012.

149. **Olesen ET, Rützler MR, Moeller HB, Praetorius HA, and Fenton RA**. Vasopressin-independent targeting of aquaporin-2 by selective E-prostanoid receptor agonists alleviates nephrogenic diabetes insipidus. *Proc Nat Acad Sci* 108: 12949-12954, 2011.

150. **Olesen ETB, Moeller HB, Assentoft M, MacAulay N, and Fenton RA**. The Vasopressin Type-2 Receptor and Prostaglandin Receptors EP2 and EP4 can Increase Aquaporin-2 Plasma Membrane Targeting Through a cAMP Independent Pathway. *Am J Physiol Renal Physiol* ajprenal. 00559.02015, 2016.

151. **Pannabecker TL, Dantzler WH, Layton HE, and Layton AT**. Role of three-dimensional architecture in the urine concentrating mechanism of the rat renal inner medulla. *Am J Physiol Renal Physiol* 295: F1271-F1285, 2008.

152. **Park E-J, Lim J-S, Jung HJ, Kim E, Han K-H, and Kwon T-H**. The role of 70-kDa heat shock protein in dDAVP-induced AQP2 trafficking in kidney collecting duct cells. *Am J Physiol Renal Physiol* 304: F958-F971, 2013.

153. **Pennell JP, Lacy FB, and Jamison RL**. An in vivo study of the concentrating process in the descending limb of Henle's loop. *Kidney Int* 5: 337-347, 1974.

154. **Phillips P, Rolls B, Ledingham J, Morton J, and Forsling M**. Angiotensin II-induced thirst and vasopressin release in man. *Clin Sci (Lond)* 68: 669-674, 1985.

155. **Piper RC, and Katzmann DJ**. Biogenesis and function of multivesicular bodies. *Annu Rev Cell Dev Biol* 23: 519-547, 2007.

156. **Pitts RF**. Physiology of the kidney and body fluids: an introductory text 1968.

157. **Promeneur D, Bankir L, Hu M, and Trinh-Trang-Tan M**. Renal tubular and vascular urea transporters: influence of antidiuretic hormone on messenger RNA expression in Brattleboro rats. *J Am Soc Nephrol* 9: 1359-1366, 1998.

158. **Promeneur D, Rousselet G, Bankir L, Bailly P, Cartron J-P, Ripoche P, and Trinh-Trang-Tan M-M**. Evidence for distinct vascular and tubular urea transporters in the rat kidney. *J Am Soc Nephrol* 7: 852-860, 1996.

159. **Rahman SS, Moffitt AE, Trease AJ, Foster KW, Storck MD, Band H, and Boesen EI**. EHD4 is a novel regulator of urinary water homeostasis. *FASEB J* fj. 201601182RR, 2017.

160. **Rainey MA, George M, Ying G, Akakura R, Burgess DJ, Siefker E, Bargar T, Doglio L, Crawford SE, and Todd GL**. The endocytic recycling regulator EHD1 is essential for spermatogenesis and male fertility in mice. *BMC Dev Biol* 10: 37, 2010.

161. **Rieg T, Tang T, Murray F, Schroth J, Insel PA, Fenton RA, Hammond HK, and Vallon V**. Adenylate cyclase 6 determines cAMP formation and aquaporin-2 phosphorylation and trafficking in inner medulla. *J Am Soc Nephrol* 21: 2059-2068, 2010.

162. **Rocha AS, and Kokko JP**. Sodium chloride and water transport in the medullary thick ascending limb of Henle. Evidence for active chloride transport. *J Clin Invest* 52: 612, 1973.

163. **Ronzaud C, Loffing-Cueni D, Hausel P, Debonneville A, Malsure SR, Fowler-Jaeger N, Boase NA, Perrier R, Maillard M, and Yang B**. Renal tubular NEDD4-2 deficiency causes NCC-mediated salt-dependent hypertension. *J Clin Inves* 123: 657, 2013.

164. **Rousselet G, Ripoche P, and Bailly P**. Tandem sequence repeats in urea transporters: identification of an urea transporter signature sequence. *Am J Physiol Renal Physiol* 270: F554-F555, 1996.

165. **Rügheimer L, Johnsson C, Maric C, and Hansell P**. Hormonal regulation of renomedullary hyaluronan. *Acta physiologica* 193: 191-198, 2008.

166. **Rügheimer L, Olerud J, Johnsson C, Takahashi T, Shimizu K, and Hansell P**. Hyaluronan synthases and hyaluronidases in the kidney during changes in hydration status. *Matrix Biol* 28: 390-395, 2009.

167. **Russo LM, McKee M, and Brown D**. Methyl-β-cyclodextrin induces vasopressin-independent apical accumulation of aquaporin-2 in the isolated, perfused rat kidney. *Am J Physiol Renal Physiol* 291: F246-F253, 2006.

168. **Salcini AE, Confalonieri S, Doria M, Santolini E, Tassi E, Minenkova O, Cesareni G, Pelicci PG, and Di Fiore PP**. Binding specificity and in vivo targets of the EH domain, a novel protein–protein interaction module. *Genes Dev* 11: 2239-2249, 1997.

169. **Sandoval PC, Slentz DH, Pisitkun T, Saeed F, Hoffert JD, and Knepper MA**. Proteome-wide measurement of protein half-lives and translation rates in vasopressin-sensitive collecting duct cells. *J Am Soc Nephrol* 24: 1793-1805, 2013.

170. **Sands J, Nonoguchi H, and Knepper M**. Vasopressin effects on urea and H2O transport in inner medullary collecting duct subsegments. *Am J Physiol Renal Physiol* 253: F823-F832, 1987.

171. **Sands JM**. Mammalian urea transporters. *Annu Rev Physiol* 65: 543-566, 2003.

172. **Sands JM**. Urine concentrating and diluting ability during aging. *Journals of Gerontology Series A: Biomedical Sciences and Medical Sciences* 67: 1352-1357, 2012.

173. **Sands JM, Gargus JJ, Fröhlich O, Gunn RB, and Kokko JP**. Urinary concentrating ability in patients with Jk (ab-) blood type who lack carrier-mediated urea transport. *J Am Soc Nephrol* 2: 1689-1696, 1992.

174. **Sands JM, and Layton HE**. Advances in understanding the urine-concentrating mechanism. *Annu Rev Physiol* 76: 387-409, 2014.

175. **Sands JM, Timmer RT, and Gunn RB**. Urea transporters in kidney and erythrocytes. *Am J Physiol Renal Physiol* 273: F321-F339, 1997.

176. **Saxena SK, and Kaur S**. Regulation of epithelial ion channels by Rab GTPases. *Biochem Biophys Res Commun* 351: 582-587, 2006.

177. **Schmidt-Nielsen B, Graves B, and Roth J**. Water removal and solute additions determining increases in renal medullary osmolality. *Am J Physiol Renal Physiol* 244: F472-F482, 1983.

178. **Sharma M, Naslavsky N, and Caplan S**. A role for EHD4 in the regulation of early endosomal transport. *Traffic* 9: 995-1018, 2008.

179. **Shayakul C, Steel A, and Hediger MA**. Molecular cloning and characterization of the vasopressin-regulated urea transporter of rat kidney collecting ducts. *J Clin Invest* 98: 2580, 1996.

180. **Simone LC, Naslavsky N, and Caplan S**. Scratching the surface: actin'and other roles for the C-terminal Eps15 homology domain protein, EHD2. *Histol Histopathol* 29: 285-292, 2014.

181. **Smith CA, Dho SE, Donaldson J, Tepass U, and McGlade CJ**. The cell fate determinant numb interacts with EHD/Rme-1 family proteins and has a role in endocytic recycling. *Mol Biol Cell* 15: 3698-3708, 2004.

182. **Smith CP, Potter EA, Fenton RA, and Stewart GS**. Characterization of a human colonic cDNA encoding a structurally novel urea transporter, hUT-A6. *Am J Physiol Cell Physiol* 287: C1087-C1093, 2004.

183. **Star RA, Nonoguchi H, Balaban R, and Knepper MA**. Calcium and cyclic adenosine monophosphate as second messengers for vasopressin in the rat inner medullary collecting duct. *J Clin Invest* 81: 1879, 1988.

184. **Stewart GS, Fenton RA, Wang W, Kwon T-H, White SJ, Collins VM, Cooper G, Nielsen S, and Smith CP**. The basolateral expression of mUT-A3 in the mouse kidney. *Am J Physiol Renal Physiol* 286: F979-F987, 2004.

185. **Stewart GS, Thistlethwaite A, Lees H, Cooper GJ, and Smith C**. Vasopressin regulation of the renal UT-A3 urea transporter. *Am J Physiol Renal Physiol* 296: F642-F648, 2009.

186. **Su H, Carter CB, Laur O, Sands JM, and Chen G**. Forskolin stimulation promotes urea transporter UT-A1 ubiquitination, endocytosis, and degradation in MDCK cells. *Am J Physiol Renal Physiol* 303: F1325-F1332, 2012.

187. **Tajika Y, Matsuzaki T, Suzuki T, Ablimit A, Aoki T, Hagiwara H, Kuwahara M, Sasaki S, and Takata K**. Differential regulation of AQP2 trafficking in endosomes by microtubules and actin filaments. *Histochem Cell Biol* 124: 1-12, 2005.

188. **Tajika Y, Matsuzaki T, Suzuki T, Aoki T, Hagiwara H, Kuwahara M, Sasaki S, and Takata K**. Aquaporin-2 is retrieved to the apical storage compartment via early endosomes and phosphatidylinositol 3-kinase-dependent pathway. *Endocrinology* 145: 4375-4383, 2004.

189. **Tamma G, Klussmann E, Maric K, Aktories K, Svelto M, Rosenthal W, and Valenti G**. Rho inhibits cAMP-induced translocation of aquaporin-2 into the apical membrane of renal cells. *Am J Physiol Renal Physiol* 281: F1092-F1101, 2001.

190. **Tamma G, Klussmann E, Oehlke J, Krause E, Rosenthal W, Svelto M, and Valenti G**. Actin remodeling requires ERM function to facilitate AQP2 apical targeting. *J Cell Sci* 118: 3623-3630, 2005.

191. **Tamma G, Wiesner B, Furkert J, Hahm D, Oksche A, Schaefer M, Valenti G, Rosenthal W, and Klussmann E**. The prostaglandin E2 analogue sulprostone antagonizes vasopressin-induced antidiuresis through activation of Rho. *J Cell Sci* 116: 3285-3294, 2003.

192. **Terris J, Ecelbarger CA, Marples D, Knepper M, and Nielsen S**. Distribution of aquaporin-4 water channel expression within rat kidney. *Am J Physiol Renal Physiol* 269: F775-F785, 1995.

193. **Terris J, Ecelbarger CA, Sands JM, and Knepper MA**. Long-term regulation of renal urea transporter protein expression in rat. *J Am Soc Nephrol* 9: 729-736, 1998.

194. **Terris JM, Knepper MA, and Wade JB**. UT-A3: localization and characterization of an additional urea transporter isoform in the IMCD. *Am J Physiol Renal Physiol* 280: F325-F332, 2001.

195. **Tsukaguchi H, Shayakul C, Berger UV, Tokui T, Brown D, and Hediger MA**. Cloning and characterization of the urea transporter UT3: localization in rat kidney and testis. *J Clin Invest* 99: 1506, 1997.

196. **Uchida S, Sohara E, Rai T, Ikawa M, Okabe M, and Sasaki S**. Impaired urea accumulation in the inner medulla of mice lacking the urea transporter UT-A2. *Mol Cell Biol* 25: 7357-7363, 2005.

197. **Vagin O, Kraut JA, and Sachs G**. Role of N-glycosylation in trafficking of apical membrane proteins in epithelia. *Am J Physiol Renal Physiol* 296: F459-F469, 2009.

198. **Verkman A**. Dissecting the roles of aquaporins in renal pathophysiology using transgenic mice. In: *Semin Nephrol*Elsevier, 2008, p. 217-226.

199. **Vesey DA, Qi W, Chen X, Pollock CA, and Johnson DW**. Isolation and primary culture of human proximal tubule cells. *Kidney Research: Experimental Protocols* 19-24, 2009.

200. **Vinay P, Gougoux A, and Lemieux G**. Isolation of a pure suspension of rat proximal tubules. *Am J Physiol Renal Physiol* 241: F403-F411, 1981.

201. **Vivas L, Chiaraviglio E, and Carrer HF**. Rat organum vasculosum laminae terminalis in vitro: responses to changes in sodium concentration. *Brain Res* 519: 294-300, 1990.

202. **Wade J, Lee A, Liu J, Ecelbarger C, Mitchell C, Bradford A, Terris J, Kim G-H, and Knepper M**. UT-A2: a 55-kDa urea transporter in thin descending limb whose abundance is regulated by vasopressin. *Am J Physiol Renal Physiol* 278: F52-F62, 2000.

203. **Wainszelbaum MJ, Proctor BM, Pontow SE, Stahl PD, and Barbieri MA**. IL4/PGE 2 induction of an enlarged early endosomal compartment in mouse macrophages is Rab5-dependent. *Exp Cell Res* 312: 2238-2251, 2006.

204. **Wei S, Xu Y, Shi H, Wong S-H, Han W, Talbot K, Hong W, and Ong W-Y**. EHD1 is a synaptic protein that modulates exocytosis through binding to snapin. *Molecular and Cellular Neuroscience* 45: 418-429, 2010.

205. **Welling PA, and Weisz OA**. Sorting it out in endosomes: an emerging concept in renal epithelial cell transport regulation. *Physiology* 25: 280-292, 2010.

206. **Yang B, and Bankir L**. Urea and urine concentrating ability: new insights from studies in mice. *Am J Physiol Renal Physiol* 288: F881-F896, 2005.

207. **Yang B, Bankir L, Gillespie A, Epstein CJ, and Verkman A**. Urea-selective concentrating defect in transgenic mice lacking urea transporter UT-B. *J Biol Chem* 277: 10633-10637, 2002.

208. **Yang J, Lane PH, Pollock JS, and Carmines PK**. PKC-dependent superoxide production by the renal medullary thick ascending limb from diabetic rats. *Am J Physiol Renal Physiol* 297: F1220-F1228, 2009.

209. **Yasui M, Zelenin SM, Celsi G, and Aperia A**. Adenylate cyclase-coupled vasopressin receptor activates AQP2 promoter via a dual effect on CRE and AP1 elements. *Am J Physiol Renal Physiol* 272: F443-F450, 1997.

210. **Yu L, Moriguchi T, Souma T, Takai J, Satoh H, Morito N, Engel JD, and Yamamoto M**. GATA2 regulates body water homeostasis through maintaining aquaporin 2 expression in renal collecting ducts. *Mol Cell Biol* 34: 1929-1941, 2014.

211. **Zelenina M, Christensen BM, Palmér J, Nairn AC, Nielsen S, and Aperia A**. Prostaglandin E2 interaction with AVP: effects on AQP2 phosphorylation and distribution. *Am J Physiol Renal Physiol* 278: F388-F394, 2000.

212. **Zhang J, Naslavsky N, and Caplan S**. Rabs and EHDs: alternate modes for traffic control. *Biosci Rep* 32: 17-23, 2012.

213. **Zhang L, Bowen T, Grennan-Jones F, Paddon C, Giles P, Webber J, Steadman R, and Ludgate M**. Thyrotropin Receptor Activation Increases Hyaluronan Production in Preadipocyte Fibroblasts CONTRIBUTORY ROLE IN HYALURONAN ACCUMULATION IN THYROID DYSFUNCTION. *J Biol Chem* 284: 26447-26455, 2009.

214. **Zhang X, Huang S, Gao M, Liu J, Jia X, Han Q, Zheng S, Miao Y, Li S, and Weng H**. Farnesoid X receptor (FXR) gene deficiency impairs urine concentration in mice. *Proc Nat Acad Sci* 111: 2277-2282, 2014.